Suivi automatique de variations modales à l'aide du technique de décrément aléatoire sans filtrage application à des enregistrements de vibrations ambiantes des bâtiments

Fatima Nasser Nasser-Barakat

UNIVERSITÉ DE GRENOBLE

THÈSE

pour obtenir le grade de

DOCTEUR DE L'UNIVERSITÉ DE GRENOBLE

Spécialité : **signal, image, parole, télécommunications (SIPT)**

Arrêté ministériel : 7 août 2006

Présentée par
Fatima NASSER-BARAKAT

Thèse dirigée par **Mme. Nadine MARTIN**

préparée au sein du
laboratoire Grenoble, images, parole, signal, automatique (GIPSA-lab)
dans **l'école doctorale d'électronique, électrotechnique, automatique et traitement du signal (EEATS)**

Automatic Modal Variation Tracking via a Filter-Free Random Decrement Technique Application to ambient vibration recordings on high-rise buildings

Thèse soutenue publiquement le **28 Mai 2015**,
devant le jury composé de:

M. Jérôme ANTONI
professor, INSA Lyon (Rapporteur)
M. Laurent MEVEL
Chargé de recherche, INRIA Rennes, (Rapporteur)
M. Philippe GUEGUEN
Directeur de recherche IFSTTAR, ISTerre Grenoble (Président, Examinateur)
M. Julien HUILLERY
Maître de conférence, Ecole Centrale Lyon (Examinateur)
Mme. Nadine MARTIN
Directeur de recherche CNRS, GIPSA-Lab Grenoble (Directrice de thèse)

Acknowledgements

As I write down this acknowledgement I am aware of the long road I have passed and the many obstacles I have overcome. And as I look back to this wonderful though tiresome journey I can't help but have immense gratitude for all the people who have shared it with me and witnessed all the ups and the downs and were there to help me through it all. Without their time, encouragement, patience and thoughtful feedback, I would not have been able to see it through. And at the end of it all, it is my pleasure to express my appreciation to all those who have contributed in a way or another to the success of this study and made it an unforgettable experience for me and to whom I owe my fulfillment and satisfaction.

I have been privileged to spend my time preparing my doctoral studies in GIPSA lab – department of image and signal that provided a professional yet welcoming environment and its members and staff will always remain dear to me.

At this moment of accomplishment, first of all I pay homage to my supervisor Dr. Nadine MARTIN. She patiently provided encouragement and advice necessary for me to proceed through the completion of my thesis and never pushed or judged but was very understanding when she knew I needed to juggle priorities.

I also deeply appreciate the assistance of all the jury members of whom I was honored and privileged to be evaluated by. First thanks to Mr. Philippe GUEGUEN who chaired the jury. Thank you to my two reviewers Mr. Jèrôme ANTONI, and Mr. Laurent MEVEL and to my examiner Mr. Julien HUILLERY for taking the time to appraise my work and to give their valuable commentary and their opinions regarding adjustments I needed to do on my thesis.

I take this opportunity to sincerely acknowledge the French Research National Agency (ANR) through RISKNAT program (project URBASIS ANR-09 RISK-009) who assisted this work and provided us in collaboration with ISTerre laboratory with all the required signals on which we applied our tests. In this regard, I can't but particularly mention Mr. Philippe GUEGUEN, the head of *ANR-URBASIS* project, for his helpful support.

I am particularly grateful to Mr. Gang FENG, responsible of the (SIPT) Signal, Image, Parole, Telecom specialty, who made the workflow smooth by providing helpful advice, and who has most patiently helped me through all the obstacles I faced during the preparation of my thesis no matter how trivial they were.

I am very fortunate to have had Zhongyang LI share my doctoral journey. He has been like a second advisor to me, ready with brilliant ideas, honest advice and encouraging words whenever I needed them. He was not only a mentor but also such a very good friend and a great source of inspiration.

It's my felicity to acknowledge the support of my very special office mates Wei, Jérémie,

Fakhri and Quentin who -as crazy as they may have been- made life in the lab very colorful and made the work settings very convivial. It is them that made arriving to work every morning a pleasure of mine.

I am also very blessed to have met and befriended a lot of fellow Lebanese colleagues that were a piece of home for me and the answer to my homesickness. I especially mention Soukayna, Rajaa, Wafaa, and Zeinab S.

Speaking of home, a great part of my gratitude goes to my family back in Lebanon. If it wasn't for their emotional support, encouragement, and continuous prayers I would have never accomplished anything in my life. To my dad, mom and three brothers and their wives I extend my truest appreciation. Thank you for helping me in every aspect of my life and for being a big part of who I am and who I aspire to become. Another big part of my support group back home are my in-laws, I thank them for their honest abutment and aid in particular my dearest Maysaa.

To my partner- not only through the preparation of my thesis but through my whole life-, to my husband Reda you have filled my life with affection and shown me that with love family and faith nothing is impossible. I owe you so much for embracing me with support and being my cornerstone. Not the least, thank you for all your delicious meals and your babysitting services.

Last but not least, to the jewels of my life, to the fruits of my loins, to Joud who has started the journey within me and his sibling yet to come who has ended it within me as well. For the both of you I give all my love and devotion.

with love,

Fatima.

Abstract

This thesis proposes a novel approach to automatically monitor the variations of the frequencies and the damping ratios of actual high-rise buildings subjected to real-world ambient vibrations. The approach aims at dealing simultaneously with the following challenges: multi-component signals recorded over the aforementioned buildings and having closely-spaced frequency modes with low, exponential and damped amplitudes of their impulse responses and contaminated with high additive noises. The approach relies on the application of the Random Decrement Technique directly over the multi-component signal under study which leads to the extraction of a Multi-mode Random Decrement Signature equivalent to the system impulse response. To characterize such a signature, we propose a signal model based on the physical structure of the building from where the modal parameters can be estimated. For the purpose of non-biased modal estimate, we propose to use an iterative method based on a Maximum-Likelihood Estimation optimized by a simulated annealing technique. In order to initialize the parameters of the latter, a first step is designed which can be considered as an independent estimator of the modal parameters. The originality of this step lies in its ability to automatically define the number of modes of the estimated signature through the use of the statistical properties of a Welch spectrum. The modal parameters estimated by the spectral-based initialization step are finally refined by the Maximum-Likelihood Estimation step. The latter reduces the bias in the estimation and yields more reliable and robust results. All these steps are defined in order to be able to automatically monitor the health of a building via a long-term real-time tracking of the modal variations over time without the need to any user intervention . In addition, the proposed approach has paid very special attention to the automatic estimation of the most problematic modal parameter, *i.e.*, the damping ratio. Such features making two of the original features as compared to existing techniques. The adaptability and functionality of AMBA is validated over six actual buildings excited by real-world ambient vibrations. From the obtained results, AMBA proved high efficiency in automatically estimating the frequencies and moreover the damping ratios in case of closely-spaced frequency modes and very low signal-to-noise ratio level. AMBA as well demonstrated a good performance for tracking the modal variations over time.

Key words Automatic modal analysis, random decrement technique, modal variation, building monitoring, time-tracking.

Contents

List of Figures

List of Tables

Chapter 1

Introduction

No matter how well they are built and designed, all structures deteriorate during their service life. Health assessment of these structures, timely prediction of their damage and opportune detection of any possible failure is crucial for safety reasons in all aspects.

The concept of diagnosing the state of the structure is generally known as Structural Health Monitoring. This monitoring is widely applied to various forms of applications, *e.g.* numerous forms of civil infrastructures, mechanical and aerospace structures, acoustical instruments and nuclear power plants.

In the field of civil engineering, the modal analysis has became a major tool in the pursuit of identifying and improving dynamic characteristics of civil engineering structures. This interest is mainly attributed to the fact that the modal parameters can provide a basis for the determination of the physical properties such as mass, stiffness and damping of the structure in question due to the direct relation between the modal and the physical parameters.

In the last two decades, the seismic vulnerability assessment has always been a hot topic in the engineering profession. In order to provide proper strategies to reduce seismic risks in urban areas, one of the most essential engineering needs is to have reliable and affordable solutions to monitor the behavior of the building in a long-term real-time manner. The continuous real-time monitoring of an in-service structure allows an optimal use of this structure, minimizes the possible downtime, and helps avoiding any catastrophic failures. This is the core idea behind the continuous vibration-based structural health monitoring, which shifts the researchers attention to the urge need of efficient and robust routines able to perform an automatic processing of large amounts of continuously collected data.

When the continuous vibration-based structural health monitoring is applied over a building structure, the ambient excitations thus play a significant role. First, because buildings are normally characterized by being of very large size and of complex design which makes them difficult to be artificially excited, and second, because the ambient vibrations are always present over the building which makes them a useful element to be continuously recorded by means of permanent installed set of sensors.

In spite of the remarkable efforts in this context, the user-know-how is not ruled out completely in most of the proposed automatic modal analysis methods, as the user intervention is still needed to manually select some parameters.

In this regard, the main idea of this thesis is to estimate the modal parameters of real-world

ambient vibrations in a reliable, robust and automatic way under the following simultaneous challenges:

- High-rise buildings;
- Multi-component signals;
- Low, exponential and damped amplitudes;
- Long time duration;
- Closely-spaced frequency modes;
- Low signal-to-noise ratio levels.

The existing methods have limitations in several aspects. Many methods to automatically estimate the modal parameters of the signal, such as the automatic frequency domain decomposition method, do not provide a reliable estimation of the damping ratio, which is the primary purpose of this thesis. Some other methods don't adapt to the context of the multi-component signals, such as the random decrement technique. To apply such methods on multi-component signals, the signal components must be first filtered. Many of the existing methods are very sensitive to noise, like the automatic covariance stochastic subspace identification method, thus higher modes or even poorly excited modes are not always identified. Other methods are not suitable for time-tracking process of the modal analysis, like the clustering algorithm and the time domain filtering method. The former requires a preliminary manual initialization before each application which lower its efficiency, and the latter, at which the whole process is specified according to the power spectral density plots of the signal response, makes the work more cumbersome in the case of unknown excitation, and closely-spaced frequency modes. The selection of the physical poles is a task very critical for almost all the existing methods. Most of them stems from the principle of a threshold-based peak detection method that requires a calibration phase prior to the analysis. Such calibration process could be very time consuming depending on the structure in question.

The type of signals that we consider in this thesis is the result of a time domain convolution between the system impulse response and the ground solicitation. Hence, this thesis is dedicated to the resolution of the following issues related to the nature of the studied signal and the aforementioned challenges:

- To estimate the modal parameters of a signal, the impulse response of the signal must be first extracted from the ground solicitations, emphasizing on the importance of having a free-decay signature that is equivalent to the system impulse response. To under go the objective of automatic modal parameter estimation, we should propose a method that doesn't need any preliminary filtering processes.

- We should design a signal model that fits the context of the multi-mode estimated signature.

- We should propose a method to automatically estimate the modal parameters of the multi-component signature. Such a method must manage the detection of the physical modes from the noisy ones, taking into account the closely-spaced frequency modes and the damped ones.

- To ensure the robustness of the automatic estimation approach, we should propose a non-biased parametric method, as the estimation by such a method doesn't depend on the resolution of the used spectral estimator.

- As the parametric method is iterative by nature, we should propose a method to solve its initialization problem.

- It is important that all steps of the algorithm account for long-term real-time tracking of modal parameters. In particular, the damping ratio must be taken into account for its importance in the health monitoring of the high-rise buildings.

This manuscript is organized in 7 chapters as follows;

In *"Chapter 2"* we give a brief overview of the topics that are in important relation to the content of this thesis. We present a literature overview of the output-only modal analysis, we also give a key lecture about the proposals of an automatic modal analysis in the literature. Then we present the delimitations and objectives of this thesis. Finally we introduce a general overview of the proposed approach of this thesis. This approach contains three main steps, each step is presented in a separate chapter, namely *Chapters 3, 4* and *5*.

"Chapter 3" is devoted to the proposition of using the Filter-Free Random Decrement Technique which is the first step of the proposed approach. We give a brief overview of the Random Decrement Technique, and then we dwell on the discussion of the proposed signal model in this thesis.

"Chapter 4" is dedicated to the proposition of a spectral-based initialization step of the modal parameter estimation. The estimation of the vector of parameters of the signal model is described in *"Chapter 5"*. We present the procedure of a parametric maximum-likelihood estimator based on a stochastic optimization technique, called simulated annealing. The results of the simulated signals are presented at the end of these two last chapters to illustrate the performance of each of the two steps in automatically estimating the modal parameters.

The application of the proposed approach over actual buildings subjected to real-world ambient vibrations is then validated in *"Chapter 6"*. We also introduce in this chapter a long-term real-time tracking of the natural frequency and the damping ratio.

In the last chapter, *"Chapter 7"*, we highlight the contributions of this work, then we provide information on some potential improvements to guide future developments.

Chapter 2

Research context

Contents

THIS chapter gives a brief overview of the topics that are in important relation to the content of this thesis. Firstly, the main aim of this work as proposed by the *ANR-URBASIS* project is discussed in section 2.1. As the core of this thesis is based on the ambient vibrations, section 2.2 examines their origin and nature in buildings. Later, the modal parameters of buildings determined under ambient vibrations are interpreted in physical terms, the manner in which these modal parameters are incorporated into this model is thus explored in section 2.3. Section 2.4 presents a summary overview of the output-only modal analysis in the literature, and introduces the background and motivations to automate such an analysis. Then the thesis delimitations and main objectives are identified in section 2.5. Finally, section 2.6 presents a general view of the proposed approach in this thesis.

2.1 Statement of problem

Urban seismic risk is increasing worldwide with the significant population growth and the excessive unplanned urban sprawl into areas susceptible to seismic hazard. Damages and destructions after strong earthquake have demonstrated that the continuous assessment and monitoring of built structures are imperative options.

In this regard, throughout the last decades, the engineers have paid a great attention to develop new theories and methods to predict and prevent the inherent consequences that can eventually cause serious damage in real structures.

This thesis is proposed in the context of *"ANR-URBASIS"*[1] project, (Agence Nationale de Recherche- Sismologie URBAine (Fig. 2.1)), whose mission was to contribute to the assessment of the seimsic vulnerability and damage using innovative processing methods (*cf.*, the web page of the project).

Figure 2.1: The lego of *ANR-URBASIS* project.

Starting from the fact that there is a great correlation between the numbers of the damaged buildings after an earthquake and that of the victims, the acquisition of prior knowledge of those buildings becomes an important tool to manage, predict and assess their vulnerability and post-seismic integrity.

ANR-URBASIS found that it is essential to develop the ways of the structural assessment and proposed to find the modal parameters, *i.e.*, natural frequencies, damping ratios and mode shapes, of a building by technological developments and signal processing algorithms that could estimate its normal period (inter-seismic). **This task constitutes the heart of the matter of this thesis**, and it is based on the concept that the extent of degradation of a building is reflected in the changes of its inherent dynamic behavior, and in turn, is dependent on the changes in the modal parameters in terms of local stiffness and damping characteristics and their variations with time. This whole process defines the basic premise of the vibration-based structural health monitoring.

Thus the vibration-based structural health monitoring and damage identification has been the subject of significant research in structural engineering in recent years [Doe+96, FDN01, Soh+04].

For civil engineering structures, ambient vibration tests are preferred over forced vibration ones because the artificial excitation of large structures having low natural frequencies is quite difficult, impractical, sometimes even impossible and expensive. In the ambient vibration tests, operation disturbances can be avoided since such kind of tests don't interfere with the normal use of the building, and the measured response is representative of the actual operating conditions of the building which vibrates due to natural excitation thus exciting devices are not needed. For the aforementioned reasons, in the context of this thesis and based on the interest of *ANR-URBASIS*, only the ambient vibrations are considered. Such

[1] http://urbasis.osug.fr/

ambient vibrations are referred to as *"seismic background noise"* in the field of geoscience.

This thesis focuses on the estimation of the natural frequencies and the damping ratios of a building but not its mode shapes. This is attributed to the general goal of *ANR-URBASIS* in monitoring the structural health and identifying the damage rather than localizing it.

This thesis emphasizes more on the estimation of the damping ratio. Such an emphasis is essentially twofold: firstly, the damping ratio parameter is of great importance in dynamic design of engineering structures. As per Newton's second law, the dynamic response of high-rise buildings is mainly controlled by their mass, their stiffness and their ability to dissipate the vibrating energy in order to reduce the stress and the induced damage. Consequently, the damping is an extremely important factor in mitigating dynamic-load-induced vibrations of such buildings.

Secondly, the estimation of the damping ratio is still posing some problems. Unlike the relatively easier and quantifiable properties, *e.g.*, mass and stiffness, through the resonant frequency, the exact amount of damping within a particular building is a complex, difficult and ambiguous quantity to ascertain. Moreover, the damping quantity varies with the amplitude of the excitation and depends on complex mechanisms within the building, *e.g.*, the intrinsic damping, the radiated damping at the foundation-ground interface, or the scattering damping into the building, many of which are still not fully understood.

The fairly large scattering of the damping estimates as compared to those of natural frequency is demonstrated in the literature [RFC10]. This scattering can be partially related to the limitations of the estimators and to the adoption of an equivalent physical model. However, appropriate damping estimate procedures are essential to minimize the error and to enhance robustness and accuracy of structural assessment.

2.2 Origin and nature of ambient vibrations in buildings

As this thesis only considers the ambient vibrations, this section is devoted to present the main sources and natures of these vibrations in buildings.

Ambient vibrations, also called seismic background noise, are vibrations from different sources, such as tidal waves of the seas and oceans, wind, industrial machinery, vehicular traffic, human activities, *etc.* (*cf.*, Fig. 2.2). A full review on the ambient vibrations is given by [BCCB06].

In the field of civil engineering, it is commonly known that sources of ambient vibrations are classified in two main types: natural and human. Such sources very often correspond to different frequency bands, especially within urban areas. Frequencies below 1 Hz are natural, while those above 1 Hz are mainly of urban origin (principally related to human activities).

- $f < 1$ Hz: The oceanic waves of large-scale (maximal energy) are of frequencies less

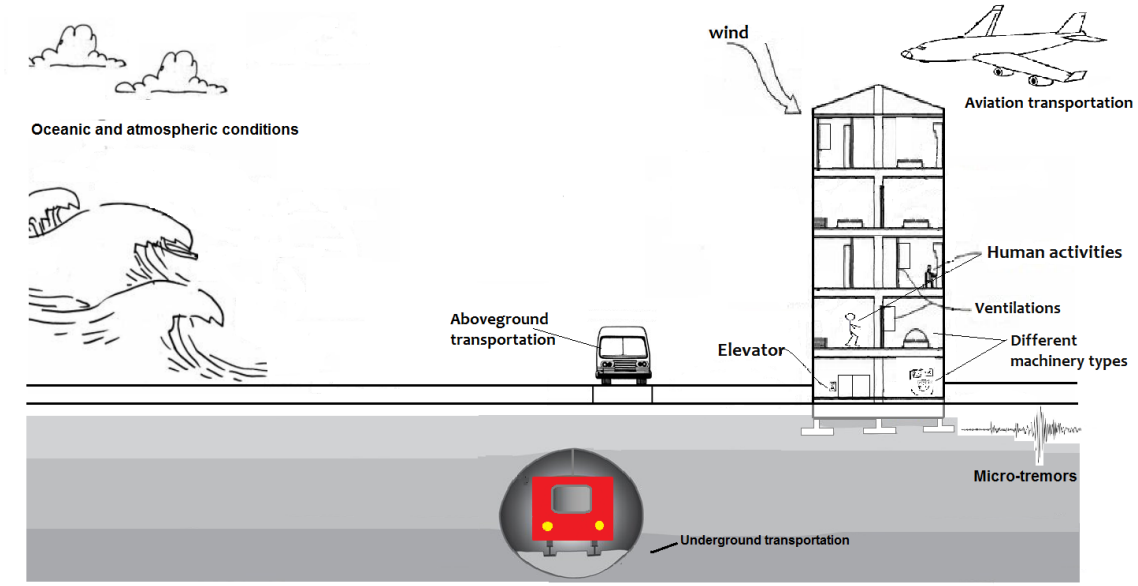

Figure 2.2: Some examples of the different sources of ambient vibrations over a building.

than 0.5 Hz, they are normally at around 0.2 Hz. When sea waves interact with coasts, this causes an ambient vibration at around 0.5 Hz. The atmospheric conditions are associated at very low frequency, much lower than 0.1 Hz, such a vibration range is almost of no interest for seismologists.

- $f = 1$ Hz: Such a frequency may be associated with the local weather, such as the wind, rain and water flows.
- $f > 1$ Hz: Such sources are essentially located at the surface of the earth, *e.g.*, industrial machinery, vehicular traffic, pedestrians, *etc.* The different human activities are highly variable between day/night and week/weekend periods, with a decrease in the amplitude at night, weekends and holidays [BCCB06].

The amplitude of the ambient vibrations is in general low, it varies in function of the proximity and the nature of the noise source. It is typically in the order of 10^{-6} to 10^{-5} m/s [BC04].

The velocities estimated by ambient vibrations are not affected by non-linearity, first because the acceleration of the observed records is small and does not vary much with time, and second because the ambient vibrations correspond to low strain of excitation that could not excite the building at the level of non-linear domain. Therefore, the ambient vibrations are appropriate for structural health monitoring in a linear regime [BC04].

For ambient vibration records, the system input is usually unknown. A critical assumption with these vibrations is that the recorded response time histories are stationary. Almost all ambient vibrations are assumed to be a white Gaussian noise as well. The hypothesis of the white Gaussian noise excitation is the key for the majority of the treatment methods.

Within *ANR-URBASIS* all the natures of these ambient vibrations are taken into consideration. The building is assumed time-invariant during the measurement period, the recorded vibrations of the building are modeled by a linear-lumped mass parameter system, and the excitation of the building is assumed to be a stationary white Gaussian noise.

2.3 Theoretical physical model

Because the main target of *ANR-URBASIS* is to evaluate the vulnerability of real urban buildings by signal processing techniques, we adopt a physical model of the building motion that is characterized by damped exponential functions.

In this section we present such a physical model for a real system. The set of equations of motion of this physical model are neither derived nor solved in this section. This is beyond the scope of this work. The main idea is only to show the assumptions and hypothesis held over the structure to yield this physical model, and to present how the model behaves and which motion does it has. The reader interested in more details can refer to [Mic07].

The physical model considered here is a model of a one-dimensional (1D) discrete beam that was proposed by Michel [Mic07], for which the masses are considered as a single point and concentrated at the floor level. Michel [Mic07] stated that if we consider a single point, *i.e.*, a single mass, per floor means that the floors are infinitely rigid and do not deform.

As per [Mic07], in the case of a lumped mass modeling of the structure, the Duhamel integral gives the elastic motion U of a building at each floor r as U_r, $\forall r \in [1, R]$, by only knowing the mass of each floor, the modal parameters, namely, the natural frequencies f_k, damping ratios ξ_k, and mode shapes Φ_k, and the ground motion $p(t)$ where k is the number of modes $\forall k \in [1, K]$.

The mode shape of the r^{th} floor $\Phi_k[r]$ depends on the number of the floor r and it participates as the weighting factor to generate the final response of the structure. The impulse response when K equals to 1 mode is thus that of a Single Degree of Freedom system and it is defined as

$$h_k(t) = \sum_{k=1}^{K} \frac{-1}{\omega_{Dk}} \exp^{-2\pi f_k \xi_k t} sin(\omega_{Dk} t + \phi_{0k}), \forall k \in [1, K], \tag{2.1}$$

with $\omega_{Dk} = 2\pi f_k \sqrt{1 - \xi_k^2}$ the pseudo pulsation of mode k, and ϕ_{0k} is the initial phase. This system being excited by the ground solicitations, the time-varying response of the mode k is obtained from the convolution with the ground solicitation $p[n]$ and is given by the Duhamel integral as following

$$\begin{aligned} y_k(t) &= \frac{-\mathfrak{p}_k}{\omega_{Dk}} \int_0^n p(t)\ h_k(t-\tau)\ d\tau \\ &= \mathfrak{p}_k\ p(t) \otimes \frac{-1}{\omega_{Dk}} \exp^{-2\pi f_k \xi_k t} sin(\omega_{Dk} t + \phi_{0k}), \forall k \in [1, K], \end{aligned} \tag{2.2}$$

with $\mathfrak{p}_k$ being the participation factor that is defined as $\mathfrak{p}_k = \frac{\sum_{fl=1}^{N} \Phi_k[fl]}{\sum_{fl=1}^{N} \Phi_k^2[fl]}$.

In fact, a building contains more than a single degree of freedom system, so that the motion of the building is then modelized as a linear superposition of the motion of all the K modes. Therefore, the dynamic response for a given floor r is obtained by superimposing the K modal responses $y_k(t)$ obtained in 2.2

$$U_r(t) = \sum_{k=1}^{K} y_k(t)\ \Phi_k[r] \tag{2.3}$$

2.4 Literature overview

This section is devoted to provide a key lecture about the concept of the Structural Health Monitoring along with the related methods used in the literature to estimate the structural modal parameters. Such an introduction aims to facilitate the understanding of such methods and the motivation which leads to the implementation of the proposed approach of this thesis.

This section can not cover the hundreds and hundreds of methods that were proposed over the years. We have chosen to focus on a handful summary of the output-only modal analysis methods in section 2.4.1 and those of the automated output-only modal analysis in section 2.4.2.

2.4.1 Output-only modal analysis

It is a true fact that any civil engineering structure begins to progressively deteriorate once it is built. This deterioration is normally attributed to aging, exposure to a normal continuous and occasional excessive loading, and adverse environmental conditions. However, the deficiencies in structures are not restricted to the aforementioned affects; poor engineering judgment, and inadequate design are other factors contributing to deficiencies at any time during the service life of the structure. Apart of the root cause, functional deficiencies are always there in civil engineering structures. Thus finding the appropriate solutions to monitor and resolve these defects is something very necessary for everyone's sake.

In this context, the methods of Structural Health Monitoring (SHM) have experienced significant developments in the past decades [Sik99, CA02, CCW03, YAB04]. Such methods are capable of providing good means to assess the validation and the continued performance

of the structure under study, *i.e.*, determining the structure ability to provide appropriate service (reliability), evaluate the necessity of maintenance (serviceability), and estimate the need for reparation or renovation of a part or the entire structure (remaining functionality) [Sik99]. The methodology provided by SHM approaches involves periodic investigation of the structure during operation.

Rytter [Ryt93] presented four levels to define the robustness of SHM:

Level I- Damage identification;

Level II- Damage localization;

Level III- Damage quantification;

Level IV- Damage prediction.

Level I defines whether the damage exists in the structure or not, level II determines the location of the damage, level III identifies the severity of the damage, and level IV predicts the remaining life time of the structure.

The first step to assess the state of a structure by means of SHM is the implementation of a global Nondestructive Damage Evaluation procedure. The latter presents the most essential part of the SHM process as it provides the primary interaction between the physical state of the structure and the analytic methods employed in the SHM process.

The civil engineering structures that have peculiar characteristics of a very large size, make impractical the application of the localized Nondestructive Damage Testing methods such as ultrasonic [Sik99]. However, a global Nondestructive Damage Evaluation technique, using the vibration characteristics of a structure, provides an efficient and effective way in assessing the condition of the overall structure.

The global Nondestructive Damage Evaluation techniques utilizing vibration characteristic generally involve two parts;

1- Data acquisition and extraction of vibration parameters. This feature is typically associated with the dynamic testing of structures. Such testing requires a source of excitation to vibrate the structure, the use of sensors to acquire time history data, and modal analysis procedures to extract modal parameters such as natural frequency and damping ratio.

2- A damage detection from the variation of the modal parameters extracted from the first part in order to identify the damage in the structure, its location and severity.

The development and implementation of SHM systems utilizing vibration characteristics of the structure have been the focus of a number of researchers. Extensive literature reviews and advances in this context have been reported by [Doe+96, Soh+04, CF04].

From the aforementioned discussion in this introductory section, it becomes clear that the measurement of structural dynamic properties such as **modal parameters** is an important step in vibration-based SHM. Theoretical background to modal testing is readily available in [MS97, Ewi00].

It is extremely very difficult to excite large civil engineering structures using controlled input, and to measure these inputs under operational conditions. Accordingly, the output-only modal analysis based on ambient vibrations has drawn significant attention in the field of civil engineering as an attractive way to tackle these problems.

Measurements under ambient vibrations have been used for the identification of damage in civil engineering structures since the 30s, namely in California by Carder [Car36]. Carder realized a number of measurements in several buildings in California and then proposed a relationship between the height and the period of the vibration of the buildings. Such a relationship is still used in the American earthquake engineering codes. Ivanovic [ITT00] summarized the tests on different civil engineering structures. In France, we cite some of the works in this sense [Bou+99, MGB08, Mic+10], all of them aimed to use these measurements to analyze the vulnerability of existing buildings.

The vibration-based damage detection methods use several aspects to identify, locate and quantify damage, *e.g.*, modal parameters and machine learning. This overview is focused on the estimation of the modal parameters and more specifically on the frequency and damping ratio.

A structure presents some changes in its structural properties whenever frequency shifts occur, this in fact makes the general basis of the development of the modal analysis methods based on the frequency changes. As per Farrar [FDN01], the changes in frequencies are unable to provide information of the damage location, *i.e.*, the spatial information. Thus the damage detection methods that depends only on the changes in the frequency are commonly Level I methods. Farrar [FDN01] claimed as well that damage detection based only on the frequency information does not provide reliable results. He explained that several combinations of damage in the structure can produce the same changes in the natural frequencies, *e.g.*, the environmental conditions. Accordingly, in the civil engineering community, especially when it comes to the application over large civil structures, the low sensitivity of the frequency shifts to damage requires either very precise measurements of the frequency change or large levels of damage.

Salwu [Sal97] discussed the methods for monitoring changes in frequency used to assess the condition of the structure. He recommended those that do not require prior theoretical models of damage, as this can introduce uncertainty to the measurement results. Recently, Clinton et al. [Cli+06] summarized the changes in fundamental frequencies of East-West and North-South of Milikian Library in California since its construction in 1967. He highlighted the frequency drops due to seismic events more or less strong. A permanent decrease in the frequency indicates the loss of rigidity of the structure. Michel et Gueguen [MG10] studied the vibration of the fundamental frequency of the Millikian Library as well during the earthquake of San Fernando with the pseudo-Wigner Ville reassignment method. They noted a slight

fall in the frequency after 70 seconds while the maximum displacement was achieved. They attributed this decline to the seismic source rather than the downward rigidity of the structure. Creed [Cre87] stated that frequency variations up to 5% may not sign the presence of damage in the structure. This level of variation can be attributed to the climatic conditions, such as temperature and humidity. Wahab et De Roek [WDR97] showed that a low change of 15°C in temperature, may cause changes in frequency between 4% and 5%. Farrar et al [Far+97] and Sohn et al [Soh+99] studied the bridge Alamosa Canyon, New Mexico. They reported a frequency variation of approximately 5% over 24 hours.

Modal analysis based on the damping ratio changes were also considered to assess the structural vulnerability by many researchers [Jea96, Jea97, MSZ99]. The fact that the damping ratio depends on the amplitude of the loading and on the frequency of the building has been extensively studied [Jea86, TYY94, Li+00, Sat+03, Dun05, Cli+06]. Damping descending with amplitude and ascending with frequency was observed in all of these studies. Sakate et al [Sat+03] studied a wide range of buildings in Japan with several types of construction and foundation. He showed that for the first mode of vibration, the damping increases with the frequency regardless of the type of construction.

One of the very well-known group of output-only modal analysis methods in the frequency domain consists of methods utilizing singular value decomposition of the cross-spectrum matrix. These methods are referred to as Frequency Domain Decomposition (FDD) method [BZA00].

The FDD is based on decomposing the power spectral density function matrix using the singular value decomposition. As per [BZA00], the FDD decomposes the spectral responses into a set of auto spectral density functions, each corresponding to a single degree of freedom system of one individual mode. Following [BZA00], this result is exact in the case where the loading is white noise, the structure is slightly damped, and when the mode shapes of close modes are geometrically orthogonal. As per Brincker words, if these assumptions are not satisfied, the decomposition into single degree of freedom systems is approximate, but still presenting significantly more accurate results as compared to the peak-picking method. The FDD can only estimate the natural frequencies and mode shapes.

A second generation of the FDD is known as enhanced FDD [BVA01]. As compared to the FDD, the enhanced FDD provides estimate of the damping ratios as well as improved estimate of the natural frequencies and mode shapes.

On 2006, Jacobsen et al. [JAB06] presented the methodology of the enhanced FDD as follows; the single degree of freedom power spectral density function, that is identified around a peak of resonance, is taken back to the time-domain using the Inverse Discrete Fourier Transform. The enhanced FDD obtains the natural frequencies by determining the zero-crossing as a function of time. Where the damping ratio is obtained using the logarithmic decrement of the corresponding single degree of freedom normalized auto-correlation function. As per Jacobsen words, the single degree of freedom function is estimated using the shape determined by the previous FDD peak picking, the latter being used as a reference vector in a correlation analysis based on the Modal Assurance Criterion. A Modal Assurance Criterion

value is computed between the reference FDD vector and a singular vector for each particular frequency line. If the MAC value of this vector is above a user-specified Modal Assurance Criterion Rejection Level, the corresponding singular value is included in the description of the single degree of freedom function. The lower this Modal Assurance Criterion Rejection Level is, the larger the number of singular values included in the identification of the single degree of freedom function will be. In the case of closely-spaced frequency modes, the beating phenomenon would be encountered, which can lead inaccurate estimation of the damping ratio.

The advantages of the FDD based methods is that they are easy and fast to use. Some drawbacks are presented by the need to fine tune the Modal Assurance Criterion level for each resonance frequency in the frequency set, which may be very time consuming procedure when a large number of modal frequencies exist.

2.4.2 Automated output-only modal analysis

In the context of dynamic structural health monitoring, where excessive data of continuously recorded structural responses are periodically collected, it is very important to develop means that can process the collected data automatically. As already presented in this chapter, one of the most commonly used techniques to evaluate the structural condition is through the analysis of the modal parameter variations [Doe+96]. Despite of the different limitations that might encounter the estimation process of the modal parameters variations, like the operational and environmental limitations [Sal97, PDR01], the continuous monitoring of the structural modal parameters still present a very reliable tool in the performance assessment [RFC08], functional deficiencies [MCC12], and emergency maintenance [RF10, Rai+12] of civil engineering structures.

However, most of the existing techniques require the human interaction at some stages while performing the identification of structural modal parameters. Consequently, a lot of research has been oriented towards the goal of providing tools that can automatically extract robust and reliable output-only modal analysis from continuously recorded structural responses. This section is devoted to the presentation of algorithms for automatic output-only modal analysis.

Recently, the development of automatic modal parameter estimation techniques has been paid a noticeable attention [PWJ97, PJZ98, JIZC99, CZJ99, Ver+02, BAJ07, RF10]. Such techniques are of utmost importance especially when large amount of data is acquired in monitoring works, as they help to limit the user interaction and to reduce the problems faced during manual data processing of limited experience users. However, the unresolved issues in these procedures like the computational time, robustness and efficiency in the estimation, especially for the damping ratios, is still the main reason for why the continuous modal testing is not widely used [RFC10].

Chronologically, one of the first proposals for automatic structural modal analysis can be ascribed to Verboven et al. [Ver+02], however, it is just in the last few years that more

attention has been promoted in this context. We cite for example those who formulated automatic algorithms to identify the modal parameters with the basis of output-only modal analysis methods in the two branches, the control theory and the conventional signal processing [BAJ07, RFC07, Der+08].

According to conventional modal analysis methods, and in order to identify all the physical modes in the frequency range of interest, the model order is usually over-specified. This mainly occurs as far as modal analysis methods based on control theory are considered. However, it is inevitable to distinguish the vibration modes from the noisy ones. This process normally demands high interaction of expert users [Sod77]. Accordingly, the stabilization diagram is always coupled with the classical modal analysis processes to do the distinguishing job. Such a job is not trivial, it could be difficult, time consuming and sometimes rather impossible depending on the quality of data, the experience of the user, and the performance of the estimator despite of all the interesting evolving in this field [LRP04, CT08]. Yet extensive intervention between the user and the estimation method is the basic impediment for continuous and automatic structural monitoring.

Peeters et al. [PDR01] proposed a criterion for automatic modal analysis via stochastic subspace identification technique. They applied their proposition on the Z24 bridge in Switzerland to monitor structural dynamic behavior *w.r.t* environmental conditions and damage changes. This technique was also applied recently to identify the environmental effects on the modal analysis of Tamar bridge [BC07]. Such technique is based on the means of stabilization diagram and the selection of the most stable poles.

On 2007, a fully automated modal analysis approach adopting the stochastic subspace identification technique is proposed by Anderson [And+07]. This approach is based on a clear stabilization diagram, thus the pole selection process is done by a graph theory. This algorithm is fast, hence could be used for monitoring routine issues. Further investigations are still taking place to increase the method efficiency and reliability.

On 2008, another proposition of an automatic output-only modal analysis based on the stochastic subspace identification technique is proposed [Der+08]. Even though this technique seems to be promising as a tracking method, but it has a huge drawback as it requires an excessive intervention from the user to set an initial set of modal parameters before launching the tracking procedure.

The literature has testified certain automatic propositions for the modal analysis methods based on conventional signal processing. Back to 2005, Guan et al. [GKS05] has proposed the so-called time domain filtering method. It serves as a tracking procedure, however, as its name suggests, it is based on the application of a filter to the system response, namely a band-pass filter in order to filter out a single mode in the spectrum. Accordingly, the frequency limit of the filter is static, more and above, the whole process is specified according only to the power spectral density plots of the signal responses. It gets more cumbersome in the case of very closely-spaced frequency modes, at which defining correctly the limits of each mode is very difficult or even impossible, so that frequency shifts are much likely to occur and thus changes in modal frequencies can not be tracked.

Brincker et al. [BAJ07] proposed an algorithm to automate the already proposed frequency domain decomposition method [BZA00], to comply the need to remove any user interaction and thus improve the SHM procedure. As per [BAJ07], it is required to define indicators that can help distinguishing between different modes and between modes and noise. If a peak is identified in the first singular value, the question is then to know whether this peak is related to a mode or a noise. Calculating the correlation between the first singular vector at the identified peak and the first singular vector at neighboring points defines the discriminator function called the modal coherence. Following [BAJ07], if the modal coherence is close to unity, then the first singular value at the neighboring point correspond to the same modal coordinate, and therefore, the same mode is dominating. This function is helpful in distinguishing between points dominated by modal information and points dominated by noise. Once a peak has been accepted as representing modal information, another discriminator function can be helpful in discriminating between different modes. In this case the discriminator is the modal domain function. Though a value of 0.8 could be considered as a good initialization for such the coherence function, however, only few suggestions are reported for the modal domain function [BAJ07].

The second order blind identification method has been recently proposed as an automated modal analysis algorithm [PKG08]. The selection of the actual structural modes is done based on the computation of a confidence factor. This method requires no selection of the model order. However, its main drawback is the need for a number of sensors greater than or equal to the number of active modes.

To sum up, we can summarize the two common drawbacks of the existing automated output-only methods as follows, most of them are:

1- Very sensitive to noise, which makes the identification of higher modes, highly damped modes, poorly excited modes and closely-spaced frequency modes are difficult to be identified and sometimes impossible to be identified.

2- Based on a threshold-based peak detection, at which a preliminary calibration process is required. Such a calibration helps developing an appropriate identification of the structural modes. The calibration gets worse in the presence of noisy measurements which results in false-alarmed peaks, *i.e.*, some noisy peaks is defined as actual modes.

In this regard, this work within *ANR-URBASIS* project is mainly challenged by the huge need of efficient and robust routines that are able to perform an online, long-term, and fully automatic processing of large amounts of continuously collected data from high-rise buildings that are subjected to ground ambient vibrations with paying a very special attention to the automatic estimation of the damping ratio.

2.5 Thesis delimitations and objectives

After the short literature overview in the last section, this section summarizes the delimitations of this thesis and points out its main objectives.

There are different types of excitations to bring the structure into vibration. The vibration test, in turn, differs with each of these types. In this thesis, we only consider the excitations that can be modeled by white noise, *i.e.*, the ambient vibrations.

As per Ewin [Ewi00], in order to carry out a successful vibration test, there exist three processes to be paid special attention. These are, the process to: (1) measure the vibrations; (2) provide the mathematical model of the structural vibrations; and (3) analyze the measured vibrations, known as "Data analysis". Practically, these three processes are coherent, so that all should work together with high accuracy whenever the aim is to identify the dynamic characteristics of the structure. This thesis mainly deals with the third process, that is the data analysis. This process makes the link between the other two processes, at which it uses the measured vibrations to identify the parameters of the mathematical model of the structure. Such parameters are the ones that describe the dynamic characteristics of the structure.

It is noteworthy that collecting the measurements is the intrinsic basis for a successful structural vibration test. Despite of the data analysis procedure and the mathematical model, if the data are not well measured, it is impossible to yield reliable dynamic characteristics of the structure. Although this thesis is all based on measured vibrations, however the process of measuring the vibration of a structure is neither described nor reported in details. This is beyond the scope of this work. It is only worth mentioning that all the vibration data of this thesis are provided to our hands by *ANR-URBASIS* project, and they were collected using a velocimeter that is connected to a Citychark (the 24 bits acquisition system) which is capable of recording the small amplitude of the ambient vibrations.

The linear lumped mass parameter model is the model used in this thesis to describe the vibrations of a structure. This model is a discrete model, at which the damping forces and the stiffness forces are assumed to be respectively proportional to the velocity and the displacements of the lumped masses.

In the context of this thesis, the data analysis procedure is denoted "*Modal analysis*" which provides an identification of the modal parameters of the building in question. The main topic of this thesis is how the variation of the parameters can be tracked over time from the measurements in a simultaneous and automatic way.

Every building does not necessary has only single degree of freedom but it normally has numbers of degree of freedom and thus characterized by different modes of vibrations. This thesis mainly considers this characteristic, and deals with an automatic and simultaneous estimation of the modal parameters of all the modes in a "*multi-component*" signal.

The physical model that we consider in this thesis shows a time domain convolution of

the force and the impulse response function of a building (*cf.*, section 2.3). The first task of this thesis is to propose a way capable of providing a free-decay signature equivalent to the system impulse response. The Random Decrement Technique is thus used for this aim. This method is widely used in the field of geoscience and it is of strong interest to *ANR-URBASIS* project.

In summary, the main context of this thesis is:

- The vibrations of the building can be modeled by a linear lumped mass parameter system.
- The excitation on the structure are stationary and can be modeled using Gaussian white noise.
- The measurements are provided to our hands by *ANR-URBASIS* and were assumed to be carried out as carefully as possible.
- The data analysis is based on the Random Decrement Technique.
- The goal of carrying out a vibration test is to identify the modal parameters.
- The modal parameters of concern are only the natural frequency and the damping ratio.
- The investigations in this thesis are based on both simulated and real-world ambient vibration data.
- The simulated data are modeled by a Timoshenko beam model. [2]

Taking into account the needs identified in the this chapter, and the aforementioned delimitations of this thesis within *ANR-URBASIS* project, this thesis aims the achievement of the following main objectives:

✓ development, implementation and validation of signal processing algorithms to provide automatic, accurate and robust estimates of the modal parameters, namely the natural frequency and the damping ratio, from data collected of high-rise buildings excited by ambient vibrations at the ground level;

✓ conception and implementation of long-term dynamic monitoring algorithm in relevant high-rise buildings to automatically and continuously estimate the variations of the natural frequencies and the damping ratios.

[2] The Timoshenko beam model is explained in details in chapter 4.

2.6 General view of the proposed approach

In view of providing a fully automated approach for vibration-based structural health monitoring, it is a challenge to fully automate the two steps of the output-only modal analysis presented in Fig. 2.3: (1) the estimation of the free-decay signature, and (2) the extraction of the structural modal parameters based on the estimated free-decay signature. The proposed approach of this thesis should, therefore, make the effort to overcome the typical drawbacks of the available automated methods. The approach should not be restricted to single degree of freedom systems, *i.e.*, it should deal with multi-mode ambient vibration signals, it should also take into consideration the estimation of the damping ratio modal parameter, and should strongly consider the closely-spaced frequency modes. It should be highly capable of distinguishing the true modes from the noisy ones without requiring any user interaction.

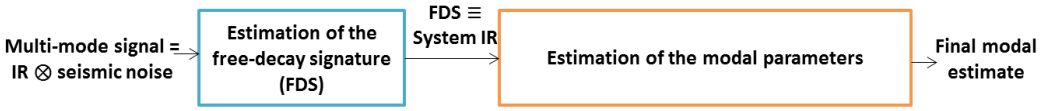

Figure 2.3: The general overview of the two steps of the output-only modal analysis.

For the estimation of the free-decay signature and as a part of *ANR-URBASIS* we chose to use the Random Decrement Technique. Usually, the multi-mode ambient vibration signal is passed through a narrow-band filter before being random decrement processed. Needless to mention that the filtering process hinders the automatic process of the modal parameter estimation. Thus, the proposed approach should avoid the filtering process prior to the RDT analysis.

As for the modal parameter estimation, and as we are taking into consideration the closely-spaced frequency modes, without any filtering processes that might destroy the free-decay signature, so the proposed approach should solve this problem.

In brief, the proposed approach of this thesis should be able to automatically and simultaneously estimate the natural frequencies and moreover the damping ratios of all the modes in the multi-mode signal under study.

Chapter 3

Filter-Free Random Decrement Technique

Contents

THE purpose of this chapter is to give the background and the motivation of using the Filter-Free Random Decrement Technique. So that it is a natural starting point in section 3.1 to give a general overview of the Random Decrement Technique itself, to present its mathematical background and to show its applicability over the signals that we consider in this thesis. The story behind the Filter-Free Random Decrement Technique is then listed in section 3.2. This section also presents the proposed signal model that is based on the Filter-Free Random Decrement Technique and consistent with the physical model that we consider in this thesis.

3.1 Random Decrement Technique

In the context of this work, we consider a physical model that shows a time-domain convolution of the force and the impulse response of the studied building. The latter is considered to be a linear and time-invariant system, where only its responses are measured. Such measurements are assumed to be stationary and distributed as Gaussian white noise. Based on all this, the main objective of this thesis is to provide a reliable and robust modal parameter

estimation, namely, the natural frequencies and moreover the damping ratios, for the data collected over high-rise buildings under ambient vibration excitation (*cf.*, section 2.5).

Concerning all the above, the first real challenge we encountered in this thesis is to find a method that is able to respect all the assumptions and delimitations of this thesis, and to meet all its objectives. Accordingly, the Random Decrement Technique (RDT) was found to have many reconciliations to the needs, assumptions and objectives of this work.

3.1.1 Description

The RDT has been described in various forms throughout literature, with almost all the forms revolving in the same context. To name but a few, H. Cole [Col68], the retriever of this method in the late 60's during his work in the analysis of the dynamic response of space structures subjected to ambient loads, introduced the RDT as a method to transform a random time series into a free-decay of the structure in question. The free decay, or the free decrement, only contains information of the structure and not the random loads. The modal parameters, especially the damping ratios, are extracted from this decrement. This is probably the explanation for the name given to the technique.

Yang and Dagalakis [YD80] stated that the RDT technique is well suited to the class of problems in which characteristics are desired of an in-service structure subjected to unknown excitation where analysis only require the measurement of the dynamic response of a structure and not the excitation.

Yang et al. [YDH80] mentioned that the method mainly analyzes the measured output of a system subjected to some ambient random input. The output of the analyzed signal which is independent of the input is the free vibration signature of the structure in question. The obtained response signatures or functions for different modes play an important role in detecting the early damage before the overall structural integrity is affected.

The technique was given a detailed mathematical basis later on by Vandiver et al. in 1982 [Van+82], who showed that it actually gives an estimate of the auto-correlation function of the system response rather than the impulse response function itself as it was previously believed.

Brincker et al. [BKJ91] said that the basic idea of this technique is to estimate the so-called Random Decrement Signatures (RDS) which can be used to characterize the stochastic time series.

Assmussen [Asm97] formulated that the RDT is a very simple, non-parametric technique, and easily implemented method for analysis of vibrations of structures loaded by stochastic forces.

Rodrigues and Brincker [RB05] presented the RDT as a time domain procedure where the structural responses to operational loads are transformed into an RDS which is proportional to

the correlation function of the system operational responses or can equivalently be considered as free vibration response. He as well introduced the several different ways to apply the RDT in operational modal analysis, at which this method could be used in modal parameter identification of the civil engineering structures. However to extract the modal parameters, this method should be accompanied by time domain or frequency domain method.

Antoni and El-Badawi [AEB11] identified the technique as a time domain blind identification technique which enables the modal parameter extraction of a system excited by unknown forces.

3.1.2 Development

The RDT was first proposed by Cole in late 60s [Col68] as an averaging method on time segments of a random time response. It was first used by Ibrahim [Ibr77] on 1977 for modal identification, and first given a detailed mathematical premise by Vandiver et al. on 1982 [Van+82].

As per Cole's words, the concept behind RDT lies in the fact that, when driven by a stationary input, the response of a linear system starting at time t_0 is composed of three parts: 1) the free response from the initial displacement at t_0, 2) the impulse response due to the initial velocity, and 3) a random component due to the load applied in the time following t_0. Therefore, if a sufficient number of segments with identical specific initial conditions are averaged, both the random and the impulse response will cancel themselves resulting in a free decaying response due to the predefined initial condition [Col68].

On 1977, it was shown that the result of the RDT is the free vibration of the system [Ibr77]. This claim was defeated later by [Van+82], they proved that the result of the RDT is a correlation function of the system.

On 1991 [BKR91] the RDT is used to estimate cross-correlation and auto-correlation functions of the system and then three different methods were investigated to identify the modal parameters. The speed and the accuracy of the RDT were compared with the Fast Fourier Transform (FFT) technique. According to [BKR91], RDT was 100 times faster than FFT. In estimating the auto-correlation of the system, RDT was also more accurate than FFT. However, FFT methods were more accurate than RDT in estimating the cross-correlation ones.

On 1997, Ibrahim et al. [IAB97] proposed the Vector-triggering Random Decrement to overcome the problems encountered from using the auto-correlation function alone, or the auto and cross-correlation of the system together for the modal analysis. In the former case, the phase data will be lost, hence the mode shapes could not be identified. In the latter case, the high noise level in the cross-correlation results in erroneous modal parameters. In the vector-triggering random decrement, the triggering conditions are defined by a vector which keeps the phase data. In the same year, Asmussen et al. [AIB97] investigated the application of the Vector-triggering Random Decrement technique to a four degree-of-freedom system as

well as to an experimental test of a bridge model.

Asmussen and Brincker on 1998 [AB98] proposed a method to calculate the variance of the random decrement signature, and fully studied the influential processing parameters of the RDT to estimate the free-decay signature. They also presented several sources of estimate uncertainties like noise, short or insufficient record length, low and variable excitation. Following [AB98], the averaging feature of the RDT plays a significant role in minimizing the estimate uncertainties under a condition of having a sufficient number of averages.

Asmussen [Asm97] has provided a thorough literature of the use of the RDT in output-only modal analysis up to 1997. After that year the RDT has continued to be extensively used, for example [RBA04, BR05, SS10, AEB11, Mik+13, Gue+14]

3.1.3 Concept

The RDT was developed by H. Cole at NASA during the late 1960s [Col68, Col71b, Col71a, Col73]. Cole's main aim was to provide "*a simple and direct method for translating the time history into a form meaningful to the observer*" [Col68].

Driven by the motive of online failure detection via monitoring the damping of a structure that is excited by white noise, which is difficult to be measured, Cole proposed a process of averaging several time segments possessing the same initial conditions to obtain a free decay. This description summarizes the concept of the RDT.

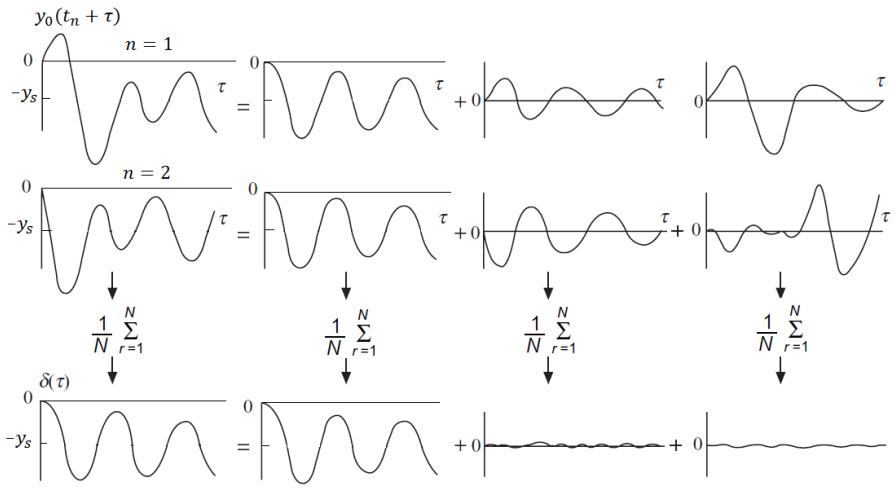

Figure 3.1: Hypothesis on Random Decrement Signature [Col73]. Cole refers to $y_0(t_n + \tau)$ as the ambient vibration measurement, and to τ as the segment length, to y_s as the triggering condition, and to $\delta(\tau)$ as the estimated RDS.

It has been shown in section (2.3) that the response of a building to a Gaussian white noise excitation is theoretically equal to the time domain convolution of force and impulse response function (*cf.*, Eq. (2.2)). According to Cole, when an enough large number of selected

segments from a sufficiently long time history of random response measurement possessing the same initial conditions are averaged, the random part of the response averages out to zero, and only the free decay (or the impulse response) survives (Fig. 3.1). This free decay is known as the Random Decrement Signature.

The detailed derivations of this technique are beyond the scope of this work. The interested reader is invited to refer to [Van+82] for more mathematical details.

Consider a discrete response time history $y[n]$, the discrete RDS $s[n]$ is then defined as the mean value of the stochastic process on the condition T_y.

$$s[n] = E[y[n + n_i]|T_{y[n]}], \tag{3.1}$$

where $y[n + n_i]$ refers to the process from which the mean value is calculated. $T_{y[n]}$ refers to the conditions that should be fulfilled.

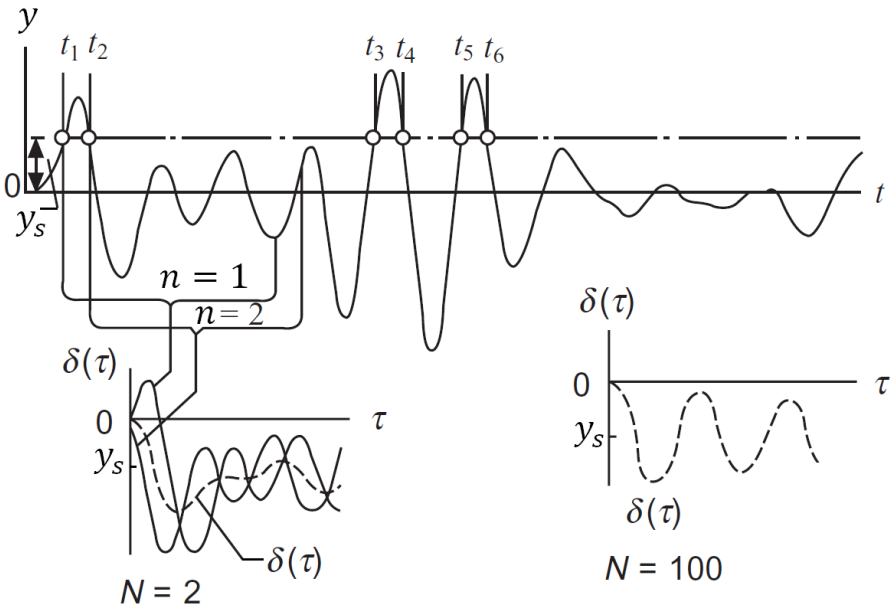

Figure 3.2: Evolution of a Random Decrement Signature [Col73]. Cole refers to $\delta(\tau)$ as the estimated RDS, N as the number of segments stacked and averaged and y_s as the triggering condition.

By assuming that the stochastic process $y[n]$ is not only stationary but also ergodic, $s[n]$ could be estimated as follows

$$s[n] = \frac{1}{N}\sum_{i=1}^{N} y[n + n_i]|T_{y[n_i]}, \tag{3.2}$$

where N is the number of points in the process which meets the triggering condition $\forall i \in [1, N]$, $y[n + n_i]$ is an ambient vibration measurement of duration n, n_i is the time instant verifying the initial conditions, and $T_{y[n_i]}$ is the triggering condition. Such a condition could be

considered in different ways for the evaluation of the RDS. Obviously, the formulation of the triggering condition controls the actual number of the triggering points N. An illustration of the process of estimating the RDS is shown in Fig. 3.2.

3.1.4 Triggering conditions

This section introduces the most well-known types of triggering conditions. The mathematical results, as mentioned earlier, are not derived but only presented.

The different triggering conditions $T_{y[n]}$ of the RDT can be formulated as in Asmussen [Asm97],

$$T_{y[n]} : \{a_1 \leq y[n] < a_2, b_1 \leq \dot{y}[n] < b_2\}. \tag{3.3}$$

where a_1, a_2, b_1 and b_2 are the triggering levels, and $\dot{y}[n]$ is the discrete time differentiation of the ambient vibration measurement $y[n]$.

As shown in Eq. (3.3), the triggering conditions can strictly specify either an amplitude or a slope level or both, leading to a variety of triggering conditions in the literature. Asmussen [Asm97] discussed the four most common triggering types according to the choice of the triggering levels a_1, a_2, b_1, and b_2.

Level Crossing ($T^L_{y[n]}$) This condition was firstly used by Cole when he first introduced the RDT [Col68]. It is the most fundamental and popular in the RDT application. It states that a triggering point is detected if the process crosses the chosen triggering level a as shown in Fig. 3.3 (a).

$$T^L_{y[n]} : \{a \leq y[n] < a + \Delta a, -\infty \leq \dot{y}[n] < \infty\}, \quad \Delta a \to 0. \tag{3.4}$$

Zero-Up Crossing ($T^Z_{y[n]}$) In this condition, a triggering point is detected if the process crosses the zero line with positive slope (Fig. 3.3 (b)).

$$T^Z_{y[n]} : \{0 \leq y[n] < 0 + \Delta a, 0 \leq \dot{y}[n] < \infty\}, \quad \Delta a \to 0. \tag{3.5}$$

Local Extrema ($T^E_{y[n]}$) In this type, a triggering point is detected if the time series has a local extremum (including both local minimum and local maximum) (Fig. 3.3 (c)). The levels a_1 and a_2 should be chosen to have equal signs in order to extract maximum information from each time segment.

$$T^E_{y[n]} : \{a_1 \leq y[n] < a_2, 0 \leq \dot{y}[n] \leq 0 + \Delta b\}, \Delta b \to 0. \tag{3.6}$$

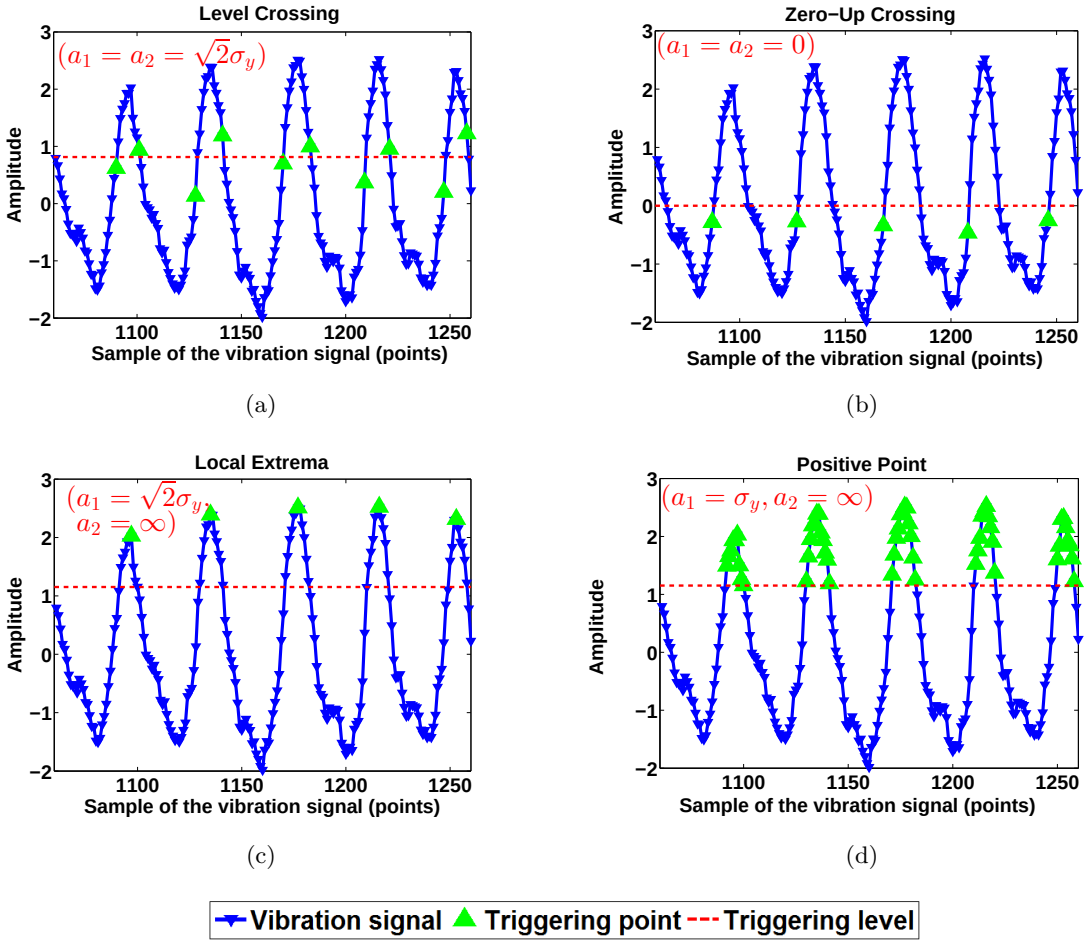

Figure 3.3: Illustration of the triggering levels for the four known triggering types on a simulated signal: (a) Level Crossing with $a = \sqrt{2}\sigma_Y$, (b) Zero-up Crossing with $a_1 = a_2 = 0$, (c) Local Extrema with $a_1 = \sqrt{2}\sigma_Y$,$a_2 = \infty$, and (d) Positive Point with $a_1 = \sigma_Y$,$a_2 = \infty$. σ_Y being the variance of the multi-component signal $y[n]$.

Positive Point ($T^P_{y[n]}$) This condition is perhaps the simplest of all triggering conditions since a triggering point is detected simply if the time series has a value in between two bounds a_1 and a_2 which are usually chosen to have equal (positive) signs (Fig. 3.3 (d)).

$$T^P_{y[n]} : \{a_1 \leq y[n] < a_2, -\infty \leq \dot{y}[n] < \infty\}. \tag{3.7}$$

3.1.5 Influential parameters

This section presents the three well-known processing parameters of the RDT that should be paid special attention while using the RDT. These parameters have high influence on the quality of the estimated RDS and thus on the estimation of the modal parameters.

Three main processing parameters of the RDT has been discussed in the literature: 1) The triggering levels, 2) the number of segments stacked and averaged, and 3) the length of the segment.

Asmussen [Asm97] illustrated that one of the difficulties in applications of the RDT is how to choose the triggering levels $[a_1,a_2]$ for a given triggering condition. Asmussen has pointed out that the optimal choice of such variable is referred to the choice which minimizes the variance of the RDSs normalized with the triggering level. Kijewski and Kareem [KK02] stated that although the triggering level has no direct effect on the variance, however, it will define the number of averaged segments. Clearly, this number should be large as much as possible to decrease the variance.

The explanation of Kijewski and Kareem [KK02] opens the discussion to another influential parameter in the RDT application. This parameter is the amount of data required to yield reliable estimates, or in other words, the required number of segments N to be stacked and averaged. As per Cole [Col68, Col71a, Col71b, Col73], this amount should be high enough for two reasons: (1) to completely remove the random part of the response, and (2) to decrease the variance normalized to N to the minimum possible. This amount, on the other hand, should not be so high in order not to higher the computation time of the RDT, nor to average out the important free decay part. Yang et al. [YDH80] for example recommended 400 to 500 segments, while others recommended at least 2000 segments like Tamura et al. [Tam+92].

The segment length is another influential parameter for the application of the RDT that was introduced by Cole [Col73]. He stated that the segment length is one of the parameters that truly influences the RDS, illustrating that it should be in the range of 10 times the period of the signal as a maximum length. It has been shown that the variance of the RDS normalized to the segment length increases with each period of oscillation [Van+82] as one moves further from the trigger condition. Thus, to achieve reliable results, the system identification should consider only the first few periods of the RDS.

3.2 Filter-Free Random Decrement Technique

3.2.1 Background and motivations

When the RDT was first proposed by Cole [Col68], it was not directly applied to a multi-component time series of the structural response, but was only based on a Single Degree of Freedom (SDOF) system. The data was necessarily filtered prior to the RDT application (*c.f*, Fig. 3.4).

However, it is well-known that filtering process is a critical step especially in situations where data are difficult to be analyzed, *i.e.*, low signal to noise ratio, closely spaced frequency modes, heavily damped modes, *etc.* Such situations are the characteristics of almost all the real-world signals that are known to have a large number of modes as well.

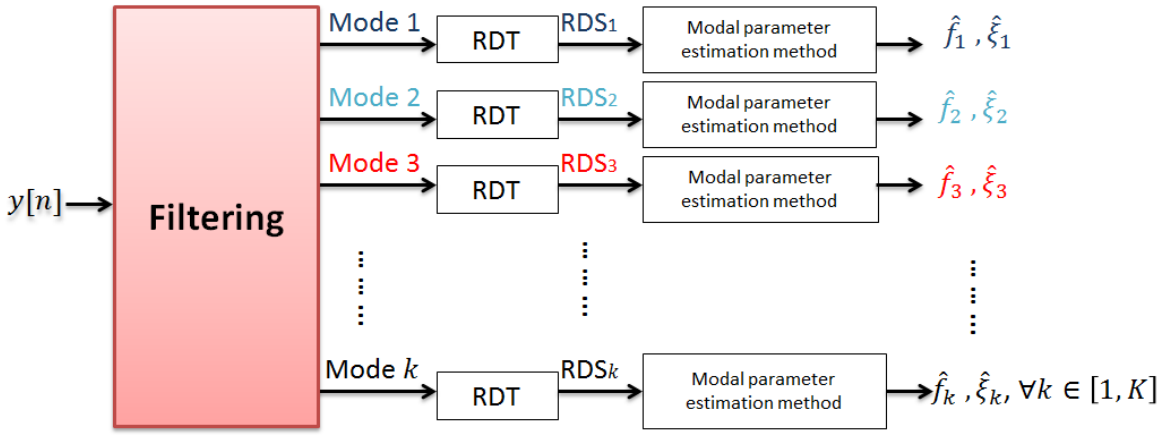

Figure 3.4: Illustration of the general concept of the Random Decrement Technique showing the filtering process as a preliminary necessary step prior to the RDT analysis over the multi-component signal in question ($y[n]$).

Accordingly, the filtering is one of the very delicate steps when dealing with the RDT. Tuning the filtering process manually is very time consuming, and it totally depends on the user.

We have made an attempt to automate the filter bandwidth setting [Nas+13]. This trail has facilitated the estimation process, and helped having reliable results. However, it doesn't rule out the user-know-how completely, as there are still several factors which require the user intervention, for example the choice of the filter type, and the filter order.

As the main objective of this thesis is to automate the estimation process of the modal parameters using the RDT, the first thing to think about is to skip the preliminary filtering process prior to the RDT analysis over multi-component signals. This concept is highly motivated by what was derived by Vandiver et al. [Van+82] on 1982. This is to say that under the conditions of a linear time-invariant system, if $y[n]$ is a SDOF system then the estimated RDS is proportional to its autocorrelation function $R_{yy}[n]$, then if $y[n]$ is a MDOF system then the estimated RDS is also proportional to the sum of all the autocorrelation functions of its modes $\sum_k R_{y_k y_k}[n]$, given that $y[n] = y_1[n] + y_2[n] + \cdots + y_k[n]$ with $y_k[n]$ being the response of mode k with all the modes being independent. Based on this fact, the procedure of skipping the preprocessing filtering process is thus applicable prior to the RDT analysis, and it has been called the Filter-Free Random Decrement Technique (FFRDT) (Fig. 3.5).

The originality of the Filter-Free RDT is its ability to: (1) avoid the difficulty encountered in the filtering process especially in situations where data are difficult to be analyzed, *i.e.*, low signal-to-noise ratio levels, closely-spaced frequency modes, and heavily damped modes, and (2) skip the required user intervention that definitely precludes the automatic estimation procedure.

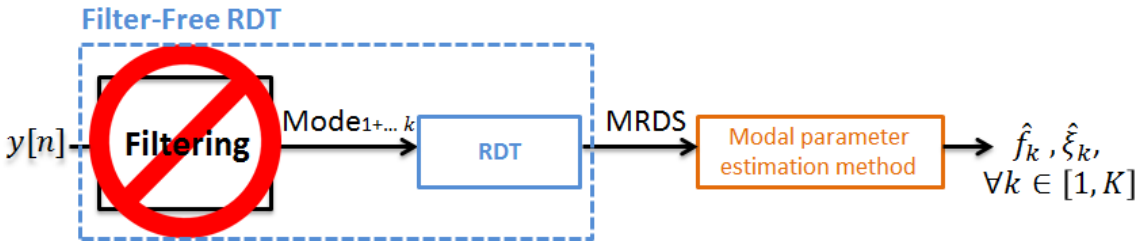

Figure 3.5: Illustration of the Filter-Free Random Decrement Technique.

The application of the RDT over multi-component signals without passing by the filtering process leads to the estimation of what we called the Multi-mode Random Decrement Signature referred to as an MRDS. Based on the latter, a signal model is proposed in this thesis as explained in the next section.

3.2.2 The signal Multi-mode Random Decrement Signature model

The measured building vibration $y[n]$ considered throughout this thesis is defined as in the physical model introduced in section (2.3) as

$$\begin{aligned} y[n] &= \mathfrak{g}[\mathfrak{n}] + e[n], \\ \text{where} \quad \mathfrak{g}[\mathfrak{n}] &= h[n] * p[n] \end{aligned} \tag{3.8}$$

$$\text{with} \quad h[n] = \sum_{k=1}^{K} A_{0k} \exp^{-2\pi f_k \xi_k n} \sin(\omega_{Dk} n + \phi_{0k}), \forall k \in [1, K], \tag{3.9}$$

where n is the normalized discrete time index, $\mathfrak{g}[\mathfrak{n}]$ is the noise-free part of the building vibration, $h[n]$ is the impulse response of a building. The initial amplitude ($A_{0k} = -1/\omega_{Dk}$) , the damping ratio (ξ_k), the natural frequency (f_k), the initial phase (ϕ_{0k}), and the number of modes (K) are the parameters that feature $h[n]$. $\omega_{Dk} = 2\pi f_k \sqrt{1 - \xi_k^2}$ is the damped pseudo-pulsation, $p[n]$ and $e[n]$ are the seismic and the additive noises respectively, both assumed to be a white Gaussian noise of zero mean and unknown variance. The convolution operator is $*$.

An RDS, regardless of whether it is a multi-mode or a single-mode, is characterized by having the same damping ratio ξ_k, natural frequency f_k and number of modes K as the impulse response $h[n]$ (Eq. (3.9)), but not the initial phase nor the amplitude because of the averaging principle of the RDT.

Considering all the above, the model of an MRDS $s[n]$ in this thesis is assumed as

$$s[n] = \mathfrak{h}[\mathfrak{n}] + v[n], \tag{3.10}$$

with

$$\mathfrak{h}[\mathfrak{n}] = \sum_{k=1}^{K} B_{0k} \exp^{-2\pi f_k \xi_k n} \sin(2\pi f_k n + \varphi_{0k}), \forall k \in [1, K], \tag{3.11}$$

where $v[n]$ is the residue of the RDT considered as an additive white Gaussian noise with zero mean and unknown variance. $\mathfrak{h}[\mathfrak{n}]$ is a deterministic multi-mode process that keeps the same characteristics as $h[n]$ of Eq. (3.9) but not for the initial amplitude B_{0k} nor the initial phase φ_{0k}. It should be noted that the term $\sqrt{1-\xi_k^2}$ of Eq. (3.9) is approximately equal to 1 in the considered model due to the fact that the range of the damping ratio in the real-world case is less than 10%.

The estimation of the modal parameters of the building vibration $y[n]$ (Eq. (3.8)) is achieved via those of the noise-free part $\mathfrak{h}[\mathfrak{n}]$ (Eq. (3.11)) of the MRDS model. To this end, a method that we have called an Automatic Model-Based Approach (AMBA) is proposed.

As we are taking into consideration the closely-spaced frequency modes without any filtering process so we proposed to use a method based on the Maximum-Likelihood Estimator (MLE). The MLE is non-linear and requires a stochastic optimization method for the parameter estimation. For this purpose, we proposed to use the Simulated Annealing technique which in turn requires an initialization of its parameters. For the latter end, we proposed a spectral-based initialization step. This step doesn't only initialize the parameters of the MLE, but also serves at automatically defining the number of modes in the estimated MRDS.

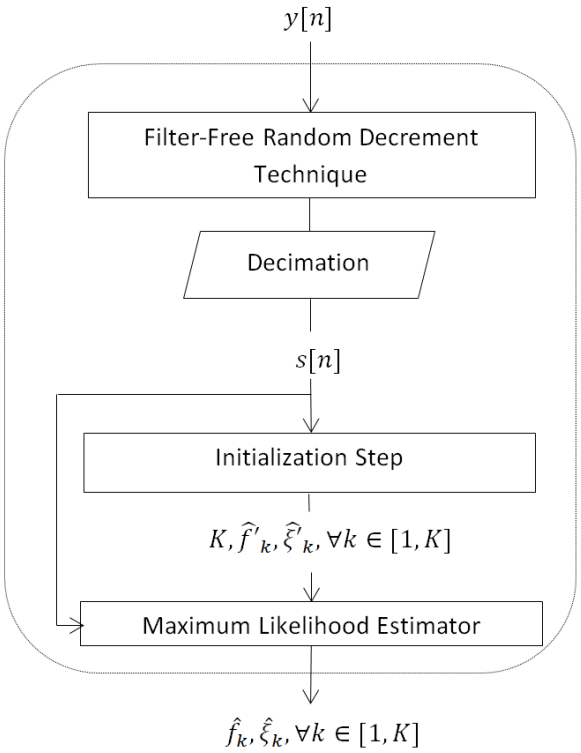

Figure 3.6: Global flowchart of the proposed approach. The approach starts by applying a FFRDT over $y[n]$. Given the MRDS $s[n]$, the approach defines the number of modes $\hat{K}$ via an initialization step followed by a non-biased estimation of the frequencies $\hat{f}_k$ and the damping ratios $\hat{\xi}_k$ via a Maximum-Likelihood Estimator.

In summary, the main steps of the proposed AMBA are illustrated in Fig. 3.6. This figure

sums up the entire estimation in three main steps:

1- Filter-Free Random Decrement Technique;

2- Initialization;

3- Maximum-Likelihood Estimation.

The last two steps of this proposition are explained in chapters 4 and 5 respectively.

The estimation process consists of determining the vector of parameters, $\boldsymbol{\theta}$, of the dimension $4 \times k$, and defined as

$$\boldsymbol{\theta} = [\boldsymbol{\theta}_1^T, \cdots, \boldsymbol{\theta}_k^T] = [B_{0k}, \xi_k, f_k, \varphi_{0k}]^T, \forall k \in [1, K], \tag{3.12}$$

where ^{T} is the transpose symbol, and B_{0k}, ξ_k, f_k and φ_{0k} are the initial amplitude, the damping ratio, the natural frequency, and the initial phase of the k^{th} mode respectively.

Under the following conditions;

$$B_{0k} > 0, \quad \xi_k > 0, \quad 0 < f_k < \frac{F_s}{2}, \quad \text{and} - \pi < \varphi_{0k} < \pi. \tag{3.13}$$

where F_s is the sampling frequency of the signal under study.

3.3 Summary

In this chapter we have presented a Filter-Free Random Decrement Technique. As the name suggests, such a technique mainly skips the essential filtering process prior to the application of the Random Decrement Technique over multi-mode signals. The Filter-Free Random Decrement Technique leads to the estimation of the Multi-mode Random Decrement Signature. Based on the latter, a signal model is proposed in this chapter. This model is consistent with the physical model that we consider in this thesis. The modal parameters of the studied building can be thus estimated from the noise-free part of the proposed signal model.

Chapter 4

Spectral-based initialization step

Contents

IN this chapter, we present an automatic method for estimating the number of modes along with the natural frequencies and the damping ratios of the Multi-mode Random Decrement Signature that was described in Chapter 3. We call the estimation technique of this chapter as an initialization step. It serves to initialize the parametric step of the approach.

In this chapter, we firstly introduce the principle of the initialization step in section 4.1, with its two main blocks: 1) Frequency estimation in section 4.2, and 2) Damping ratio estimation in section 4.3. The chapter ends up with the application of this step over simulated signals in section 4.4. The latter section also includes a presentation of the continuous beam model used to simulate the signals, as well as a study of the influential RDT parameters that should be set for more reliable estimations.

4.1 Principle of the initialization method

The main objective of the initialization step is to estimate the number of modes in the MRDS under study, and to provide a rough estimation of the natural frequency and the damping ratio of each of the estimated modes.

In multi-mode context, the modes can be identified by finding the corresponding frequency. The damping ratios of each of the modes can be then calculated from the amplitude variations on the frequency mode. It is commonly known that the spectral analysis is a well-adapted tool to achieve such estimation.

In the context of our work, in order to keep the best frequency resolution of the spectral analysis and to minimize the data redundancy, we choose to take two segments of the MRDS. One segment at the beginning of the MRDS and one at the end. The two chosen segments have the same length $L_t = 2/3L_{rds}$, with 50% of overlapping (Fig. 4.1(a)). This is due to the fact that the segment length should be sufficiently long to guarantee the frequency resolution of the spectrum. Throughout the entire length of the MRDS, we assume that the damping ratio is constant. Accordingly, the use of two segments is enough.

To illustrate the concept of the initialization step, we simulated a signal by the continuous beam model described in section 4.4.1. The signal is of 180000 points length, sampled at 200 Hz, consists of three modes located at 1 Hz, 2 Hz, and 5 Hz and damped by 1%, 2% and 3% respectively. The filter-free RDT is applied over this signal, and the MRDS is estimated as in Fig. 4.1 (a).

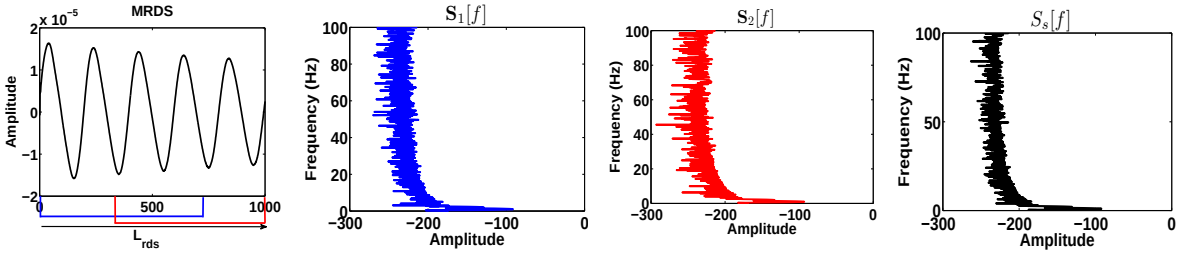

(a) (b) (c) (d)

Figure 4.1: (a) The MRDS is split up into two segments of equal length $L_t = 2/3L_{rds}$ with 50% overlapping, (b) and (c)the periodograms of the two segments respectively, (d) the estimated Welch spectrum averaged on $\mathbf{S}_1[f]$ and $\mathbf{S}_2[f]$.

We choose then to calculate a smoothed periodogram on each segment using a *Hamming* window to have more distinct frequency representation of the mode. The two applied windows are defined as $\mathbf{W}_1 = [0, 2/3L_{rds}]$ and $\mathbf{W}_2 = [2/3L_{rds}, L_{rds}]$ on the two segments respectively.

The windowing of the two segments yields two periodograms $\mathbf{S}_1[f]$ (Fig. 4.1 (b)) and $\mathbf{S}_2[f]$ (Fig. 4.1 (c)), from where the damping ratio is estimated. The averaging of $\mathbf{S}_1[f]$ and $\mathbf{S}_2[f]$ results in the estimated Welch spectrum $\mathbf{S}_s[f]$ (Fig. 4.1 (d)), from where the frequency is estimated.

4.2 Frequency estimation via an automatic peak-detection method

In order to be able to make a robust estimation of the number of modes of the MRDS, we need to develop a robust peak-detection method that is able to extract the peaks of interest from those due to the variance of the considered spectral estimator.

The detection of peaks with a fixed threshold as in [RMB07] becomes very difficult to be used over signals that present strongly modulated and damped amplitude. So we need a peak-detection method that is robust and moreover adaptive to such signals. Therefore, we propose to apply the iterative peak-detection process that was proposed by [Dur99] over the estimated Welch spectrum of $s[n]$.

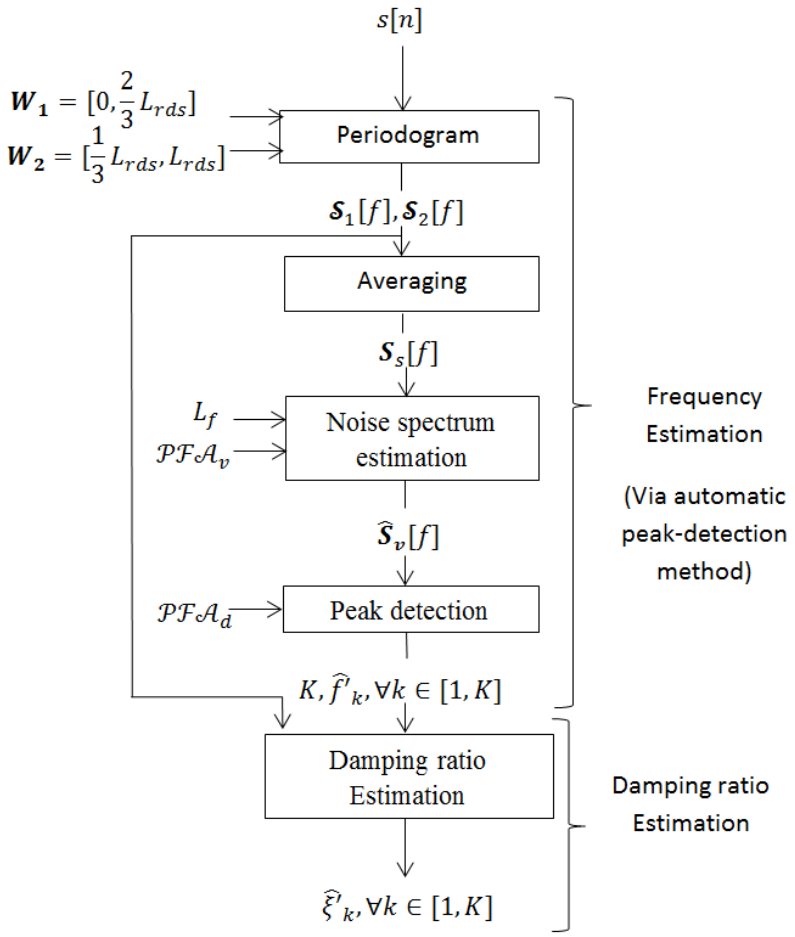

Figure 4.2: Decomposition of the "initialization step" block of Fig. 3.6

In section 4.2.1, we propose to construct a hypothesis test of Neyman-Pearson to detect the peaks of the spectrum $S_s[f]$. This test needs the noise spectrum to be estimated. In our work, it is estimated similarly to [Dur99] by a P-pass filter and is denoted $\hat{S}_v[f]$. The estimation process of the noise spectrum is described in section 4.2.2. The complete initialization

algorithm is shown in Fig. 4.2.

4.2.1 Hypothesis test for the detection and removal of peaks

A peak detection method associated with the statistical properties of the spectrum estimator must allow for an automatic interpretation of the spectrum contents.

The spectrum of s[n] of Eq. (3.10) can be expressed as

$$\mathbf{S}_s[f] = \mathbf{S}_\mathfrak{h}[f] + \mathbf{S}_v[f], \tag{4.1}$$

where $\mathbf{S}_\mathfrak{h}[f]$ is the spectrum of the noise-free part $\mathfrak{h}[\mathfrak{n}]$, and $\mathbf{S}_v[f]$ is the spectrum of the random part $v[n]$. The purpose of the detector is to decide for each frequency f of the spectrum $\mathbf{S}_s[f]$ whether $s[n]$ consists of only noise $v[n]$, or the sum of $\mathfrak{h}[\mathfrak{n}]$ and the noise $v[n]$. For that purpose, a statistical test between the two hypotheses can be written as

$$T[f] = \frac{\mathbf{S}_s[f]}{\mathbf{S}_v[f]} \underset{\mathcal{H}_0}{\overset{\mathcal{H}_1}{\gtrless}} \lambda, \tag{4.2}$$

with $T[f]$ a random variable, λ the detection threshold, and the two hypotheses being defined as

$$\begin{aligned} \mathcal{H}_0 &: \mathbf{S}_s[f] = \mathbf{S}_v[f], \\ \mathcal{H}_1 &: \mathbf{S}_s[f] = \mathbf{S}_\mathfrak{h}[f] + \mathbf{S}_v[f], \end{aligned} \tag{4.3}$$

In this study, the probability density of $\mathcal{H}_1$ is unknown, so the spectral peak detector as proposed in [Dur99] is applied. Such a detection is based on the Neyman-Pearson test where the probability of false alarm $\mathcal{PFA}$ is given *a priori* to be able to fix the threshold λ such as

$$\mathcal{PFA} = \int_\lambda^{+\infty} p_{T(f)|\mathcal{H}_0}(x)dx, \tag{4.4}$$

$\mathcal{PFA}$ is likely to retain $\mathcal{H}_1$ while $\mathcal{H}_0$ is true. $p_{T(f)|\mathcal{H}_0} = \chi^r_2$ is the probability density of $T(f)$ under the hypothesis $\mathcal{H}_0$. Indeed, it has been shown in [Dur99] and [Mar11] that all the Fourier estimators under the hypothesis $\mathcal{H}_0$ can be considered proportional to a random variable following a χ^r_2 distribution of degree of freedom r, with r being dependent on the number of segments and their overlapping.

The noise spectrum $\mathbf{S}_v[f]$ is unknown and therefore must be estimated. Consequently, the quality of the detection depends, on the one hand, on a well-chosen $\mathcal{PFA}$, and on the other hand, on a good estimation of the noise spectrum.

In the complete approach (Fig. 4.2), this detection method is used twice with two different probabilities of false alarms. In estimating the noise spectrum, the peaks verifying the

hypothesis $\mathcal{H}_1$ should be removed by this statistical test with a probability of false alarm noted as $\mathcal{PFA}_v$ (*cf.*, section 4.2.2). In the peak detection, the test is applied with another probability of false alarm noted as $\mathcal{PFA}_d$ (*cf.*, section 4.2.3).

4.2.2 Noise spectrum estimation by P-pass filtering

The noise spectrum is uniquely associated with the random part of the signal (*cf.*, Eq. (3.10)). The estimate of the noise spectrum is important as the detection method is dependent on the noise spectrum of the estimated noise Eq. (4.2).

Two types of errors can be encountered in the estimation of the noise spectrum: the underestimation and the overestimation. In the first case, some of the modes can be wrongly identified as noise. In the second case, noise peaks could be considered as modes and cause false alarms. These two errors should be avoided in order to ensure the robustness of the approach.

The estimator of the noise spectrum extracts the random part of the spectrum by eliminating the deterministic one. There are a lot of methods in the literature that are proposed to estimate the noise spectrum. These methods are mainly of two types: (1) mono-pass filtering methods, (2) and multi-pass filtering methods. The former type extract the noise spectrum directly as the output of the nonlinear filter. We recall a few methods of this category, the median filter, and the percentile filter [Wan03], more complex mono-pass filters can also be found in [CB02].

However, a common drawback of the mono-pass filtering methods is that the quality of estimate is purely dependent on the nature of the estimator and the chosen parameters. For example, the median filter is highly dependent on the choice of the window length, despite of its simplicity, however, it tends to underestimate the noise spectrum. On the other hand, the percentile filter changes with different values of the percentile [Dur99].

Contrary to the mono-pass filtering methods, the multi-pass ones involve several steps. At the cost of a greater complexity, a good estimate by a multi-pass method is less dependent on the setting. In summary, the multi-pass filtering methods generally have the advantage of being robust and adaptive [FF99].

For all the aforementioned reasons, in this thesis we propose to estimate the unknown noise spectrum $\mathbf{S}_v[f]$ as $\hat{\mathbf{S}}_v[f]$ through an iterative process; namely, the P-pass filtering technique that was developed in [Dur99], and shown in Fig. 4.3.

4.2.2.1 Configuration

The first pass of the P-pass filtering technique is a median filter

$$\hat{\mathbf{S}}_1[f] = FILTER\{\mathbf{S}_s[f - \frac{(L_f - 1)}{2}, \cdots, f + \frac{(L_f - 1)}{2}]\}, \tag{4.5}$$

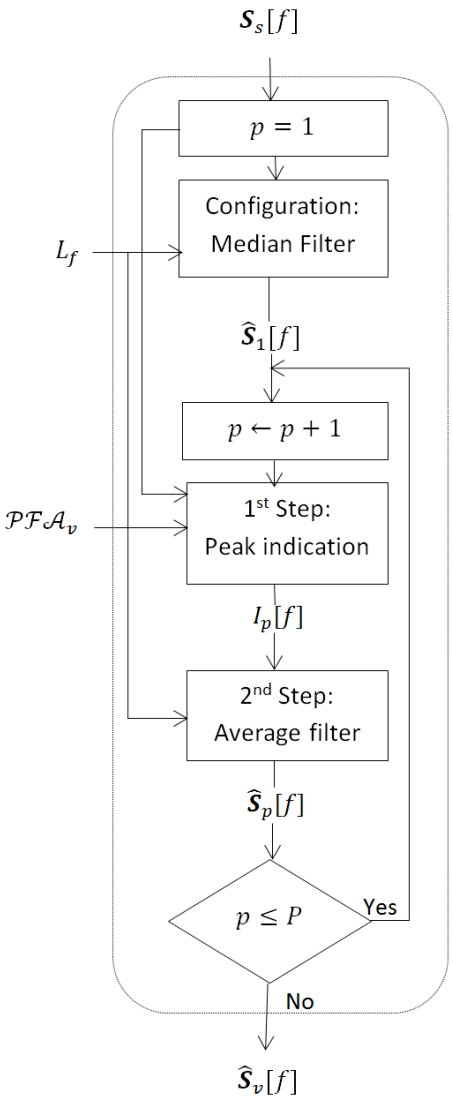

Figure 4.3: Decomposition of the block "noise spectrum estimation" in Fig. 4.2, done by a multipass filtering with P passes.

where $\hat{\mathbf{S}}_1[f]$ is the noise estimation of the first iteration, L_f is an odd integer specifying the length of the sliding filter window. Normally this length is defined as

$$3B(\frac{F_s}{f_{res}}) \leq L_f \leq 4B(\frac{F_s}{f_{res}}), \tag{4.6}$$

with B being the number of bins between the two zeros of the main lobe of the chosen window function, for $Hamming$ window $B = 4$. F_s is the sampling frequency of the signal, and f_{res} is the frequency resolution of the spectrum.

In the following $P-1$ iterations, the noise spectrum is refined at each iteration p with two steps given $p \in [2, P]$. In the first step, the peaks of $\mathbf{S}_s[f]$ are classified into two hypothesis

$\mathcal{H}_1$ and $\mathcal{H}_0$ by applying the hypothesis test described in section 4.2.1, with a probability of false alarm referred to as $\mathcal{PFA}_v$ and the most recent estimated noise spectrum $\hat{\mathbf{S}}_{p-1}[f]$. This step is explained in section 4.2.2.2.

The second step applies an average filter to $\mathbf{S}_s[f]$ by only using the part corresponding to the hypothesis $\mathcal{H}_0$ as explained in section 4.2.2.3. The refined spectrum is denoted as $\hat{\mathbf{S}}_p[f]$. The final noise spectrum $\hat{\mathbf{S}}_v[f]$ is the output of all the P iterations. The choice of the number of P is set to 3 to 5 iterations, since experimentally the noise spectrum stops changing after such a range.

4.2.2.2 Peak indication

From the estimated noise spectrum $\hat{\mathbf{S}}_{v_{p-1}}[f]$ in the pass $p-1$, we seek to compute a modified spectrum on which the detected peaks are removed and an average filtering is performed to update the estimated noise spectrum. Indeed, we must first indicate the peaks of the spectrum by the method described in paragraph 4.2.1 as

$$\mathbf{S}_s[f] \underset{\mathcal{H}_0}{\overset{\mathcal{H}_1}{\gtrless}} \lambda \times \hat{\mathbf{S}}_{v_{p-1}[f]}, \tag{4.7}$$

where λ is calculated with a probability of false alarm $\mathcal{PFA}_v$ only used during the estimation of the noise spectrum.

Then an indication function $I_p[f]$ is derived from 4.7 as

$$I_p[f] = \begin{cases} 0, & \text{if } \mathbf{S}_s[f] \text{ verify the hypothesis } \mathcal{H}_1 \\ 1, & \text{if } \mathbf{S}_s[f] \text{ verify the hypothesis } \mathcal{H}_0 \end{cases} \tag{4.8}$$

4.2.2.3 Average filtering of the peak-free spectrum

An average filter is then applied on the peak-free spectrum $\mathbf{S}_s[f] \times I_p[f]$ by

$$\hat{\mathbf{S}}_p[f] = \frac{\sum_{i=f-L_f}^{f+L_f} (\mathbf{S}_s[i] I_p[i])}{\sum_{i=f-L_f}^{f+L_f} I_p[i]}. \tag{4.9}$$

where L_f is an odd integer specifying the length of the sliding filter window and being defined as in Eq. (4.6).

4.2.3 Peak detection

As soon as the noise spectrum is estimated, the peaks of the spectrum $\mathbf{S}_s[f]$ can be calculated using Eq. (4.2) where

1- λ in Eq. (4.2) is deduced from another probability of false alarm $\mathcal{PFA}_d$ as in Eq. 4.4.

2- $\mathbf{S}_v[f]$ in Eq. (4.2) is substituted using the estimated noise spectrum $\hat{\mathbf{S}}_v[f]$ of paragraph 4.2.2.

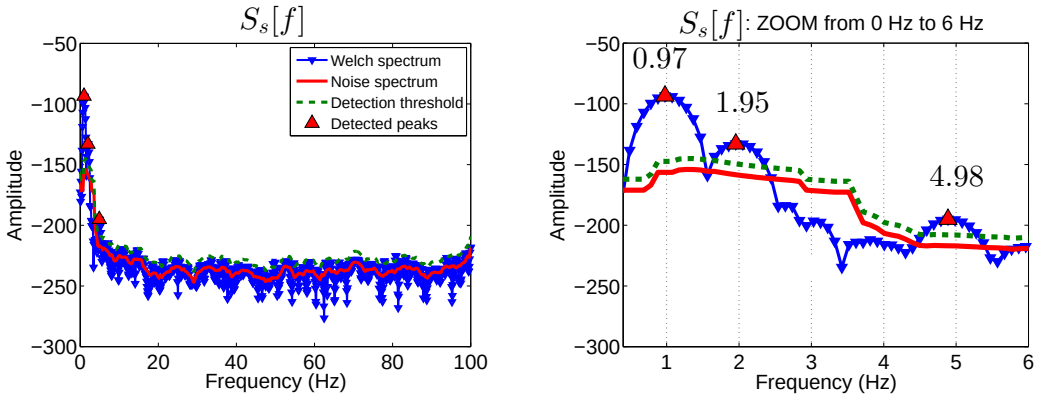

(a) (b)

Figure 4.4: Application of the peak detection method on the spectrum of Fig. 4.1, (a) the noise spectrum estimate and the detection threshold over Welch spectrum, (b) a zoom on the three detected modes with the theoretical values 1Hz, 2Hz, and 5Hz.

The peak detection is illustrated in Fig. 4.4 with the same simulated signal as in section 4.1. The detection threshold is calculated with a probability of false alarm $\mathcal{PFA}_v = 0.1$, and another probability of false alarm of the noise spectrum estimation $\mathcal{PFA}_d = 0.1$.

Fig. 4.4 presents the proper functionality of the frequency estimation of the initialization step, the three modes of interest are being correctly identified with reasonable frequency location as compared with the theoretical ones, with a normalized error $e_{\hat{f}'} = |f - \hat{f}'\,|\,/f \leq 0.03$ %. The estimated values of the frequency are presented in Tab. 4.1.

The detected frequencies are considered as the initialization results of the mode frequencies, and defined as

$$\{\hat{f}'\}, k \in [1, K]. \tag{4.10}$$

4.3 Damping ratio estimation

Hereby, we address the issue of estimating the damping ratio for all the estimated modes of the MRDS. The estimation is acheived using the ratio of the spectra of two neighboring segments over $s[n]$.

In section (4.1) we explained that $s[n]$ is analyzed over two segments. Hereinafter, each segment is expressed in the time-domain in a vector form as

$$\mathbf{s}_1 = [s[1], \cdots, s[\frac{2}{3}L_{rds}]], \tag{4.11}$$

$$\mathbf{s}_2 = [s[1 + \frac{1}{3}L_{rds}], \cdots, L_{rds}]], \tag{4.12}$$

where $\mathbf{s}_1$ and $\mathbf{s}_2$ are the MRDS on the first and the second segment respectively. Further on, $\mathbf{s}_1$ and $\mathbf{s}_2$ can be decomposed as the sum of modes

$$\mathbf{s}_j = \sum_{k=1}^{K} \mathbf{s}_{j,k}, \forall k \in [1, K], \tag{4.13}$$

where $j = 1, 2$ being an index to present the two vectors, and $\mathbf{s}_{1,k} = [s_k[1], \cdots, s_k[2/3L_{rds}]]$, and $s_{2,k} = [s_k[1+1/3L_{rds}], \cdots, s_k[L_{rds}]]$ are the RDS vectors of the mode k (Eq. (3.10)) over each segment.

For each segment j we have

$$\mathcal{FT}\{\mathbf{s}_j\} = \sum_{k=1}^{K} \mathcal{S}_{j,k}[f] = \mathcal{S}_j[f]. \tag{4.14}$$

At frequency f_k with

$$\mathcal{FT}\{\mathbf{s}_{j,k}\} = \mathcal{S}_{j,k}[f], \tag{4.15}$$

where $\mathcal{FT}\{.\}$ denotes the Discrete Fourier Transform, and $\mathcal{S}_{j,k}$ is the vector of the spectrum denoted as $\mathcal{S}_{j,k}[f]$.

Since if the power of the modes are independently distributed in the frequency-domain, then

$$\mathcal{S}_j[f_k] = \mathcal{S}_{j,k}[f_k]. \tag{4.16}$$

Therefore

$$\frac{\mathcal{S}_2[f_k]}{\mathcal{S}_1[f_k]} = \frac{\mathcal{S}_{2,k}[f_k]}{\mathcal{S}_{1,k}[f_k]}. \tag{4.17}$$

If we assume that the noise in the MRDS is sufficiently reduced, then according to Eq. (3.10), the estimation of the peak amplitude becomes

$$\frac{\mathcal{S}_2[f_k]}{\mathcal{S}_1[f_k]} = exp^{-\alpha \frac{1}{3} L_{rds}}, \tag{4.18}$$

where $\alpha = 2\pi f_k \xi_k$, with f_k and ξ_k being the frequency and the damping ratio of the MRDS for each mode k, $\forall k \in [1, K]$. For each detected peak at the two time instants $1/3L_{rds}$ and $2/3L_{rds}$ we estimate the damping ratio as

$$\hat{\xi}'_k = \frac{\log\left(\mathcal{S}_1[f_k]\right) - \log\left(\mathcal{S}_2[f_k]\right)}{2\pi f_k \frac{L_{rds}}{3}}. \tag{4.19}$$

In Tab. 4.1 we present the damping ratio estimated by the initialization step for each of the detected peaks of the signal in Fig. 4.4. The estimation for the three modes are in well accordance with the simulated values, 1%, 2%, and 3% for the three modes respectively. Their normalized error is very small $e_{\hat{\xi}'_k} \leq 0.18\%$, which indicates the proper applicability of the proposed initialization step (more verification is held in the next section 4.4).

Table 4.1: The estimated frequencies $\hat{f}'_k$ and damping ratios $\hat{\xi}'_k$, along with their normalized errors of each mode of the MRDS using the initialization step.

Mode	$\hat{f}'_k$	$e_{\hat{f}'_k}$	$\hat{\xi}'_k$	$e_{\hat{\xi}'_k}$
1^{st}	0.97	0.03	1.18	0.18
2^{nd}	1.95	0.025	1.85	0.07
3^{rd}	4.98	0.004	2.94	0.02

4.4 Application of the initialization step over simulated signals

In the context of this thesis we mainly consider the characterization of the vibrations of actual high-rise buildings. Indeed, the analytical investigation of vibrations of damaged building is a complicated problem. This problem may be simplified if a building can be represented in the form of a beam with corresponding boundary and loading conditions. Thus a question arises: to what type of beam can be associated a building? [CBH08].

As per Chesnais et al. words [CBH08], a great part of existing buildings were built before the definition of seismic codes. So the question of their seismic assessment is of first importance. The large number of buildings and the general lack of information make inappropriate the use of sophisticated computing methods. However, the experimental modal shapes suggest using continuous beam models to describe the first horizontal modes of vibration of usual regular buildings. The interest of such modelling lies in the efficiency of the analytical formulation for understanding the dynamics of a real structure. Applications concern as well prediagnosis as strategies of reinforcement. The shear beams and bending beams are the two

simple models usually considered in this approach. But can buildings behave differently? And how can we determine the more appropriate model for a given structure?

The next section responds to these questions in the sense that fits our problem. We mainly present a brief description of the Timoshenko beam model that we used to generate our simulated signals. No detailed mathematical derivations of this model is given, this is beyond the scope of this work. This model is provided to our hands by *ANR-URBASIS*. The interested reader in such details is invited to refer to [Bou+05, Mic07, Per+13].

4.4.1 Modeling of the building by Timoshenko beam

Simple models of the bending and shear beams are characterized by their frequency ratios which are respectively equal to $6.3, 17.5, 34.3, \cdots$ and $3, 5, 7, \cdots$. Due to the comparable stiffness of the floors and the walls, neither the bending component nor the shear one would dominate the behavior of structures. The continuous Timoshenko beam reflects these two types of behavior and allows for better modelling of buildings [Mic07].

Timoshenko beam is a representation for composing behavior in bending and shear behavior of a structure [Bou+05, Per+13]. C is the dimensionless parameter of the Timoshenko beam that characterizes the effects of bending versus shear, it is defined as

$$C = \frac{EI\pi^2}{4\mathcal{K}H^2}, \tag{4.20}$$

where EI is the bending stiffness, $\mathcal{K}$ is the shear stiffness, and H is the total height of the beam. The C parameter characterizes the structural system and its adherence to a particular building is very interesting to understand its dynamic behavior information.

Fig. 4.5 shows that the coefficient C can be determined only by the ratio $\frac{f_1}{f_2}$. Boutin et al. [Bou+05] found a good agreement between the values of C determined by the structural parameters and derived for building plans with those determined from the frequencies. According to these authors, the use of frequencies allows a better estimate of this parameter for existing buildings. The parameter C and the first natural frequency f_1 are therefore sufficient to calculate all the beam. It is then possible to determine the movement of the building for a given load. In the cases where no sufficient measures for determining a mode shape are realized, this beam model can be used.

Recall from the physical model that we consider in this thesis (*c.f.* section 2.3), for a given solicitation $U_s(t)$, the dynamic response $U^{tot}(t)$ of a model of discrete 1D beam is given by Eq. (2.2) and called Duhamel integral

$$\begin{aligned} \{U^{tot}(t)\} &= \{U_p(t)\} + \{U(t)\} \\ \{U(t)\} &= [\phi]\{y\}(t) \\ \forall k \in [1, N] \quad y_k(t) &= \frac{-p_k}{\omega_{Dk}} \int_0^t U_p''[n] \exp^{-\xi_k \omega_k[n]} sin(\omega_{Dk}[n]) dn. \end{aligned} \tag{4.21}$$

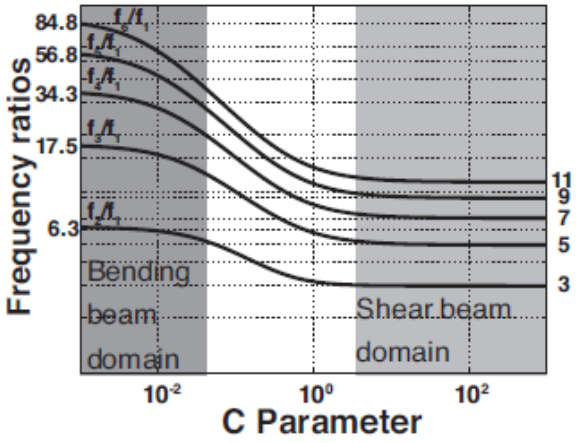

Figure 4.5: Frequency ratio as a function of the dimensionless parameter C for a continuous Timoshenko beam. The limits of this beam model are the bending and shear models [Mic07].

It only requires knowledge of the modal parameters (frequencies, mode shapes and damping ratio) and the participation coefficient p_k. It is this coefficient which determines the amplitude of each mode in the response of the structure. When the load is controlled (*Input-Output Modal Analysis*), this coefficient is directly obtained by the records. In the case of ambient vibrations (the context of this thesis), the discrete model allows estimation of the relevant participation coefficient under the condition of making an assumption on the masses of floors. It may be noted that if the mass of the floors is assumed to be constant, the participation coefficients p_k of each mode k no longer depends on the mass and defined as

$$p_k = \frac{\{\phi_k\}^T[M]\{1\}}{\{\phi_k\}^T[M]\{\phi_k\}} = \frac{\sum_{i=1}^{N} \phi_{ij}}{\sum_{i=1}^{N} \phi_{ij}^2}. \tag{4.22}$$

As part of this work, we assume that we have the least amount of information on the structure, as we are dealing with the problem of actual buildings. Besides, at each level of the continuous beam, an ambient vibration is generated as the dynamic response of this model which is excited by a ground solicitation assumed to be stationary Gaussian white noise.

4.4.2 Setting of the RDT parameters

While working with the RDT, one should not turn a blind eye towards its processing parameters. In this section we are mainly focused on the RDT parameters that are of high interest to physicists. The length of the ambient vibration signal that should be recorded comes primarily. As the physicists equip buildings with machines to record the vibrations, so it is very important for them to know the quantum required to be recorded of these vibrations to

assure reliable and robust estimations. They are mainly interested to know the amount of the necessary recorded data that is able to carry out the estimation to the fullest. Accordingly, the two parameters that we studied are the length of the recorded ambient vibration signal L_{sig} (points) and the length of the RDS L_{rds} (points).

4.4.2.1 Over SDOF systems

The study of this section is accomplished by simulating the response of a SDOF system with $K = 1$ in Eq. (3.9).

In the aim of evaluating the influence of the L_{sig} and L_{rds} parameters over the natural frequency f and the damping ratio ξ, a study is held on the number of periods in the vibration signal N_{sig} and the RDS N_{rds} which are deduced respectively from $N_{sig} = L_{sig} * R$ and $N_{rds} = L_{rds} * R$, with $R = f/F_s$ being the normalized frequency f per sampling frequency F_s.

In this study, N_{sig} ranges from 500 to 3700, because the number of periods of the recorded signal should be neither too long to prevent losing the time resolution of the signal, nor too short to assure it contains a large number of averaged segments that yield the exponentially decaying form. N_{rds} on the other hand ranges from 3 to 12 according to the suggested values in [Col68].

In order to estimate the accuracy of the estimation of the damping ratio ξ, for each configuration set (N_{sig}, N_{rds}), a Monte Carlo simulation of 100 noise realizations is held with:

- The normalized frequency $R = f/F_s$, with f and F_s being generated randomly as $F_s \sim \mathcal{U}(50, 300)$ and $f \sim \mathcal{U}(0.1, F_s/10)$, where $\mathcal{U}$ is a uniform distribution.
- The damping ratio ξ ranges from 1% to 5% to be consistent to the case of the actual buildings.

An estimated damping ratio is computed at each realization as $\hat{\xi}_k$ as in Eq. (4.19). The accuracy of the estimation is quantified by the error, the bias and the variance as follows

$$E = \frac{1}{D}\sum_{i=1}^{D}\frac{|\xi - \hat{\xi}_i|}{\xi}, \tag{4.23}$$

$$Bias = \frac{1}{D}\sum_{i=1}^{D}\frac{\xi - \hat{\xi}_i}{\sigma_\xi}, \tag{4.24}$$

$$Variance = \frac{1}{D-1}\sum_{i=1}^{D}(\xi - \bar{\xi}_i)^2, \text{with} \quad \bar{\xi}_i = \frac{1}{D-1}\sum_{i=1}^{D}(\hat{\xi}_i), \tag{4.25}$$

where ξ is the simulated damping ratio, D is the number of the noise realizations, $\hat{\xi}_i$ is the estimated damping ratio $\forall i \in [1, D]$, and σ_ξ, $\bar{\xi}_i$ are the standard deviation and the mean value of the simulated damping ratio respectively.

Only the results in terms of their error are presented in Fig. 4.6, since the bias and the variance are not significantly different for different configurations and are very weak in the order of 10^{-3} and 10^{-5} respectively. The influence of the configuration set up is distinguished by two groups of the damping ratio: (1) $\xi \leq 3\%$ (Fig. 4.6 (a)), (2) $3\% < \xi \leq 5\%$ (Fig. 4.6 (b)) since the influence of the parameters over the estimation is different in the two groups.

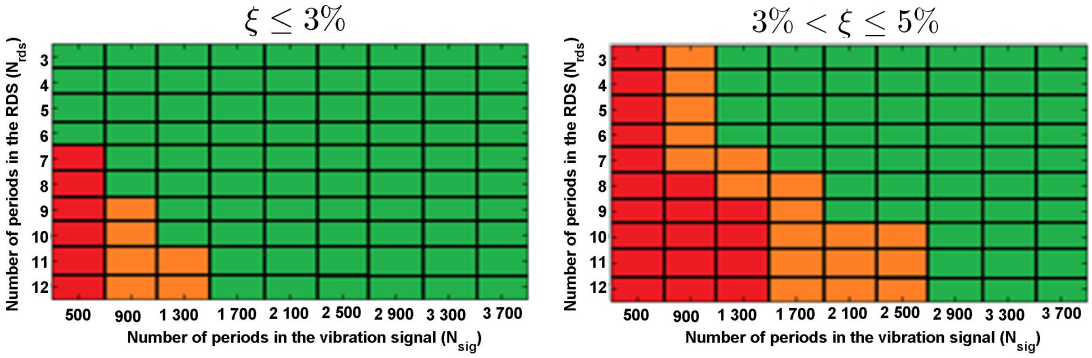

Figure 4.6: The estimated damping ratio error E of: (a) $\xi \leq 3\%$ and (b) $3\% < \xi \leq 5\%$. Good regions with $E \leq 10\%$ (green), intermediate regions with $10\% < E \leq 20\%$ (orange) and bad regions with $E > 20\%$ (red).

The green region shows an error of estimation $E \leq 10\%$, the orange region $10\% < E \leq 20\%$, and the red region $E > 20\%$. Accordingly, it is always recommended to be in the green region for acceptable damping ratio estimations in the context of this thesis. However, as the real-world signals are multi-mode, it is important to manage the parameter setting of the RDT when dealing with MDOF systems, a concept that is explained in the next section.

4.4.2.2 Over MDOF systems

When dealing with MDOF systems, as the case of the real-world signals, the parameters of the RDT (L_{sig} and L_{rds}) are set up by choosing R, N_{rds} and N_{sig} as follows:

- $R = min(\tilde{f})/F_s$, $\forall k \in [1, K]$ where $min(\tilde{f})$ indicates the minimum value of the detected peaks over the MDOF signal under study, thanks to an automatic peak detection method (this method is explained in chapter 4, section 4.2).
- N_{rds} is set from the recommended green region of Fig. 4.6.
- N_{sig} should be verified to respect the green region of Fig. 4.6. If it is not the sace, less reliable estimation results should be expected.

Once the configuration parameters are well chosen for the system under study, then our proposition of the initialization step could be safely applied over the multi-component signal in question. The extracted MRDS in this case is expected to be well estimated, and thus ready to hold the estimation process of the modal parameters.

4.4.3 Simulated signals: result analysis and discussion

Six 50-storey building models are simulated using the aforementioned Timoshenko beam model (section 4.4.1) to evaluate the effectiveness of the initialization step in: (1) defining a robust number of the modes of the signal in question, and (2) providing a rough estimation of a natural frequency and a damping ratio for each of the defined modes.

The acceleration response of the top floor of each of the simulated buildings is then computed and denoted Top_1 to Top_6 respectively. The simulated signals are categorized as: well-spaced modes, quasi-spaced modes, and closely-spaced modes as shown in Tab. 4.2. This is in the purpose of showing the applicability of the proposed initialization step in detecting the interested peaks under different categorizations.

Table 4.2: The simulated signals are denoted as Top_1, Top_2, Top_3, Top_4, Top_5, and Top_6, where f indicates the simulated frequency in (Hz) and ξ the simulated damping ratio in (%).

	Well-separated modes				Quasi-separated modes				Closely-spaced modes			
	Top_1		Top_2		Top_3		Top_4		Top_5		Top_6	
Mode k	f	ξ	f	ξ	f	ξ	f	ξ	f	ξ	f	ξ
1^{st}	1	1	1	0.5	0.4	1	0.4	0.5	1	1	1	0.5
2^{nd}	2	2	2	0.7	1.2	2	1.2	0.7	1.2	2	1.2	0.7
3^{rd}	5	3	5	1	2	3	2	1	NA	NA	NA	NA
4^{th}	7	4	7	1.5	NA	NA	NA	NA	NA	NA	NA	NA

All the six simulated signals are generated with a length of 360000 points, and a sampling frequency of 200 Hz. The application of the initialization step is tested under different signal-to-noise ratio levels (SNR) 0 dB, 9 dB, and 15 dB, as the existence of noise in the analyzed signal adds more challenge for the peak detection algorithm.

The Filter-Free RDT is applied over the multi-component simulated signals in question,the setting of the RDT parameter is done as explained in section 4.4.2.2. The estimated MRDS is then decimated to a Nyquist rate of 20 Hz to reduce the computation time. The triggering condition used in this section is the positive point type (*cf.*, section 3.1.4). Indeed, due to the high content of noise we chose to use the positive point triggering condition, so that sufficient triggering points are available. On the other hand, using triggering bounds close to zero might introduce false triggering points which increase the uncertainty of the estimated MRDS.

In order to describe the applicability of the proposed initialization step, a Monte Carlo procedure over 100 runs is applied.

The application of the initialization step, on the Welch spectrum of the MRDS of the six simulated signals is illustrated in Figs. 4.7, 4.8 and 4.9. The number of modes K of the MRDS $s[n]$ are estimated as the number of the detected peaks. In [Dur99] a spectral window matching technique is used to estimate the frequency of the peak; however, in this study, since only rough estimates are desired in the initialization step, the maximum of the bell shape is defined to be the position f of each peak.

Tab. 4.3 presents a summary of the number of periods of the MRDS (N_{rds}) chosen in the parameter setting of the FFRDT, the values of the probability of false alarm of both the $\mathcal{PFA}_d$ for the peak removal in the noise detection and the $\mathcal{PFA}_v$ for the peak detection, and the theoretical values of the location of each mode, along with the representation of each signal in its associated figure. It is worth noting that the choice of both $\mathcal{PFA}_d$ and $\mathcal{PFA}_v$ is empirical. In our case we have chosen them both to have the same value to keep the coherence between the peak elimination by $\mathcal{PFA}_v$ and the peak detection by $\mathcal{PFA}_d$. It should be noted as well that for the sake of clarity, the scale of the figures are not unified.

Table 4.3: The number of modes of interest, the SNR levels, the chosen N_{rds}, $\mathcal{PFA}_d$ and $\mathcal{PFA}_v$ for each of the six simulated signals (Top_1 to Top_6), along with the theoretical location of the modes f, and the figure that illustrates the peak detection process.

Simulated signal	No. of modes of interest	SNR level (dB)	N_{rds}	$\mathcal{PFA}_d$	$\mathcal{PFA}_v$	f (Hz)	Illustration in Fig.
Top_1	4	15	5	0.04	0.04	[1, 2, 5, 7]	4.7 (a)
		9	5	0.06	0.06		4.7 (b)
		0	5	0.09	0.09		4.7 (c)
Top_2	4	15	5	0.09	0.09	[1, 2, 5, 7]	4.7 (d)
		9	5	0.17	0.17		4.7 (e)
		0	5	0.15	0.15		4.7 (f)
Top_3	3	15	5	0.01	0.01	[0.4, 1.2, 2]	4.8 (a)
		9	5	0.1	0.1		4.8 (b)
		0	7	0.09	0.09		4.8 (c)
Top_4	3	15	5	0.01	0.01	[0.4, 1.2, 2]	4.8 (d)
		9	5	0.03	0.03		4.8 (e)
		0	7	0.02	0.02		4.8 (f)
Top_5	2	15	12	0.1	0.1	[1, 1.2]	4.9 (a)
		9	12	0.09	0.09		4.9 (b)
		0	12	0.1	0.1		4.9 (c)
Top_6	2	15	12	0.08	0.08	[1, 1.2]	4.9 (d)
		9	12	0.09	0.09		4.9 (e)
		0	12	0.08	0.08		4.9 (f)

When performing modal analysis, one of the key decisions that must be done upon starting to analyze the data is to decide how many modes are there in the frequency range of interest.

The red triangles mark the detected peaks in Figs. 4.7, 4.8 and 4.9. It happens sometimes that some peaks other than those of interest are detected as well, these peaks might be of

interest meaning in certain aspect. However, in the context of our thesis, we mainly consider the actual buildings that have a frequency range less than 10 Hz, so that our study is normally restricted to such a range.

In the example of the six simulated signals in this section, we can ignore all the detected peaks above the highest frequency mode in the signal, *e.g.*, for Top_1 all the detected peaks above 8 Hz are ignored. So that in the figures only the peaks marked with the green label are considered, otherwise they are ignored.

The N_{rds} for each of the six signals is chosen based on the category that this signal belongs to, *i.e.*, for the well-separated modes, an N_{rds} of 5 periods is enough to carry out the peak detection process, however, when the modes are getting closer and more contaminated in noise, *e.g.*, when an SNR is equal to 9 and 0 dB, the N_{rds} is chosen to be higher, 7 for the case of quasi-spaced modes, and 12 for the closely-spaced ones. Indeed, the frequency resolution gets better with longer analysis window, and thus allows identifying the closely spaced modes.

The estimated results of the mean frequencies and damping ratios for all the six simulated signals are shown in Fig. 4.10 and Fig. 4.11 respectively. The first bar for each mode represents the simulated value and the subsequent bars illustrate the result of the mean of the estimated values with the three different SNR levels 15 dB, 9 dB, and 0 dB respectively. Error bars representing one standard deviation are also shown.

The frequency estimate by the initialization step are more reasonable than those of the damping ratio estimate as compared to the theoretical values of each. The former present an error of utmost 10%, however the error of the latter sometimes reached to 30% especially when the SNR is 0 dB and the modes are closely spaced. This is in addition to the fact that the estimation of the damping ratio is more problematic than that of the frequency, there is another reason for the less accurate estimates of the damping ratios by a spectral-based methods like the initialization step. This reason is the short MRDS length that inhibits accurate estimation of damping, particularly for systems possessing closely spaced modes with high damping ($\xi \geq 3\%$) and high frequency. This length is restricted to be less than or equal to 12 periods, $L_{rds} \leq 12$, in order to maintain low variance of the estimated MRDS normalized to the MRDS length [Col73].

The powerful features of the peak detection method lend itself to convenient and accurate definition of the number of modes of the signal in question. Due to two false-alarm probabilities, the peak detection from the noise spectrum is relatively flexible. So as with the Hypothesis test that takes into account the properties of the estimator, the manual selection of the detection threshold is avoided. In addition, the estimated noise spectrum from the Welch spectrum ensures robustness of the peak detection method vis-à-vis the very low SNR level.

It is not the intention that the initialization step gives accurate estimation of the natural frequency and the damping ratio of these modes, only rough estimates are desired, the refinement of such estimates by the MLE step is explained in full details in Chapter 5.

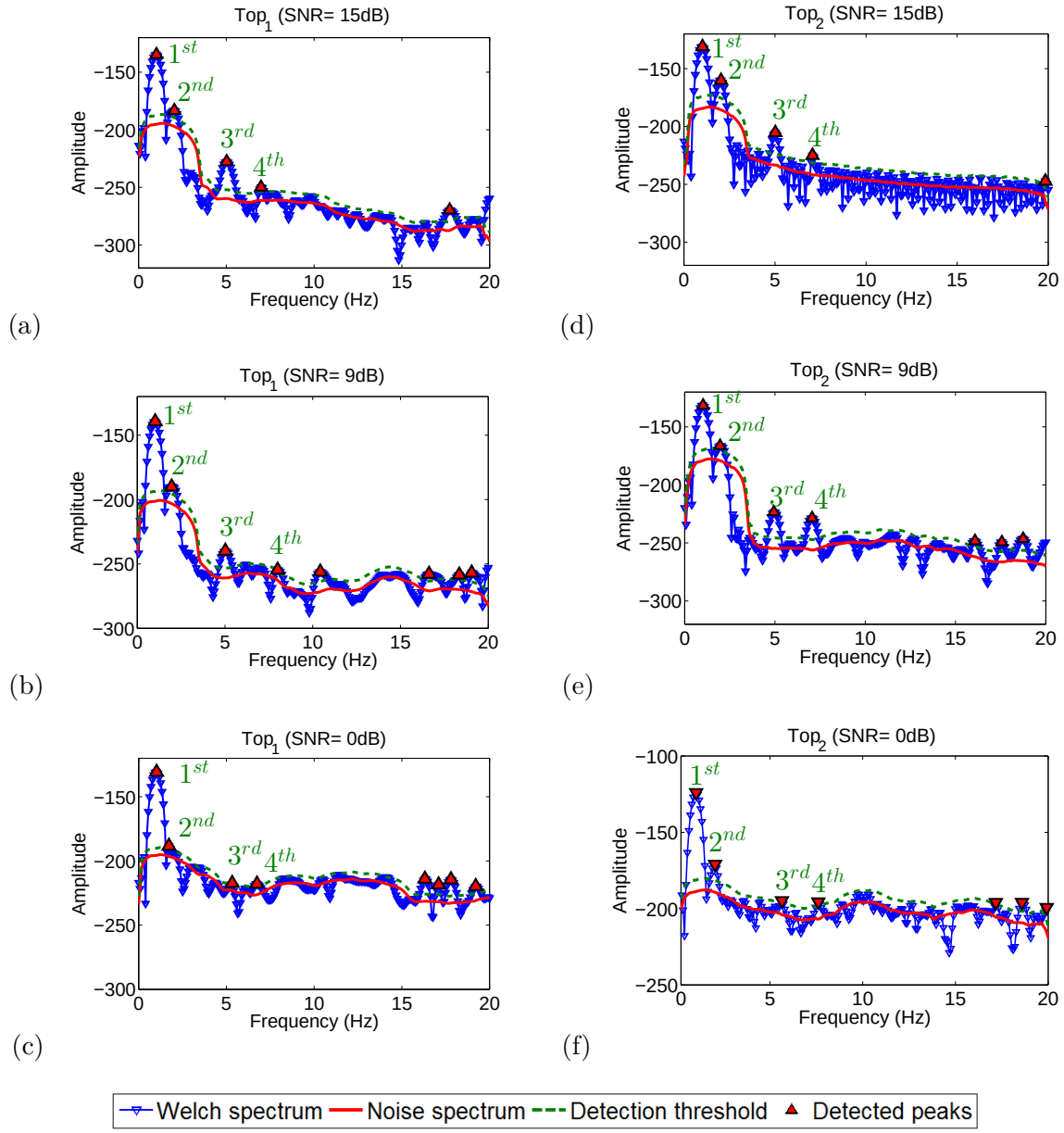

Figure 4.7: Application of the automatic peak detection method over the Welch spectrum of the MRDS of Top_1 with the SNR level of (a) 15 dB, (b) 9 dB, and (c) 0 dB, and over that of Top_2 with the SNR level of (d) 15 dB, (e) 9 dB, and (f) 0 dB. The modes of interest are labeled in green.

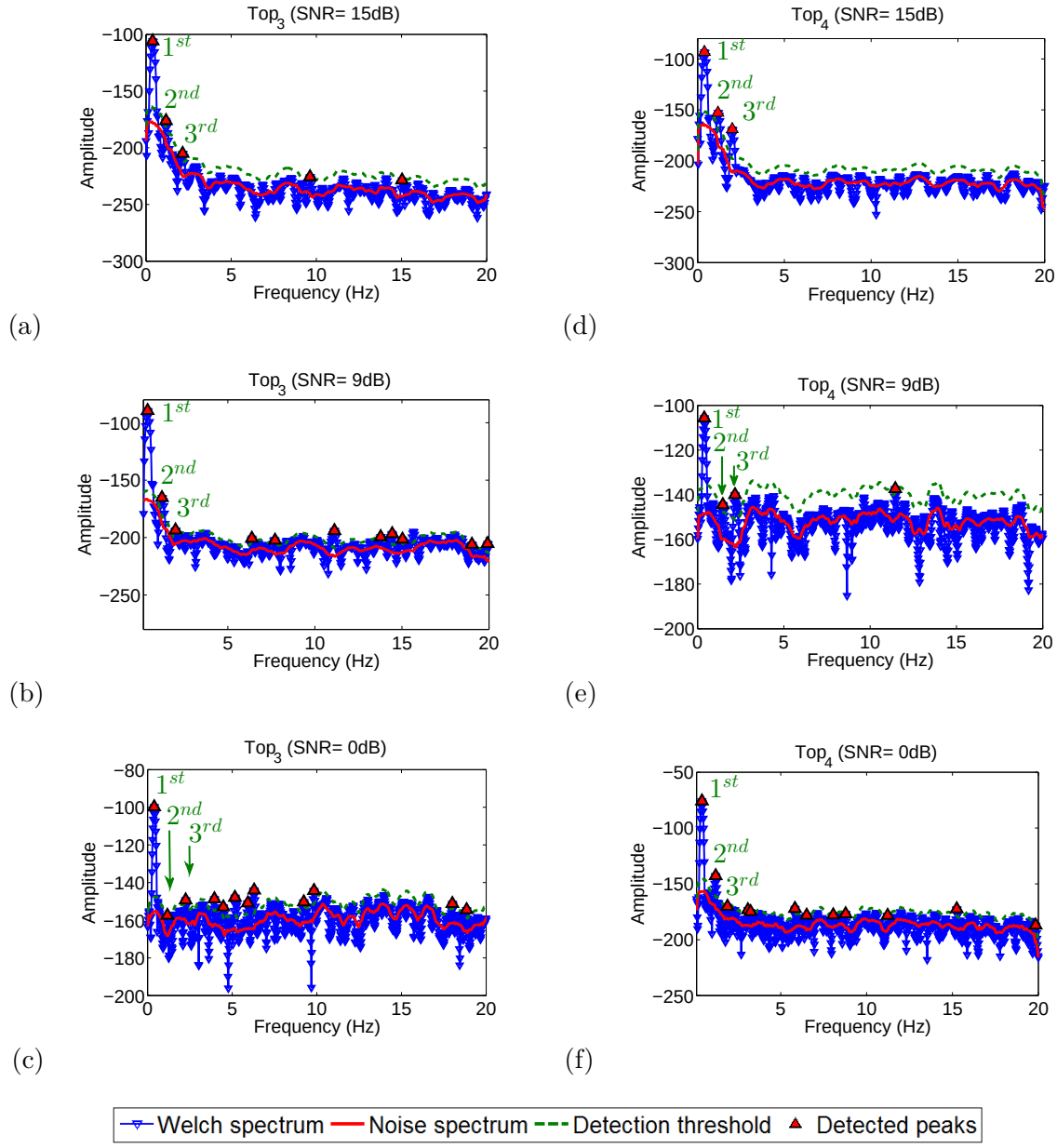

Figure 4.8: Application of the automatic peak detection method over the Welch spectrum of the MRDS of Top_3 with the SNR level of (a) 15 dB, (b) 9 dB, and (c) 0 dB, and over that of Top_4 with the SNR level of (d) 15 dB, (e) 9 dB, and (f) 0 dB. The modes of interest are labeled in green.

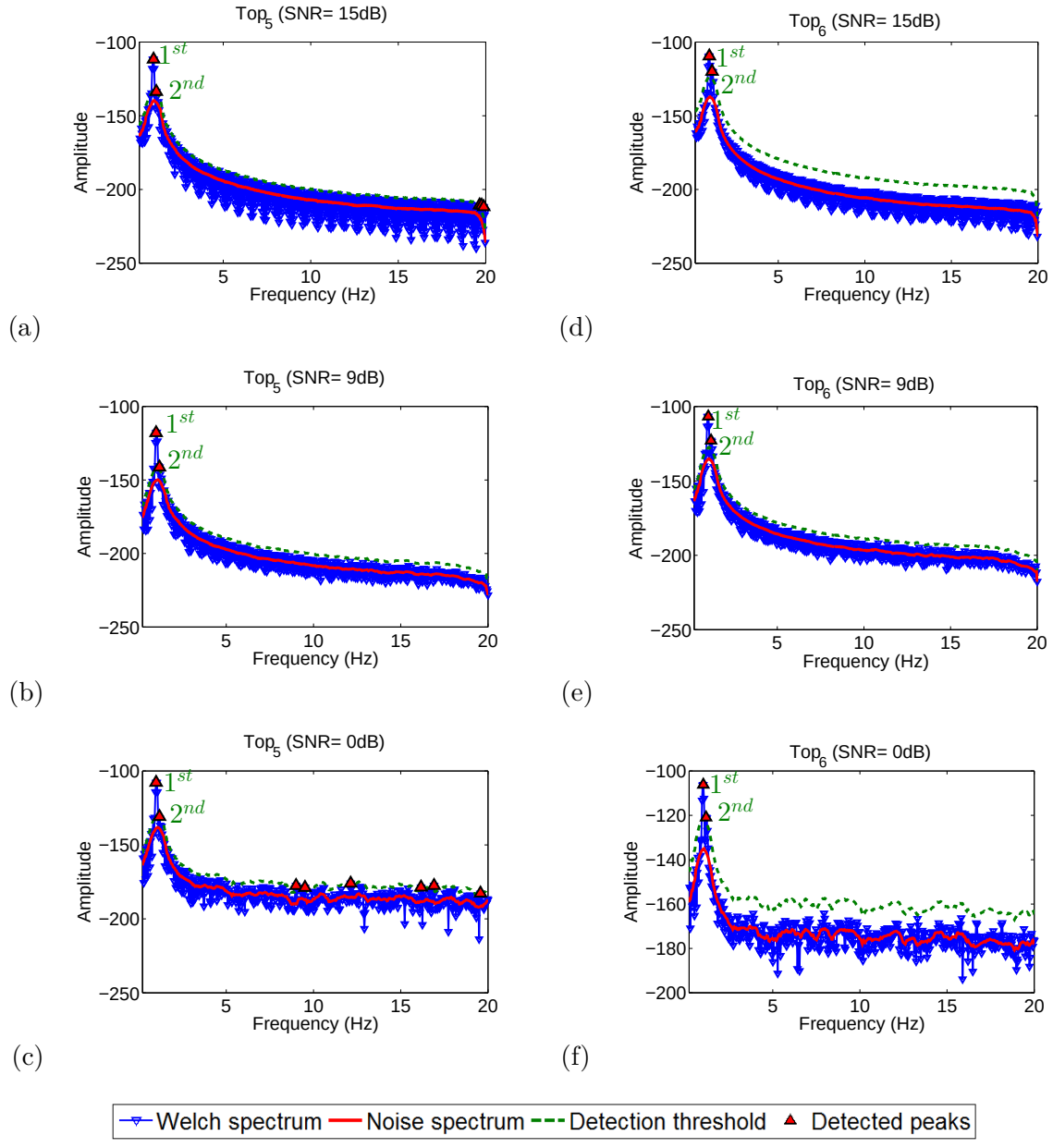

Figure 4.9: Application of the automatic peak detection method over the Welch spectrum of the MRDS of Top_5 with the SNR level of (a) 15 dB, (b) 9 dB, and (c) 0 dB, and over that of Top_6 with the SNR level of (d) 15 dB, (e) 9 dB, and (f) 0 dB. The modes of interest are labeled in green.

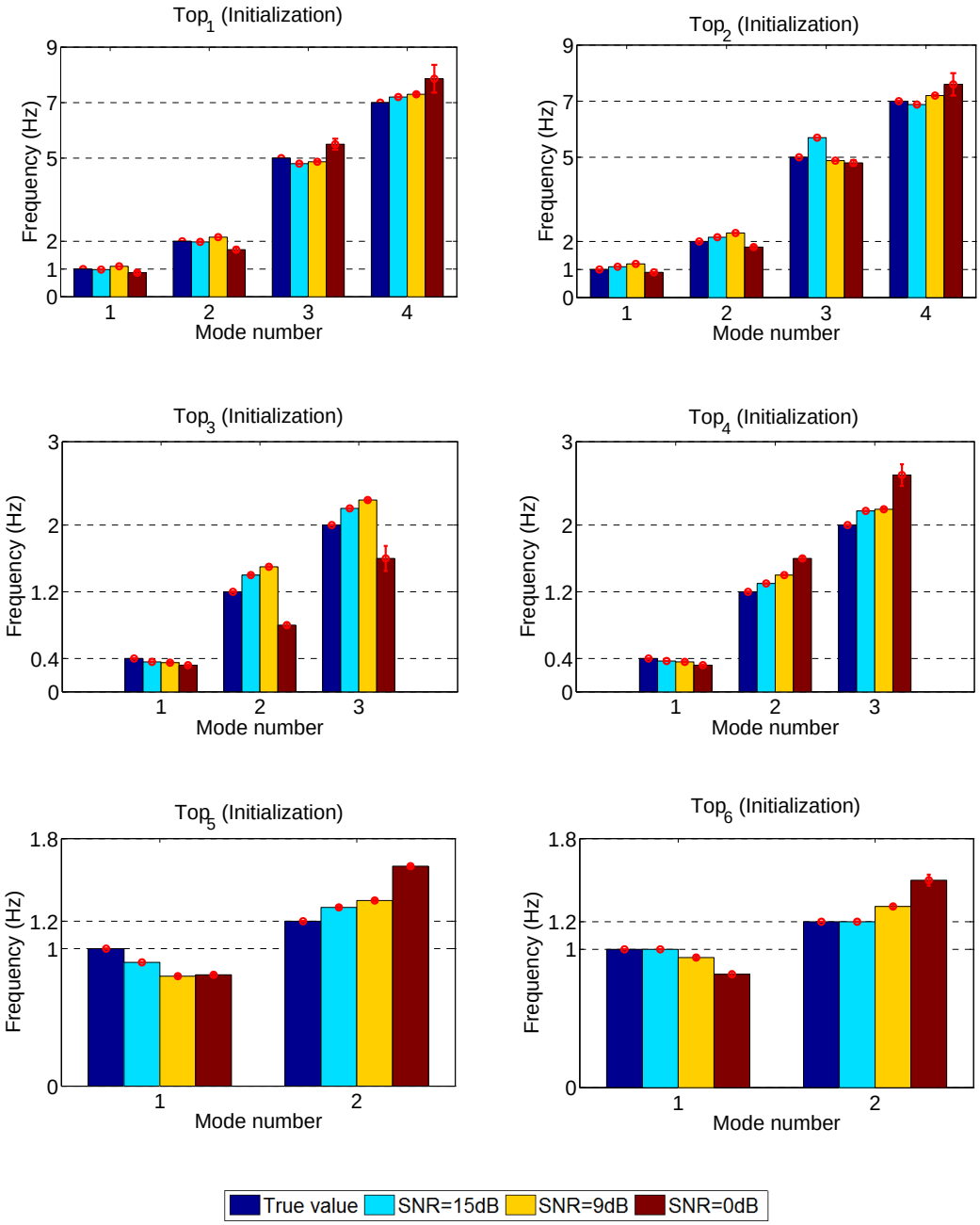

Figure 4.10: Mean frequency estimates by the initialization step for the three different SNR levels ($15dB$ blue, $9dB$ yellow, $0dB$ dark red), and their associated true values (dark blue), along with their standard deviations for Top_1 (top left) to Top_6 (bottom right).

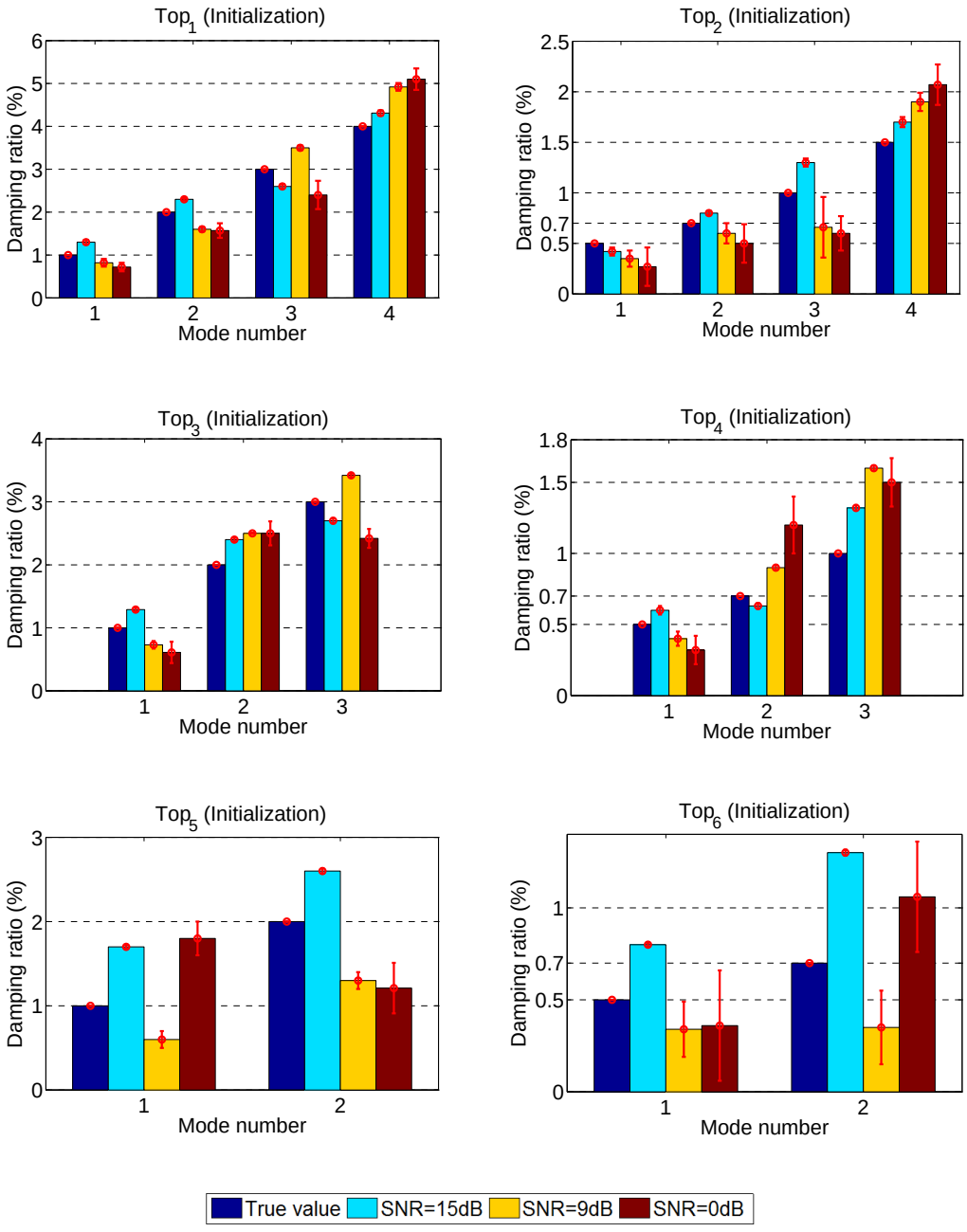

Figure 4.11: Mean damping estimates by the initialization step for the three different SNR levels ($15dB$ blue, $9dB$ yellow, $0dB$ dark red), and their associated true values (dark blue), along with their standard deviations for Top_1 (top left) to Top_6 (bottom right).

4.5 Summary

In this chapter, a spectral-based method is proposed. It is based on a Welch spectral estimation of the multi-mode Random Decrement Signature that was modeled in Chapter 3. The simulated results in this chapter showed that the initialization step is able to not only define the number of modes of the multi-mode Random Decrement Signature in an automatic manner, but also to estimate the frequencies and the damping ratios of all the defined modes simultaneously and automatically.

As to detect the peaks by the initialization step, an iterative peak-detection process is proposed to be used. This technique successfully works with the type of our signals that present strongly modulated and damped amplitudes.

The proposed method does not explicitly handle a robust modal parameter estimation, the latter are to some extent biased. Such estimation are enough to initialize the iterative step of our proposed approach, the Maximum-Likelihood Estimation process of the next chapter 5.

Chapter 5

Parametric Maximum-Likelihood Estimation Step

Contents

IN the previous chapter, we have proposed to roughly estimate the natural frequency and the damping ratio along with the number of modes of the signal model Multi-mode Random Decrement Signature via a spectral-based initialization step. In this chapter, we proceed to estimate the vector of parameters of this model $\boldsymbol{\theta}$ (Eq. 3.12) by a parametric Maximum Likelihood Estimator. Based on a stochastic optimization technique, called simulated annealing, we propose to maximize the likelihood function under the constraints of a positive amplitude and damping ratio, and a positive frequency belonging to a given frequency band.

Section 5.1 of this chapter is devoted to the procedure of maximum likelihood, while sections 5.2 to 5.4 focus on the description and analysis of the different parameters involved in the technique of simulated annealing. We present at the end of this chapter, the results over simulated signals in section 5.5.

5.1 Estimation by maximum likelihood

In this section we recall the expression and properties of the Maximum Likelihood Estimator (MLE) and its relationship with the least-square estimator.

Likelihood function

The basic idea of the MLE, as the name suggests, is to estimate the parameter vector $\boldsymbol{\theta}$ of a model by maximizing the joint density function $l(\boldsymbol{\theta})$, called likelihood function, for all the observations as

$$l(\boldsymbol{\theta}) = f(s[1], \cdots, s[L_{rds}]|\boldsymbol{\theta}), \tag{5.1}$$

where $\boldsymbol{\theta}$ is the parameter vector defined in Eq. (3.12).

The maximum likelihood estimator is then defined as

$$\hat{\boldsymbol{\theta}}_{MLE} = \underset{\boldsymbol{\theta}\in\mathbb{R}^{4k}}{\arg\max}\, l(\boldsymbol{\theta}). \tag{5.2}$$

Properties of Maximum Likelihood Estimator

The MLE is a standard approach to parameter estimation. It has many asymptotic properties in estimation: sufficiency (complete information about the parameter of interest contained in its MLE estimator); consistency (true parameter value that generated the data recovered asymptotically, i.e. for data of sufficiently large samples); efficiency (lowest-possible variance of parameter estimates achieved asymptotically); and parameterization invariance (same MLE solution obtained independent of the parametrization used).

Relation to least-squares estimation

Given that the noise is white and Gaussian, the maximization of the likelihood is equivalent to the minimization of the least squares (LS) [Jab+07]

$$\hat{\boldsymbol{\theta}}_{MLE} = \hat{\boldsymbol{\theta}}_{LS} = \underset{\boldsymbol{\theta}\in\mathbb{R}^{4k}}{\arg\min}\, LS(\boldsymbol{\theta}), \quad \text{with} \quad LS(\boldsymbol{\theta}) = \sum_{n=-L/2}^{L/2} |s[n] - \mathfrak{h}[\mathfrak{n};\boldsymbol{\theta}]|^2. \tag{5.3}$$

$LS(\boldsymbol{\theta})$ is the least-square function. $s[n]$ is the MRDS (Eq. (3.10)), $\mathfrak{h}[\mathfrak{n};\boldsymbol{\theta}]$ is the noise-free part of Eq. (3.10) where all its parameters are defined by $\boldsymbol{\theta}$.

We aim to find $\boldsymbol{\theta}$ that minimizes $LS(\boldsymbol{\theta})$ in order to find the optimum parameter set.

5.2 Stochastic optimization

The function to be minimized in this part is called the "objective function". Due to the non-linearity of the latter and to the constraints of our problem (Eq. (3.13)), the choice of the optimization method is crucial for the quality and the accuracy of the estimation.

In our case, the presence of the local minima of $LS(\boldsymbol{\theta})$: (1) makes it impossible to obtain an analytic expression of the estimator, because the traditional optimization technique

[Ste88, Bro70] such as gradient descent, the Gauss-Newton method, *etc.*, do not guarantee convergence to a global optimum; and (2) obliges the use of a stochastic optimization method.

The metaheuristic methods are the stochastic optimization methods that appeared in 1980s as generic heuristics, that is to say, extensible and / or adaptable to a large number of problems without any changes or major changes in the main structure of the algorithm.

These methods are iterative and therefore easy to implement and based on a random sampling of the objective function without the use of gradient information. Their main interest, compared to the conventional methods, lies in their ability to extract the global optimum. Indeed, during their iterations, the objective function is possible to accept a solution which deteriorates the objective function in order to escape a local optimum.

It is worth mentioning that such metaheuristic methods have some issues for the users to solve [Dré+03]: (1) The selection of the initialization point of the algorithm, and (2) The setting of the number of iterations and thus the execution time. These issues are more difficult to deal with in the case of non-linearity of the objective function and the presence of correlations between the parameters.

The choice of metaheuristic, its design and settings are therefor up to the user. These choices must adapt to the problems to achieve the optimum solution with acceptable accuracy at a reasonable computational time. For the context of our problem, we opted the method of simulated annealing based on the work of Jabloun [Jab+07].

5.3 Simulated annealing principle

The simulated annealing is proposed by Krikpatrick et al. [KGV83] as a new iterative optimization method that avoids being trapped in the local minimum. This method is, on the one hand, based on the Metropolis algorithm [Met+53] which allows to describe the evolution of a thermodynamic system, and on the other hand, is inspired by a process used in metallurgy. Technically, a material having a high initial energy is cooled by dosing the decrease of the temperature. The cooling should be gradual so that the equilibrium of the thermodynamic is established. Meanwhile, if local defects occur due to a rapid cooling, they are removed by local heating (annealing). By analogy with this physical process, the objective function is the energy of the system and the temperature is a fictitious parameter to be controlled.

The main steps of the simulated annealing are shown generally in Fig. 5.1. They include:

- **An initialization step** in which an initial solution is determined.
- **An iteration body** of Q iterations. Each iteration has two steps
  - **Candidate selection** for generating candidates (potential solution). This step is controlled by the temperature and the Metropolis acceptance rule.
  - **Control step** Controls the temperature and the candidate generation range.

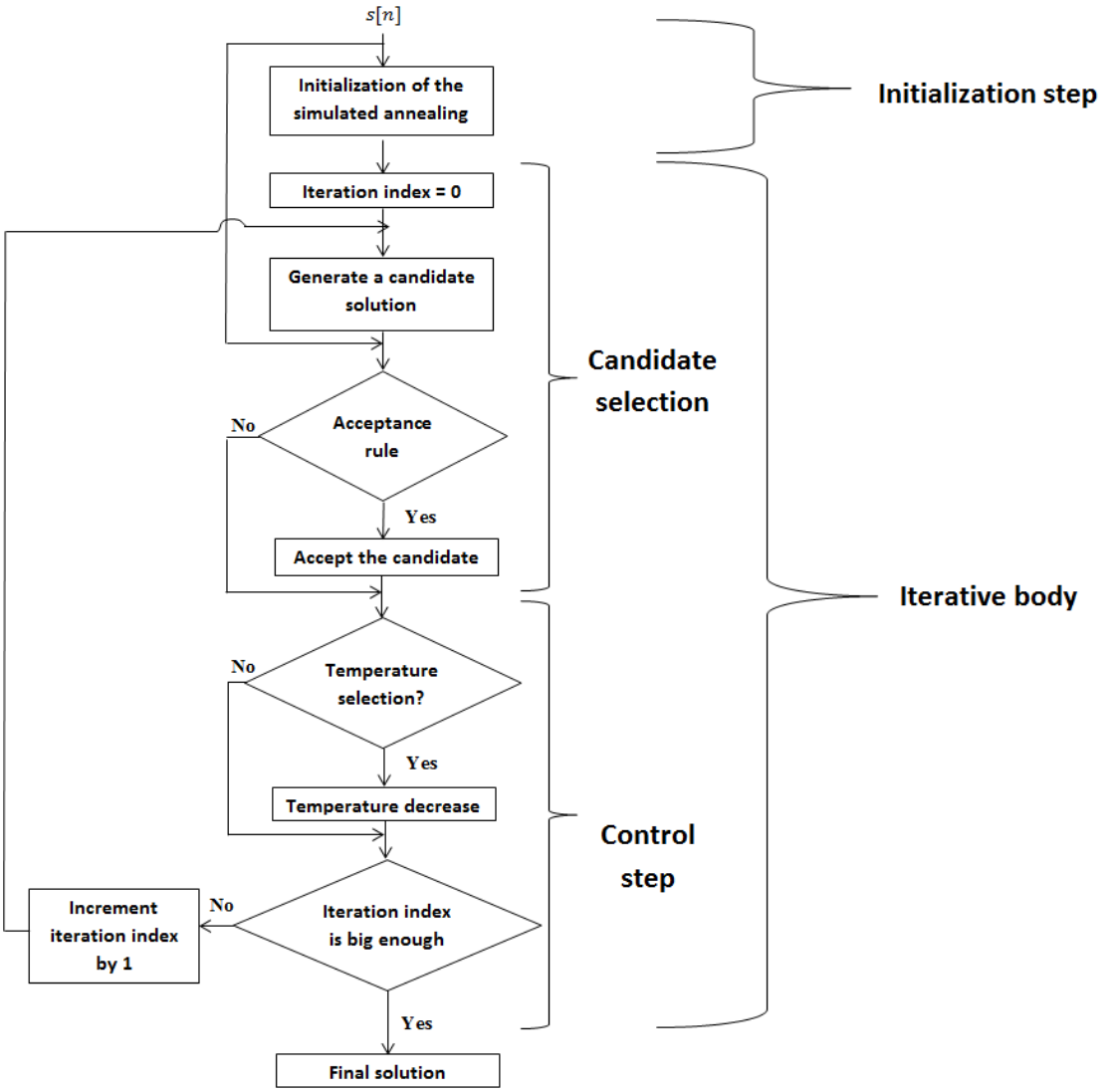

Figure 5.1: Flowchart of the simulated annealing technique

As regards the theoretical convergence of simulated annealing, it was established that the simulated annealing converges asymptotically to a global optimum under the following conditions [HS89]: (1) the reversibility, and (2) the connectivity of the search space. The former allows the return to a previous iteration of the solution, and the latter allows reaching any potential candidate solution from any other candidate solution for a finite number of elementary changes.

Under these conditions, the convergence is ensured regardless of the initialization state. Other conditions [AF87] have been studied as a function of the probability of acceptance. It was also shown that reliable initialization of the algorithm increases the probability of

convergence.

In the following we detail the two main steps of the simulated annealing and the necessary parameters for their operation.

5.4 Simulated annealing configuration

In this section, we explain on one hand the parameters needed to run the simulated annealing, and on the other hand, we specify the choice we have adopted to solve our problem (Eq. (5.2)).

5.4.1 Initialization step

A good initialization of the model parameters $\boldsymbol{\theta}$ (Eq. 3.12) reduces the computation time and simplifies the adjustment of parameters involved in the operation of the simulated annealing algorithm.

In our case, we propose to initialize $\boldsymbol{\theta}$ for each mode k using the method that we proposed in Chapter 4. In summary:

- ξ_k: is intialized by Eq. (4.19);
- f_k: is initialized by Eq. (4.10) as $\{\hat{f}'\}$;
- B_{0k}: is the amplitude of $\{\hat{f}'\}$ on the spectrum $\mathbf{S}_s[f]$ (Eq. (4.1));
- φ_{0k}: is initialized by 0.

5.4.2 Iteration body

In this section, the steps in each iteration of the simulated annealing are presented.

5.4.2.1 Candidate selection

The simulated annealing selects candidates that are generated randomly in a way that the selected solution converges to the global optimum asymptotically. There are two steps in the selection of each candidate solution, the first is the candidate selection and the second is the decision of acceptance according the metropolis rule.

Candidate generation

Let's denote the solution of δ of the previous iteration $q-1$ as δ_{q-1}, where $\delta \in \boldsymbol{\theta}$. We generate a new candidate in the current iteration q by

$$\delta_{q,can} \sim \mathcal{N}(\delta_{q-1}, \sigma^2_{\delta q}), \tag{5.4}$$

where $\mathcal{N}(\delta_{q-1}, \sigma^2_{\delta q})$ denotes a normal distribution of mean δ_{q-1} and variance $\sigma^2_{\delta q}$.

$\sigma^2_{\delta q}$ is therefore the parameter generation range of δ in iteration q.

The same procedure is done independently on all the parameters in $\boldsymbol{\theta}^{(q-1)}$ and finally a candidate parameter set $\boldsymbol{\theta}^{(q)}_{can}$ is generated as

$$\boldsymbol{\theta}^{(q)}_{can} \sim \mathcal{N}(\boldsymbol{\theta}^{q-1}, \boldsymbol{\sigma}^2_q) \tag{5.5}$$

where $\boldsymbol{\theta}^{q-1}$ is the parameter set of the previous iteration and $\boldsymbol{\sigma}^2_q$ is the set of candidate generation ranges.

Acceptance rule

Then a decision is made to accept or reject the generated candidate $\delta_{q,can}$ based on a Metropolis rule described as follow;

- Firstly, generate a random variable u according to a uniform distribution $\mathcal{U}$, $u \sim \mathcal{U}(0,1)$;
- Then evaluate

$$\epsilon_{\boldsymbol{\theta}} = exp\Big(\frac{LS(\boldsymbol{\theta}^{(q-1)}) - LS(\boldsymbol{\theta}^{(q)})}{\mathcal{T}_q}\Big). \tag{5.6}$$

  where $\mathcal{T}_q$ is the temperature of iteration q.

$$\text{if}: \begin{cases} u < \epsilon_{\boldsymbol{\theta}}, & \text{accept the candidat as} \quad \boldsymbol{\theta}^q = \boldsymbol{\theta}^q_{can} \\ \text{otherwise}, & \text{reject the candidate by} \quad \boldsymbol{\theta}^q = \boldsymbol{\theta}^{q-1}. \end{cases} \tag{5.7}$$

5.4.2.2 Control step

Two important parameters should be considered to control a simulating annealing process, the temperature control and the candidate generation range.

Temperature control

As per Jabloun [Jab07], the control of the temperature is a very crucial point because it must avoid getting stuck in one of the following cases:

- If the temperature decreases rapidly, the establishment of the thermodynamic equilibrium will not have time to settle.
- If the global optimum is still far and the temperature is very low, this leads to a low of acceptance rate that may lead to a non-optimal solution.

- If the global optimum is close enough and the temperature is high enough, the acceptance rate will be high as well. The algorithm then continues to accept solutions that increase the objective function, thereby contributing to a loss of time before freezing on the optimal solution.

A proper initialization and a suitable choice of the decaying law of the temperature allow rectifying these three cases.

In the context of our work, we considered the following;

- Generate $u \sim \mathcal{U}(0,1)$;
- Then generate a random variable by the Bernouilli distribution $\zeta \sim \mathcal{B}(\rho), \rho = 0.01$. The parameter ρ is fixed empirically in a way that the final result approaches at best the optimal solution.

If $u < \zeta$, then $\mathcal{T}^{(q+1)} = (1 - \epsilon_{\mathcal{T}})\mathcal{T}^{(q)}$, $\epsilon_{\mathcal{T}} = 0.02$.

The initial temperature $\mathcal{T}^{(0)}$ corresponds to the objective function of the initial parameter set $LS(\boldsymbol{\theta}^{(1)})$.

Candidate generation range

We define a range centered on the current solution for each parameter in $\delta \in \boldsymbol{\theta}$. The selection of the new solution is then in this vicinity through a perturbation mechanism. This mechanism is to change the current solution by sampling the objective function with a Gaussian distribution centered around a current solution with the variance defined by the above mentioned range. Therefore, such a range is an important parameter to ensure convergence of the simulated annealing.

To tune the candidate generation range $\sigma^2_{\delta q}$ of parameter δ_{q-1};

- Generate $u \sim \mathcal{U}(0,1)$;
- Then generate a random variable by the Bernouilli distribution $\zeta \sim \mathcal{B}(\rho), \rho = 0.01$.

If $u < \zeta$, reduce the candidate generation range by $\sigma^2_{\delta q} = (1-\epsilon_q)\sigma^2_{\delta(q-1)}$, where $\epsilon_q = 0.99$.

5.5 Application of the Maximum-Likelihood Estimation step over simulated signals

The application of the MLE, and thus the complete proposed approach AMBA, in terms of accuracy and reliability of estimates, is investigated on the same six simulated signals that

were generated by the Timoshenko beam model in Chapter 4 (*cf.*, section 4.4.3). These signals are presented in Tab. 4.2.

In order to describe the robustness of AMBA, a Monte-Carlo procedure over 100 runs is applied.

The estimated results of the mean frequencies and damping ratios for all the six simulated signals are shown in Fig. 5.2 and Fig. 5.3 respectively. The first bar for each mode represents the simulated value and the subsequent bars illustrate the result of the mean of the estimated values with the three different SNR levels equal to 0 dB, 9 dB, and 15 dB respectively. Error bars representing one standard deviation are also shown.

Fig. 5.2 shows that the frequencies of the six simulated signals are estimated with high precision across all modes and all forms of configurations as their relative error of estimation is less than 5%. The error becomes noticeable ($E \leq 10\%$) only for the modes where the damping ratio is $3 < \xi \leq 4\%$, even though this error is only on the order of a few percent of the true value. These estimations are not deteriorated until the SNR reaches $0dB$, where the error is then $10\% < E \leq 30\%$, and the noise variance is equal to the average signal power.

It is seen from Fig. 5.3 that the mean values for all damping ratio estimates fall in the correct range of damping and the errors are acceptable. The most significant outliers occur for the modes with $\xi \geq 3\%$ and low energy (high frequencies). Given that the modes in higher frequencies damp faster than those of their lower counterparts, then their energies of vibration are much weaker, making them indistinguishable from noise. Moreover, the amplitude of the RDS gets smaller at its end.

As the amplitude for highly damped modes get smaller rapidly, then the estimations will be biased by this reduction and the error will be rather high. The error of the modes possessing both high damping and high frequency becomes higher when the noisy observation is generated with low SNR level.

The estimations of weakly damped modes with damping ratio $\xi \leq 1\%$ show excellent agreement with the simulated values. This is true for all simulated scenarios, especially for the fundamental modes. This could be attributed to the fact that the fundamental modes are usually characterized by low damping ratios and lower frequencies, as compared to the other modes of the signal. As for the moderately damped modes with damping ratio $1 < \xi \leq 2\%$, the estimates are less accurate than those modes damped with $\xi \leq 1\%$. However, the mean of their estimates are still very close to the simulated values, even when the SNR is low.

Nevertheless, the simulated results suggest positively that the proposed method is capable of yielding very good estimation results. It exhibits very good performance, and it is robust despite low SNR levels, thanks to the noise reduction of the resulting RDS that is achieved by the time averaging procedure of the RDT of different time segments having same initial conditions.

For the purpose of comparison, the classical RDT with the preliminary manual filtering process is applied over the six simulated signals. The *Butterworth* filter is used to filter the

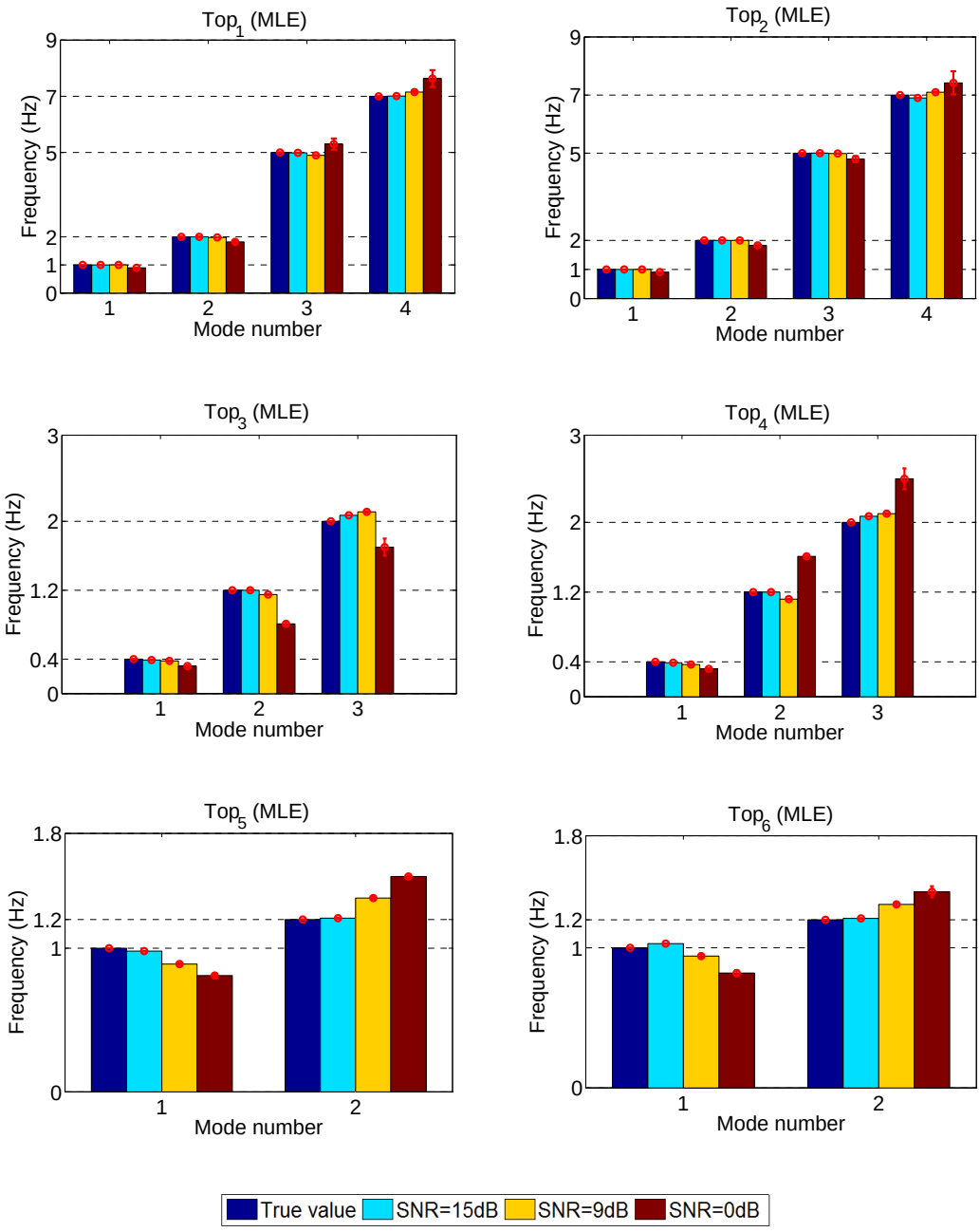

Figure 5.2: Mean frequency estimates by the MLE step for the three different SNR levels ($15dB$ blue, $9dB$ yellow, $0dB$ dark red), and their associated true values (dark blue), along with their standard deviations for Top_1 (top left) to Top_6 (bottom right).

signals under study. In order to get the order and the bandwidth needed to filter each mode k, the *Butterworth* was designed by supplying it with the desired configuration of: pass-band corner frequency W_p, stopband corner frequency W_s, passband ripple R_p, and stopband attenuation R_s.

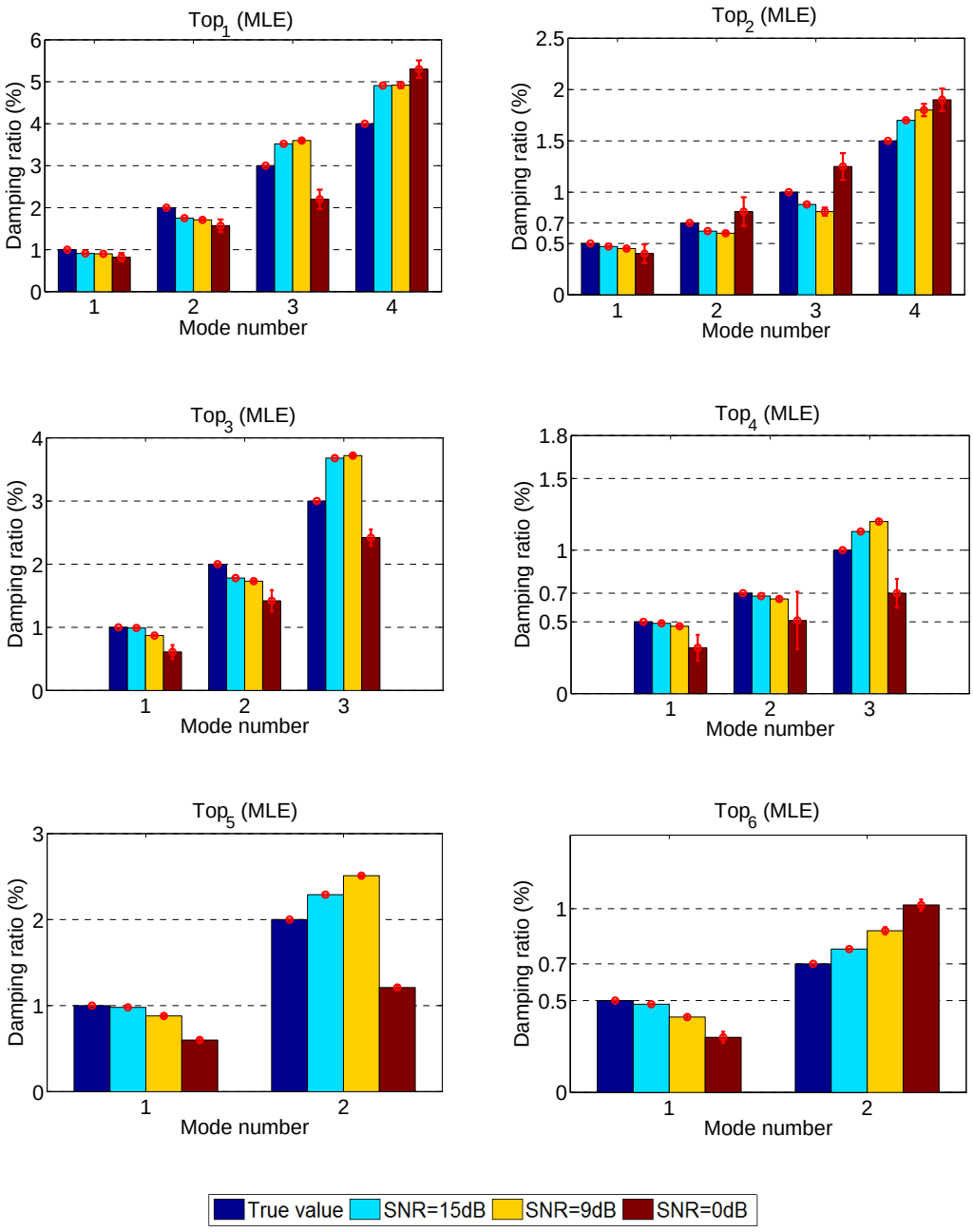

Figure 5.3: Mean damping ratio estimates by the MLE step for the three different SNR levels ($15dB$ blue, $9dB$ yellow, $0dB$ dark red), and their associated true values (dark blue), along with their standard deviations for Top_1 (top left) to Top_6 (bottom right).

The comparative results are shown in Figs. 5.4 and 5.5 in terms of the estimation error of the frequencies and the damping ratios respectively. The error being calculated as $e = |x - \bar{x}|/x$ for both the automatic and the manual estimation approaches, where x describes a natural frequency or a damping ratio of the mode under study.

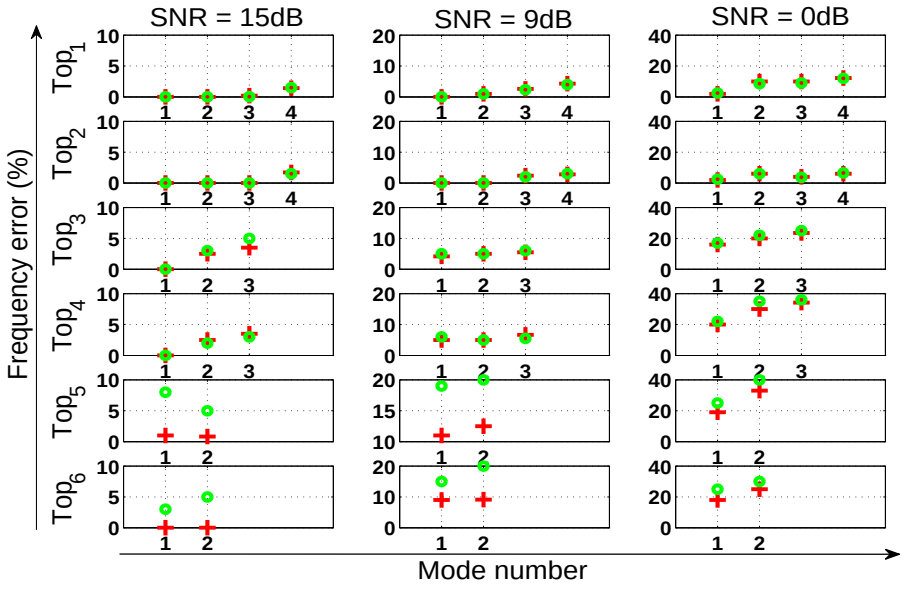

Figure 5.4: Estimated frequency with the automatic estimation approach (filter-free RDT) (+), and the manual estimation approach (RDT pre-processed by filtering) (o).

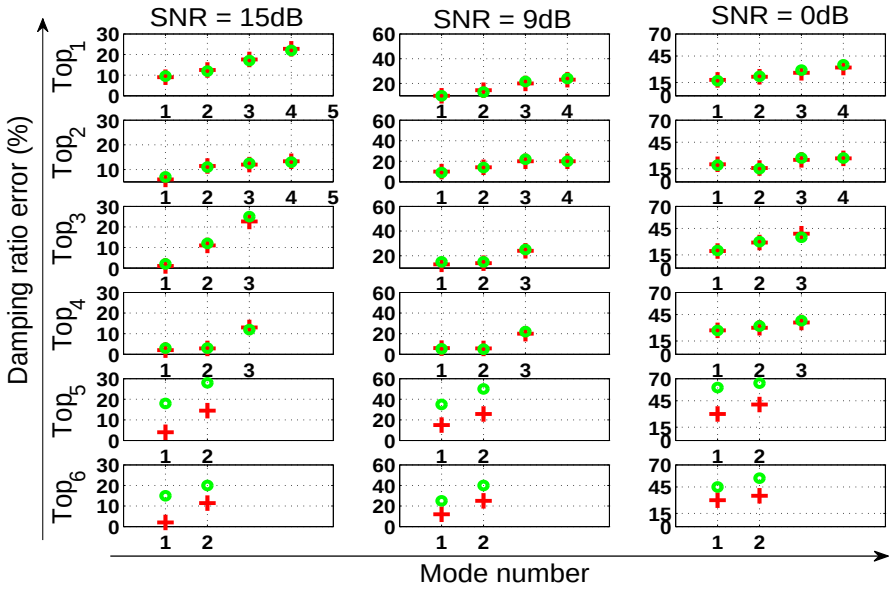

Figure 5.5: Estimated damping ratio with the automatic estimation approach (filter-free RDT) (+), and the manual estimation approach (RDT pre-processed by filtering) (o).

The modal estimation of the signals of the first two categories in Tab. 4.2 (Top_1, Top_2, Top_3 and Top_4) , where the modes are sufficiently spaced, exhibit nearly the same estimation results of frequency and damping ratio for both approaches (automatic and manual). The frequency estimation error e in Fig. 5.4 is less than 10%, and that of the damping ratio in Fig. 5.5 is less than 20%. This is due to the possibility of setting the filter bandwidth conveniently.

The estimation results of the frequency and damping ratio were deteriorated when the SNR is 0dB, the error thus becomes noticeable ($e \geq 30\%$).

Whereby, for the signals of the 3rd category in Tab. 4.2 (Top_5 and Top_6), with the closely spaced modes, the setting of the filter bandwidth becomes much harder. Thus, the mode is always susceptible to frequency shifts relative to the true value; hence the overall modal estimates of the manual method are biased. For the closely spaced modes, the accuracy of the proposed automatic approach is higher than that of the manual one, as it imposes no filtering process, and no filter bandwidth settings are required. The error of the frequency estimations of the proposed automatic method presents more than 20% gain as compared to the manual one. The error of the damping ratio estimations on the other hand are improved by 15% as well.

In the manual method, it is worth noting that the problem of setting the filter bandwidth for closely spaced modes becomes more difficult when the damping of the modes is high. This explains the higher estimation error of Top_5 as compared to Top_6 using the manual method for both frequency and damping ratio estimations (Fig. 5.4 and Fig. 5.5).

The comparative results indicate the reliability of the automatic proposed approach (AMBA) in this thesis. AMBA is capable to give very accurate results simultaneously and automatically of all the modes of the signal under study. Besides, it shows its importance for the cases where filtering becomes very difficult like the case of closely spaced modes, hence assuring the prominence of the elimination of the filtering process prior to the RDT analysis for more reliable modal estimation.

5.6 Summary

In this chapter, we presented the Maximum-Likelihood Estimation procedure that is used to estimate the model parameters of Eq. (3.10). We explained that the likelihood function is non-linear with respect to its parameters, and it has several local minima, thus the conventional optimization techniques do not guarantee the convergence to the global minimum; accordingly, we chose to use a stochastic optimization technique; namely, the simulated annealing.

We presented how to set the parameters of the simulated annealing algorithm. We discussed as well the role, and the choices that we opted to our problem and to the constraints imposed on our model.

We also illustrated that if the parameters of the simulated annealing are well set, the convergence of the simulated annealing is ensured and the realization of an optimal solution is possible.

The simulated results showed that the natural frequencies and the damping ratios estimated by the Maximum-Likelihood Estimation are very reliable and robust.

Indeed, the Maximum-Likelihood Estimation procedure is relatively time consuming as

compared to the initialization step of the previous chapter, but truly effective. The frequencies and moreover the damping ratios were ameliorated by 10% and 30% respectively.

Maximum-Likelihood Estimation procedure has successfully handled the very critical situations like the closely spaced frequency modes with very low signal-to-noise-ratio level.

Chapter 6

Application of AMBA over Actual Buildings subjected to Real-World Ambient Vibrations

Contents

THIS chapter is aimed at the discussion of the accuracy and efficiency of the Automatic Model-Based Approach in assessing the frequency and the damping ratio when applied over actual buildings subjected to real-world ambient vibrations. Section 6.1 presents the application of AMBA over six actual high-rise buildings, and proposes a way to automatically set the required length of the MRDS to yield reliable estimate. Section 6.2 discusses the applicability of AMBA in the long-term real-time tracking of the modal parameters over three actual buildings.

6.1 Estimation of the modal parameters by AMBA: Application to six actual buildings

6.1.1 Selection of the best N_{rds}

As the frequency resolution of the Welch spectrum increases with the length of the MRDS (N_{rds}), we decided in this chapter to apply AMBA over the whole range of N_{rds} that was precised in section 4.4.2.1, that is to say, in the range of 3 to 12 periods.

To select the best N_{rds}, we propose to calculate a normalized error E between $s[n]$ and the reconstructed one $\hat{s}[n]$ based on the estimated parameters as

$$E = \frac{\sum_n |s[n] - \hat{s}[n]|^2}{\sum_n (s[n])^2}. \tag{6.1}$$

Consider all the above, the best N_{rds} that is able to give the most reliable and robust estimation among the others is the one that is able to:

- detect the maximum number of modes as long as a physical interpretation can be established,
- provide the most stable normalized error E (Eq. 6.1), with respect to N_{rds}, which indicates the stability of the frequencies and the damping ratios as well.

The region with the highest number of modes is automatically identified by specifying the first N_{rds} that detects such a number of modes and the last N_{rds} with the same number of modes. Over this unique region, the algorithm then proceeds to calculate the normalized error E as in Eq. (6.1) sequentially for all the consecutive N_{rds} of this region. As long as E is stable the algorithm considers one zone, otherwise it defines a new zone. Then for each defined zone the standard deviation of the associated E of each corresponding N_{rds} is then defined as σ_E. The zone with the lowest σ_E will be considered as the zone of interest, and thus will define the best N_{rds}.

These criteria are applied throughout the whole validation process of AMBA over all the chosen actual buildings in this chapter.

6.1.2 Description of the six buildings under study

This thesis only considers the ambient vibrations. Hence, for this chapter we test AMBA over six actual high-rise buildings subjected to real-world ambient vibrations, three of them are in Beirut (Lebanon) and the other three are in Grenoble (France). All of these signals are provided to our hands by *ANR-URBASIS*.

The buildings of Beirut (Fig. 6.1) are the three towers of the Cap-sur-ville project. They were constructed in 1995 in the Eastern side of Beirut. Following [GVM12], the tower with 21 stories is named W, the other two towers with 18 and 16 stories are named V and X respectively.

Based on [GVM12], the construction design is the same for the three towers, they are all designed in reinforced concrete panels fixed to reinforced concrete frame elements, and settled inside the sandstone at 20 m depth. These towers are about 50 m apart from each other, and they are all constructed over the same geological formations. Two stories of car park occupy

Figure 6.1: Perspective view of the three towers W, V and X of the Cap-sur-ville project in Beirut (Lebanon).

most of the buried foundation part of the three towers. The only difference is in terms of height, as each of them has different number of stories.

In [GVM12] they detailed that each tower is instrumented at the top with a Taurus seismic station (Nanometrics) associated to a velocimeter. This sensor has a frequency response in the 0.033 Hz − 40 Hz frequency band. The sampling frequency is 200 Hz.

The three buildings of Grenoble (France) are Mont-Blanc, Belledonne, and Arpej II towers. Mont-Blanc and Belledonne are two of the three Ile Verte towers (Fig. 6.2). [Mik+13, MGC12] studied these buildings and provided a full description of their structure as follows; these stand-alone towers are 30-story reinforced concrete buildings. The structure is a rhombus of 40 × 20 m. The velocimeter is used at the top of each building to record the ambient vibrations. The sampling frequency is set to 50 Hz.

Figure 6.2: Perspective view of Belledonne and Mont-Blanc towers in Grenoble (France).

Following [MGC12, Val+14], Arpej II is one of the two twin 16-storey reinforced concrete buildings (Length × Thickness × Height = 28 × 12 × 56 m) built in the 1970s on the Grenoble university campus (Fig. 6.3). The storey height is regular between the 2nd and the 16th floors (3.3 m) and taller at the first floor (5.5 m). Its structure is composed of a reinforced concrete frame with two reinforced concrete shear walls at the extremities in the transverse

direction and a reinforced concrete shear wall core for lift shafts and stairwells. The ambient vibrations of Arpej II were recorded at the top of the building using a velocimeter. The sampling frequency is set to 200 Hz.

Figure 6.3: Perspective view of Arpej II tower in Grenoble (France).

The real-world ambient vibration recordings of the signals considered in this chapter are of different durations. Tab. 6.1 presents the length of each of the signals. These lengths are converted into number of periods using the following formula (*cf.*, section 4.4.2.1)

$$N_{sig} = \frac{L_{sig} \times min(\tilde{f})}{F_s}, \tag{6.2}$$

where N_{sig} is the number of periods of the minimal frequency within the total length of the signal, L_{sig} is the length of the signal in points, $min(\tilde{f})$ the minimum frequency detected over the signal under study by the automatic peak-detection method (*cf.*, section 4.2), and F_s is the sampling frequency (Hz).

For all the six signals under study, we do the analysis uniquely on the data of the longitudinal direction. The estimated MRDS, from the first step of AMBA, is then decimated to a Nyquist rate of 20 Hz to reduce the computation time and provide better modal estimate. This decimation value is equal for all the signals of the towers W, X, V, and Arpej II as they have the same sampling frequency (200 Hz). The signals of Mont-Blanc and Belledonne are not decimated as their sampling frequency is already small (50 Hz).

The results of [GVM12, Mik+13, MGC12, Val+14] presented in Tabs. 6.2 and 6.3 are used as a reference for comparing with the obtained results by AMBA in this chapter.

Starting with the three towers of Beirut, the authors of [GVM12] found that the same fundamental frequency is obtained in the two horizontal directions for the three towers. Considering the towers as continuous beams, they observed the classical series of bending frequencies (fundamental and overtones) for shear beam in the three towers (*i.e.* $f_2/f_1 = 3$, $f_3/f_1 = 5$,

Table 6.1: The length of the six studied signals measured at Beirut (W, V and X) and at Grenoble (Mont-Blanc, Belledonne and Arpej II).

Signal length	W	V	X	Mont-Blanc	Belledonne	Arpej II
L_{sig} (Points)	720000	720000	720000	174000	174000	180000
minutes	60	60	60	58	58	15
N_{sig} (Periods)	2592	3348	3024	2958	3062	1143

Table 6.2: The modal frequency values of towers W, V, and X estimated in [GVM12] using Fast Fourier Transform applied over ambient vibration recordings made in the three towers in the longitudinal (Long.) direction. Italic values are related to the torsion modes that are observed in Long. direction.

mode	Tower W Long. (Hz)	Tower V Long. (Hz)	Tower X Long. (Hz)
1	0.72	0.84	0.93
2	*1.16*	*1.34*	*1.46*
3	2.39	2.83	3.15
4	*3.51*	*4.10*	*4.52*
5	4.57	5.30	5.92
6	*6.41*	*7.26*	*8.12*

$f_4/f_1 = 7$) in the longitudinal direction. As a consequence, they assumed the intermediate frequencies, the ones in italic case in Tab. (6.2), to be corresponding to the torsion mode that is only observed on the longitudinal direction for towers W and V, and on both horizontal components for tower X. According to [GVM12] such observations are considered as the proof of some variations of the building design of the tower X.

As per [Mik+13], the behavior of Mont-Blanc and Belledonne is quite similar. Their fundamental mode are at 0.65 Hz (Transverse), 0.84 Hz (Longitudinal), 0.67 Hz (Transverse) and 0.89 Hz (Longitudinal) for Mont-Blanc and Belledonne towers respectively. A torsion mode was observed close to 1 Hz. All these values were also observed by [MGC12] using an

Table 6.3: The modal frequency values of towers Arpej II, Mont-Blanc and Belledonne estimated by [Val+14] using Fourier analysis and Frequency Domain Decomposition of ambient vibrations. Long. and Trans. indicates the estimation in Longitudinal and Transverse directions respectively.

	Velocimeter				
	Freq. (Hz)- Long.		Freq. (Hz)-Trans.		Freq. (Hz) Torsion
	Mode 1	Mode 2	Mode 1	Mode 2	
Arpej II	1.27	4.96	1.12	4.37	1.37
Mont-Blanc	0.85	3.26	0.66	2.64	0.96
Belledonne	0.88	3.17	0.68	2.78	1.00

extensive modal analysis with multichannel recordings.

[Mik+13, MGC12] illustrated that Mont-Blanc and Belledonne towers can be considered as being identical in terms of design, shape and height. However, the obtained modal frequency values provide information on the existence of slight differences due to the presence of differences in design or due to the elastic property variations.

6.1.3 Actual buildings: result analysis and discussion

The estimated frequency and damping ratio values that are assessed by AMBA when applied on towers W, X and V in Beirut are respectively presented in figures 6.4, 6.7, and 6.8, and on towers Mont-Blanc, Belledonne, and Arpej II in Grenoble are as well respectively illustrated in figures 6.9, 6.10, and 6.11.

Each of the aforementioned figures contain three subfigures: (a) the estimated frequency Hz, (b) the estimated damping ratio %, and (c) the normalized error E (Eq. (6.1)). The abscissa for all the figures are the number of periods of the MRDS (N_{rds}) varying from 3 to 12 periods. For the sake of clarity, different scales were used for different figures. The frequency and damping of the different modes are associated by the same color and the same line style between subfigures (a) and (b) in all the figures.

All of these figures are split into different zones by a vertical black line, based on the values of the N_{rds} and the associated estimates of frequency and damping ratio. The splitting process is mainly related to the criteria to classify the best N_{rds} that is able to carry out the most reliable estimates, as discussed earlier in section 6.1.1.

For each of the studied buildings, Tab. 6.4 presents a summary of the chosen direction of study, the modes of interest in such a direction, the probability of false alarm of both the test threshold $\mathcal{PFA}_d$ and the noise spectrum $\mathcal{PFA}_v$ that are required for the automatic peak detection method, along with the representation of each signal in its associated figure. As already explained in section 4.4.3, the choice of $\mathcal{PFA}_d$ and $\mathcal{PFA}_v$ is empirical. In the context of our work, the reason for choosing the same value for both of them is attributed to the fact that we want to keep the coherence between the peak elimination by $\mathcal{PFA}_v$ and the peak detection by $\mathcal{PFA}_d$.

Tabs. 6.5 and 6.6 present the mean estimate of the associated frequency and damping ratio of the zones of interest for the buildings of Beirut and Grenoble respectively.

In this study, the positive point triggering condition of the Random Decrement Technique is used for all the studied signals.

In order to validate the correctness of the obtained results, we compared the mean values of the estimated frequencies to the work of [GVM12, Mik+13, MGC12, Val+14]. The comparison for the towers of Beirut and Grenoble is presented in Figs. 6.5 and 6.12 respectively.

As for tower W and based on the *a priori* information about the signal from [GVM12]

Table 6.4: The chosen direction of study, the modes of interest in such a direction, $\mathcal{PFA}_d$ and $\mathcal{PFA}_v$, along with the representation of the modal parameters of each signal in its associated figure.

	Tower	Direction of study	Modes of interest	$\mathcal{PFA}_d$	$\mathcal{PFA}_v$	Illustration in Fig.
Beirut (Lebanon)	W	Longitudinal	6	0.035	0.035	6.4
	V	Longitudinal	6	0.04	0.04	6.8
	X	Longitudinal	6	0.055	0.055	6.7
Grenoble (France)	Mont-Blanc	Longitudinal	2	0.06	0.06	6.9
	Belledonne	Longitudinal	2	0.065	0.065	6.10
	Arpej II	Longitudinal	2	0.02	0.02	6.11

(*cf.*, Tab. 6.2), it can be seen on Fig. (6.4 (a)) that AMBA is able to estimate the seven modes of interest starting from N_{rds} equal to 8 periods. Thus the algorithm defines the region of interest from N_{rds} equals to 8 to N_{rds} equals to 12 periods. The modes over this region are located at around 0.7 Hz, 1.13 Hz, 2.38 Hz, 3.48 Hz, 4.50 Hz, 6.41 Hz, and 6.88 Hz, which are in a well match with the modes estimated by [GVM12] as shown in Fig. (6.5 (a)). It is worth mentioning here that the seventh mode at around 6.88 Hz was not treated in [GVM12] but it was clearly visible in Fourier Transform, the method they used to estimate the modal frequencies of the signal of tower W. The interested reader could refer to [GVM12] for more clarifications.

Fig. (6.4 (b)) and Fig. (6.4 (c)) show respectively the estimated damping ratio and the estimated normalized error E. As shown on the figures, the zone of N_{rds} between 8 and 12 is split into two zones: (1) $8 \leq N_{rds} \leq 10$, and (2) $10 \leq N_{rds} \leq 12$. The zone with the lowest σ_E is highlighted in bold indicating the zone of interest from where the best N_{rds} can be selected.

The first zone, $8 \leq N_{rds} \leq 10$, shows a lower standard deviation ($\sigma_E = 0.0015$) which indicates more stability for the estimated damping ratios and natural frequencies. Even though, the damping ratios of the 2^{nd}, 4^{th} and 6^{th} modes are not as stable as the other three modes, and sometimes they show lower values as compared to their previous modes as can be seen in Tab. 6.5. However, this is attributed to the fact that these modes are from the torsion direction that were only observed in the longitudinal direction. This observation is true for all the other buildings. Generally, the estimation of the modal parameters is less reliable when different directions are considered.

As compared to towers W and V, the slightly higher fundamental frequency of tower X as shown in Tab. 6.5 and Fig. 6.7 is explained by the shortest height of this tower as it has the least number of stories among the other two towers. The signal-to-noise ratio of this tower is the lowest, as it is known to increase with the number of stories, thus it is the tower that is more sensitive to noise.

Table 6.5: The mean and the standard deviation estimate by AMBA of the modes of interest of the signals of Towers W, V and X for both the frequency and the damping ratio.

	Tower W				Tower V				Tower X			
Region of interest	$8 \leq N_{rds} \leq 10$				$6 \leq N_{rds} \leq 8$				$10 \leq N_{rds} \leq 12$			
mode	$\bar{f}$	σ_f	$\bar{\xi}$	σ_ξ	$\bar{f}$	σ_f	$\bar{\xi}$	σ_ξ	$\bar{f}$	σ_f	$\bar{\xi}$	σ_ξ
1	0.69	0.0010	0.68	0.0173	0.83	0.0057	0.80	0.0306	0.90	0.0035	0.59	0.0057
2	*1.13*	0.0065	0.80	0.0577	*1.30*	0.0058	0.60	0.1442	*1.43*	0.0061	0.59	0.0119
3	2.37	0.0057	0.97	0.0100	2.81	0.00058	1.27	0.0306	3.12	0.0058	1.15	0.0503
4	*3.48*	0.0058	0.57	0.0173	*4.06*	0.0058	0.69	0.0635	*4.50*	0.0058	0.91	0.0228
5	4.52	0.0017	1.86	0.0173	5.57	0.0417	1.16	0.0200	5.92	0.0172	0.84	0.0300
6	*6.46*	0.011	0.55	0.0451	*7.49*	0.0936	1.07	0.1002	*8.07*	0.0172	0.33	0.0308
7	6.88	0.011	1.68	0.0153	NA	NA	NA	NA	NA	NA	NA	NA
Normalized Error E:												
$\bar{E}$	0.0014				0.0077				0.0205			
σ_E	0.0015				0.0011				0.0004			

Table 6.6: The mean and the standard deviation estimate by AMBA of the modes of interest of the signals of Towers Mont-Blanc, Belledonne and Arpej II for both the frequency and the damping ratio.

	Tower Mont-Blanc				Tower Belledonne				Tower Arpej II			
Region of interest	$8 \leq N_{rds} \leq 10$				$8 \leq N_{rds} \leq 10$				$9 \leq N_{rds} \leq 11$			
mode	$\bar{f}$	σ_f	$\bar{\xi}$	σ_ξ	$\bar{f}$	σ_f	$\bar{\xi}$	σ_ξ	$\bar{f}$	σ_f	$\bar{\xi}$	σ_ξ
1	0.83	0.00006	0.57	0.0300	0.87	0.0058	1.06	0.0900	1.27	0.0058	1.06	0.0473
2	1.07	0.1002	0.69	0.0635	1.23	0.0577	1.14	0.3259	5.02	0.0063	2.65	0.0451
3	3.20	0.0100	1.49	0.0153	3.03	0.0115	0.52	0.3676	NA	NA	NA	NA
4	NA	NA	NA	NA	3.27	0.0005	1.16	0.0643	NA	NA	NA	NA
Normalized Error (E):												
$\bar{E}$	0.0110				0.0309				0.0373			
σ_E	0.0004				0.0005				0.0005			

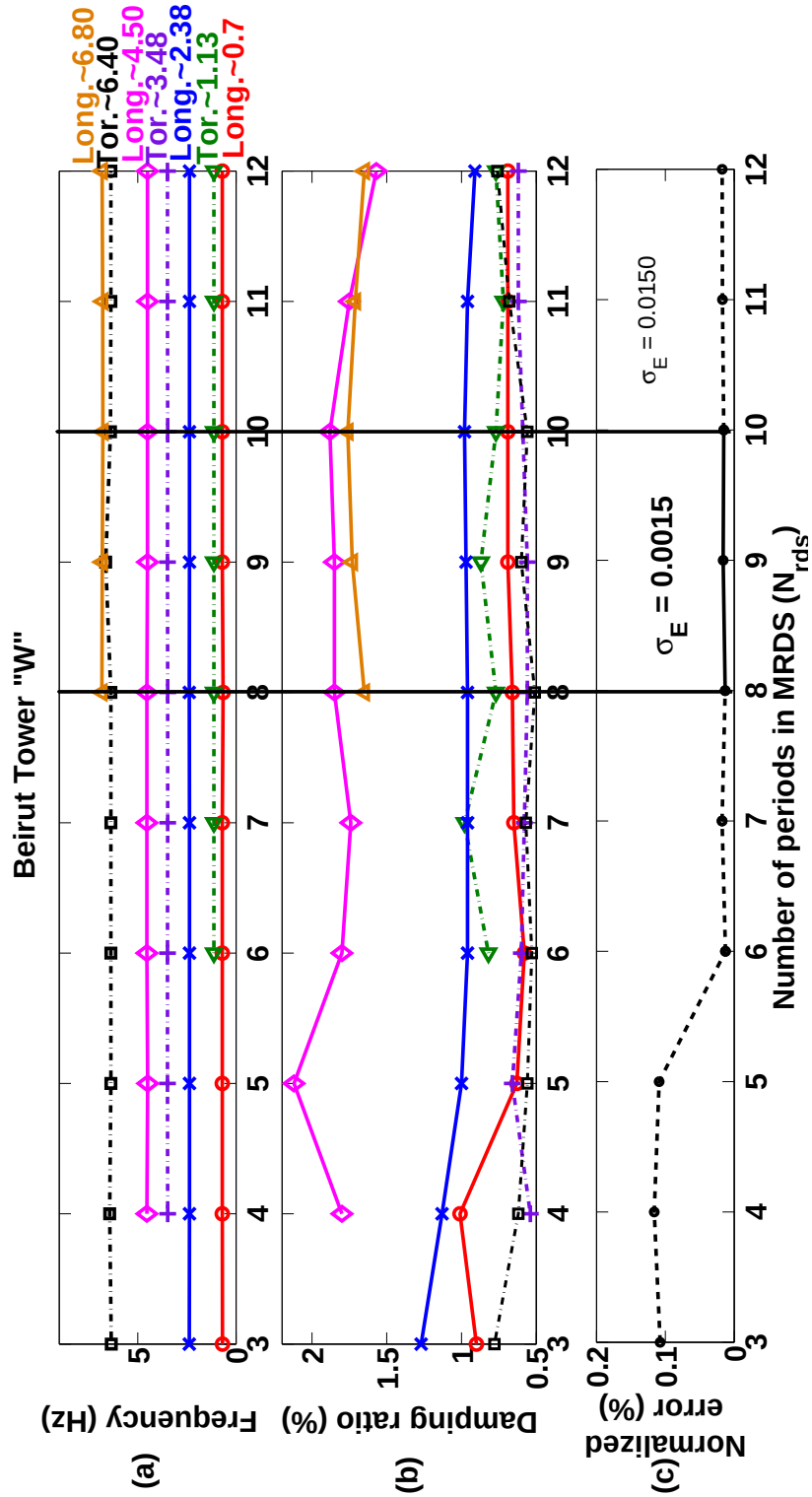

Figure 6.4: (a) The frequency, (b) the damping ratio and (c) the normalized error estimated by AMBA for tower W in Beirut (Lebanon) in the longitudinal (long.) direction. Tor. indicates the torsion modes observed in the long. direction. σ_E is the standard deviation of the normalized error. The region of interest is indicated by bold σ_E.

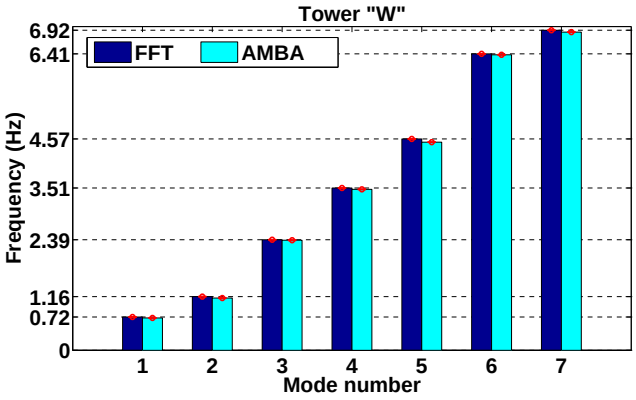

(a)

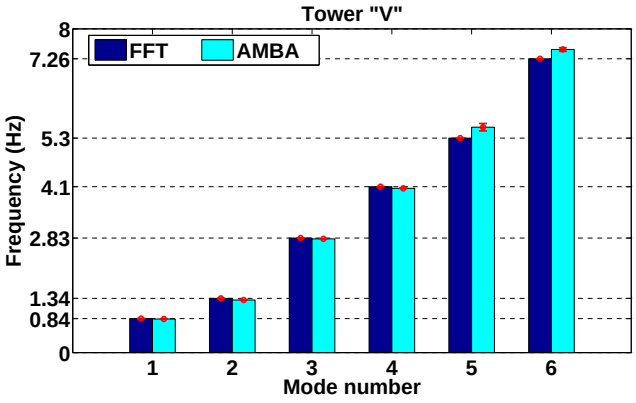

(b)

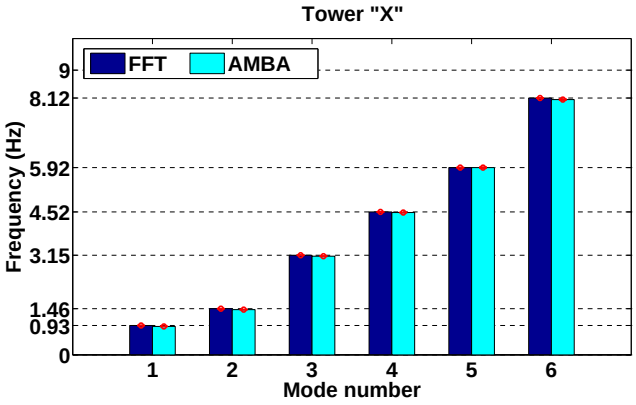

(c)

Figure 6.5: Mean frequency estimates for the different N_{rds} in the region of interest (light blue), and their associated values that were estimated in [GVM12] by using the Fast Fourier Transform (FFT) (dark blue), along with their standard deviations using AMBA for (a) Tower W, (b) Tower X, and (c) Tower V.

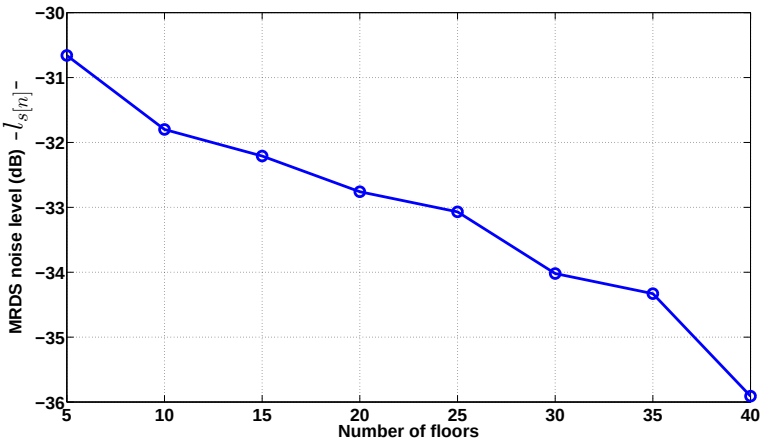

Figure 6.6: The relation between the building height and the noise level of the MRDS based on a two-mode simulated signal of 360000 points with $f = [1, 5]$ Hz and $\xi = [1, 1.5]\%$ and sampled at 200 Hz.

Tower V (Fig. 6.8) experiences a median values for both the fundamental frequency and the normalized error E among towers W and X. This is also explained by its median number of stories.

The lower the number of stories is, the bigger the effect of the noise in the overall analysis result will be. This can be justified by the ascending order of the mean normalized error $\bar{E}$ of the three towers W, V and X as shown in Tab.6.5 respectively with respect to their number of stories.

To justify this conclusion, we studied the influence of the number of stories, r, on the estimation of the MRDS. For this purpose, a two-mode signal is simulated with a length of 360000 points, sampled at 200 Hz, with the modes being located at 1 Hz and 5 Hz and damped by 1% and 1.5% respectively.

For each r being varied from 5 to 40 floors, we fixed the variance of the seismic noise $p[n]$ and the additive one $e[n]$, and applied 100 noise iterations. At each iteration, the MRDS of the noisy signal $y[n]$ and the noise-free signal $\mathfrak{g}[\mathfrak{n}]$ of Eq. (3.8) are estimated as $s[n]$ and $s_{\mathfrak{g}}[n]$ respectively. The normalized noise level in the estimated MRDS is then denoted $l_{s[n]}$ and computed as

$$l_{s[n]} = \frac{\sum_n |s[n] - s_{\mathfrak{g}}[n]|^2}{\sum_n |s_{\mathfrak{g}}[n]|^2}. \tag{6.3}$$

Fig. 6.6 shows clearly that as the number of stories increases, the noise level decreases. This means that the short buildings are more influenced by noise as compared to their taller counterparts.

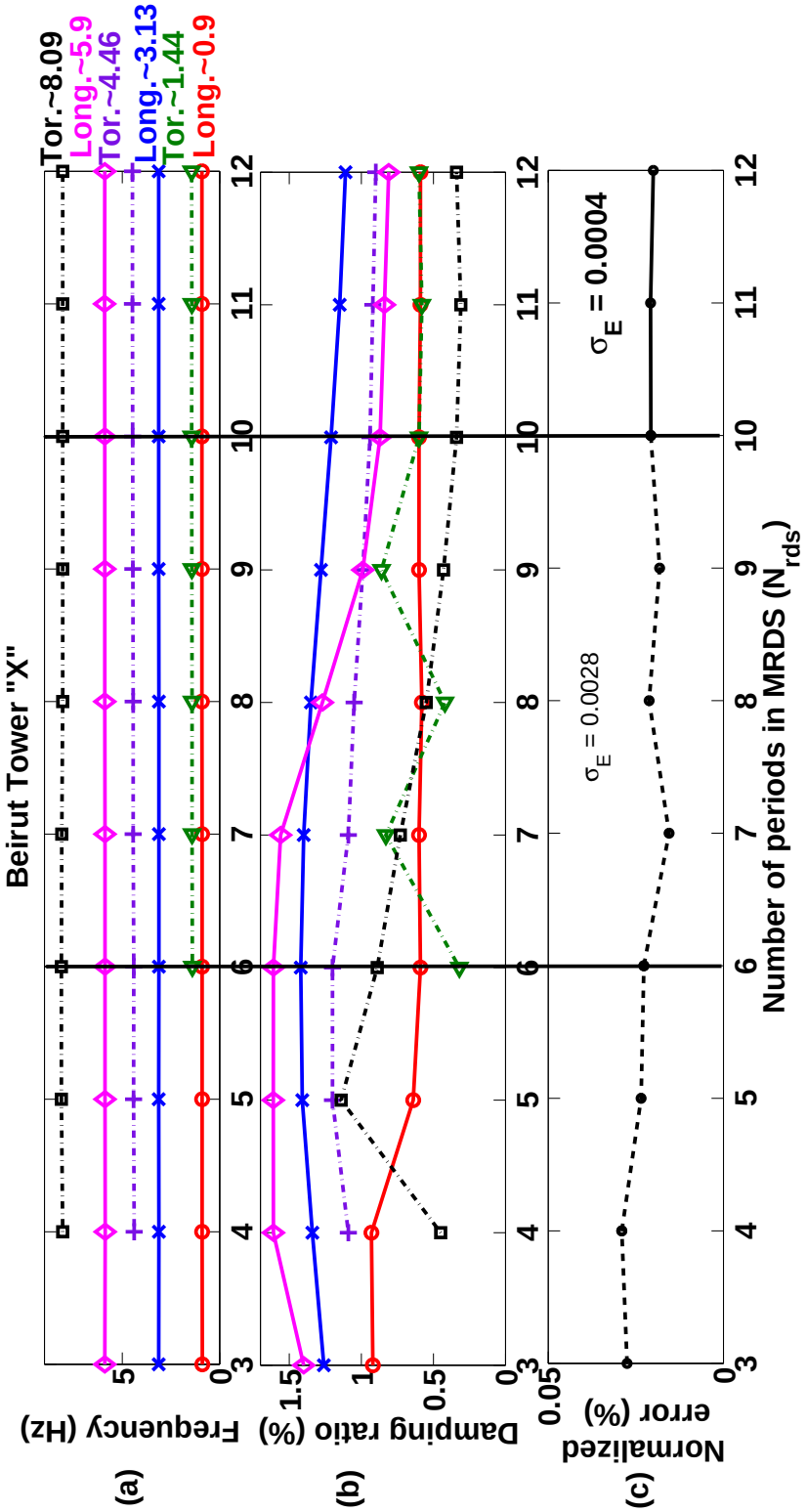

Figure 6.7: (a) The frequency, (b) the damping ratio and (c) the normalized error estimated by AMBA for tower X in Beirut (Lebanon) in the longitudinal (long.) direction. Tor. indicates the torsion modes observed in the long. direction. σ_E is the standard deviation of the normalized error. The region of interest is indicated by bold σ_E.

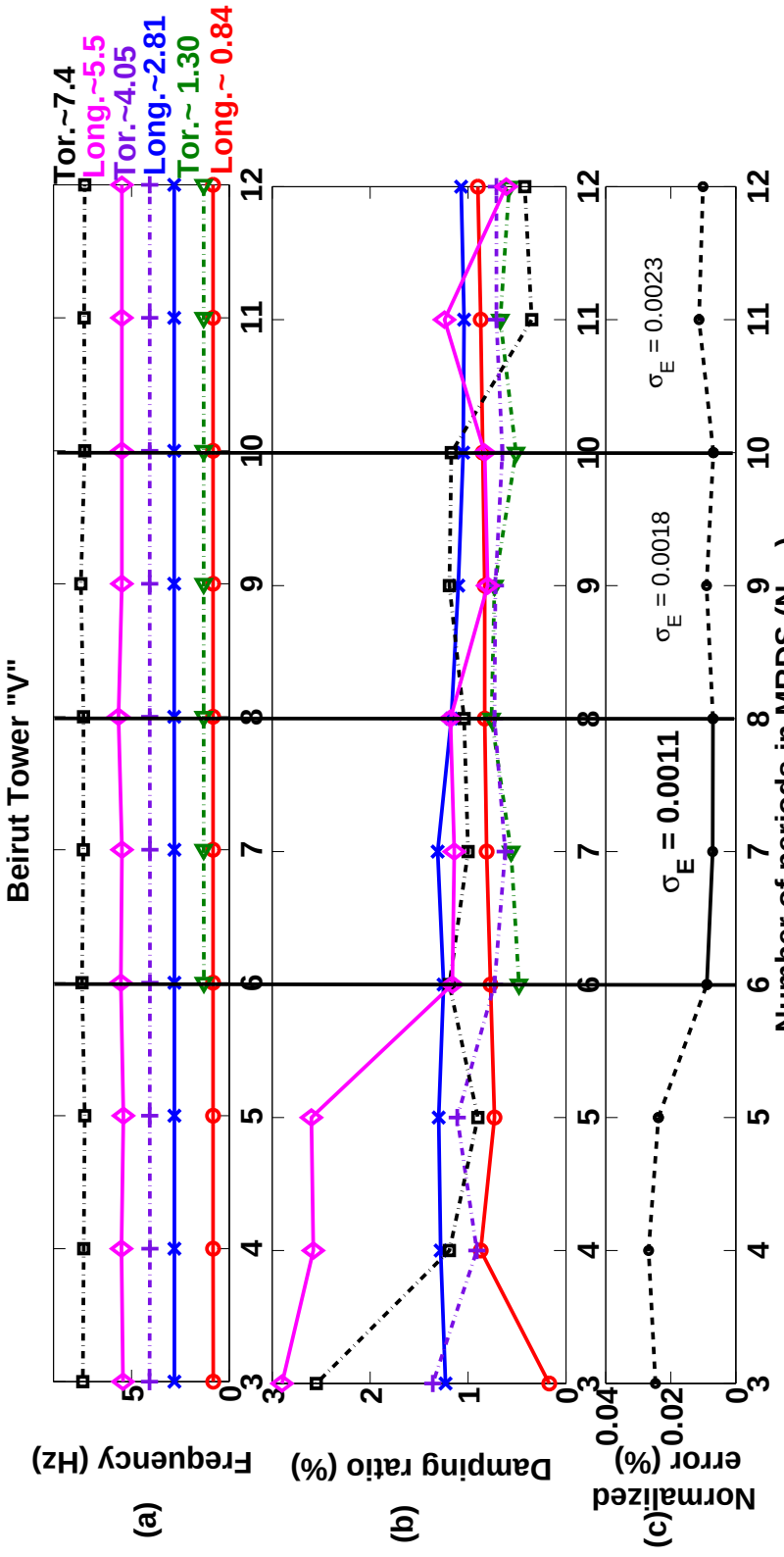

Figure 6.8: (a) The frequency, (b) the damping ratio and (c) the normalized error estimated by AMBA for tower V in Beirut (Lebanon) in the longitudinal (long.) direction. Tor. indicates the torsion modes observed in the long. direction. σ_E is the standard deviation of the normalized error. The region of interest is indicated by bold σ_E.

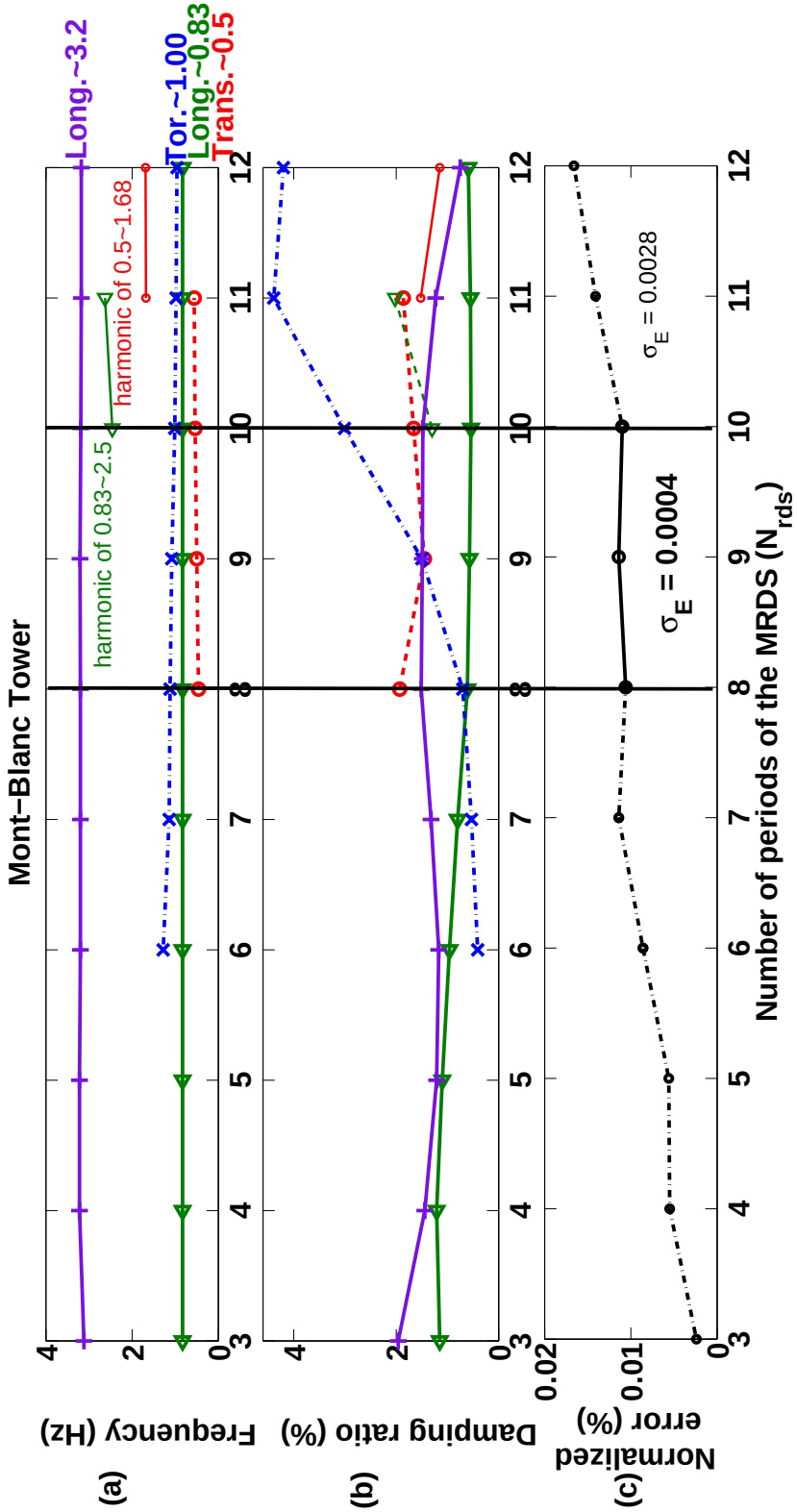

Figure 6.9: (a) The frequency, (b) the damping ratio and (c) the normalized error estimated by AMBA for tower Mont-Blanc in Grenoble (France) in the longitudinal (long.) direction. Tor. and Trans. indicates respectively the torsion and the transverse modes observed in the long. direction. σ_E is the standard deviation of the normalized error. The region of interest is indicated by bold σ_E.

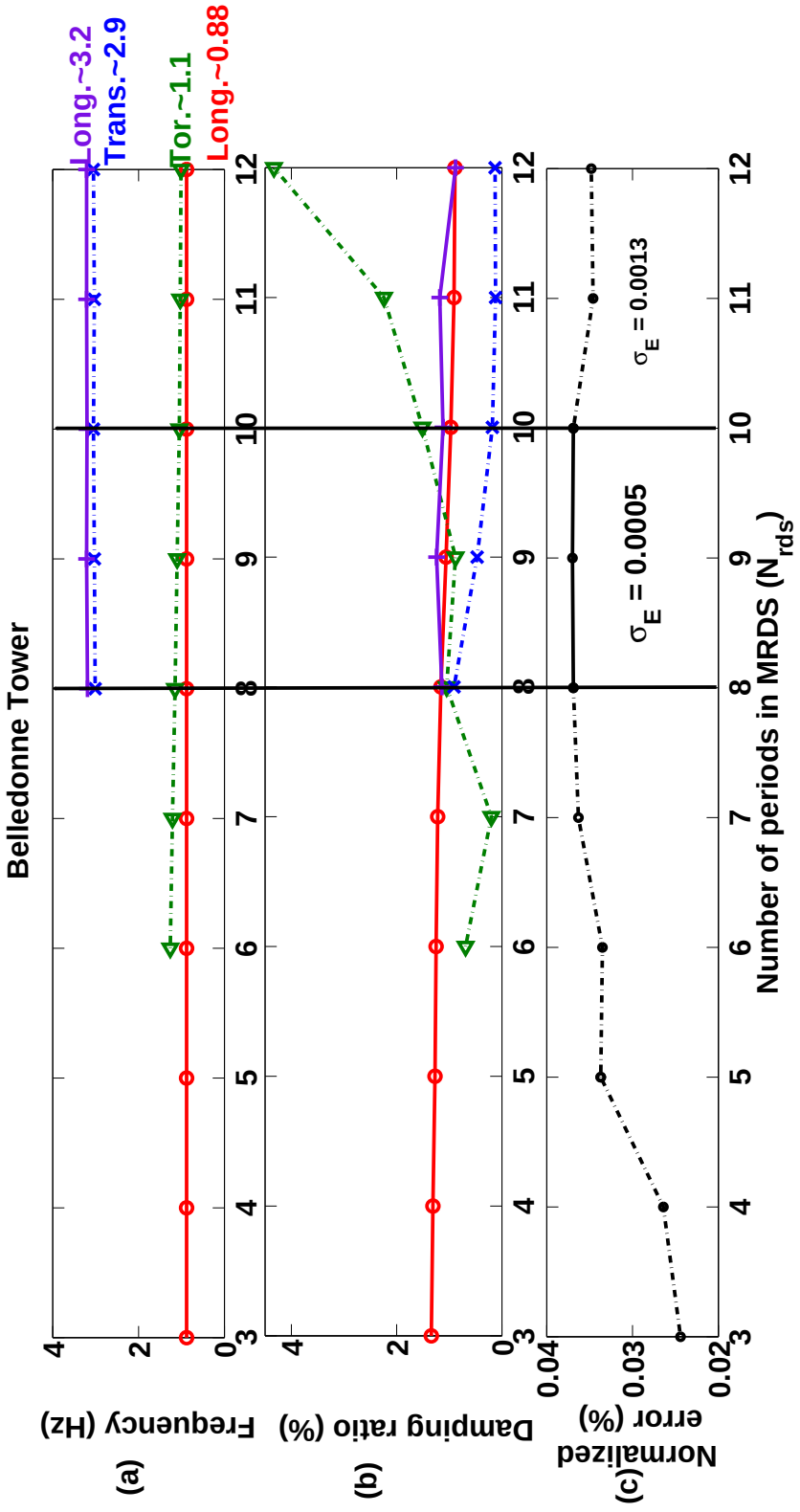

Figure 6.10: (a) The frequency, (b) the damping ratio and (c) the normalized error estimated by AMBA for tower Belledonne in Grenoble (France) in the longitudinal (long.) direction. Tor. and Trans. indicates respectively the torsion and the transverse modes observed in the long. direction. σ_E is the standard deviation of the normalized error. The region of interest is indicated by bold σ_E.

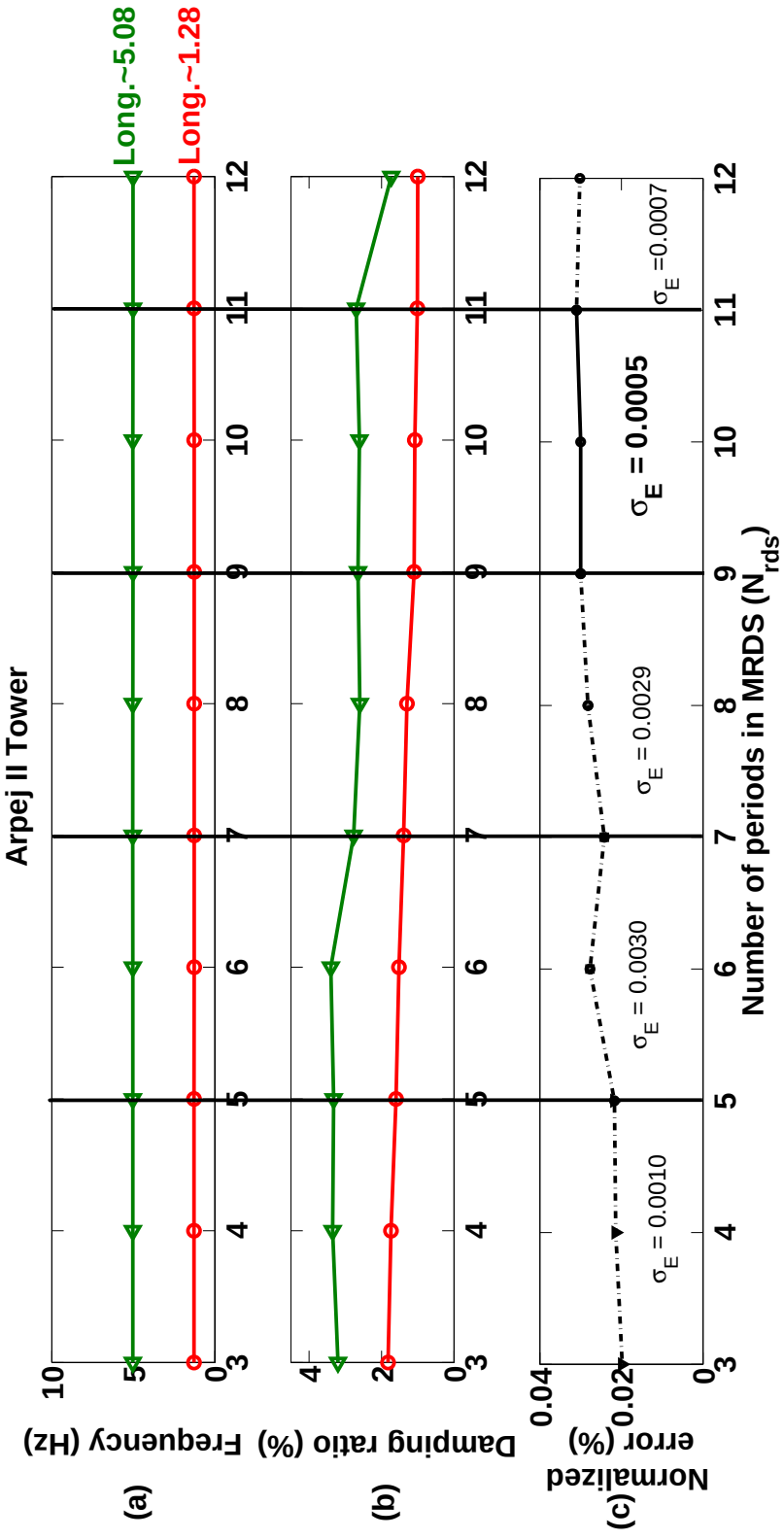

Figure 6.11: (a) The frequency, (b) the damping ratio and (c) the normalized error estimated by AMBA for tower Arpej II in Grenoble (France) in the longitudinal (long.) direction. σ_E is the standard deviation of the normalized error. The region of interest is indicated by bold σ_E.

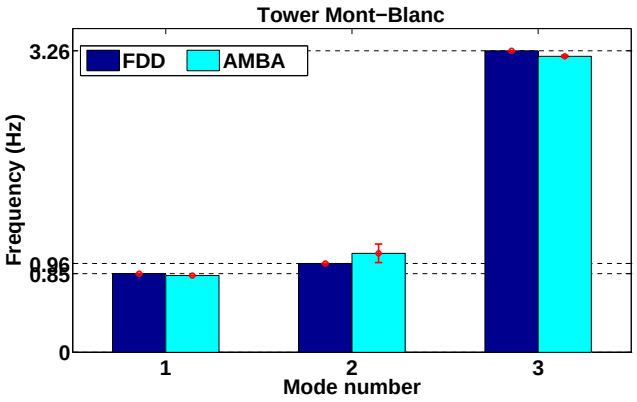

(a)

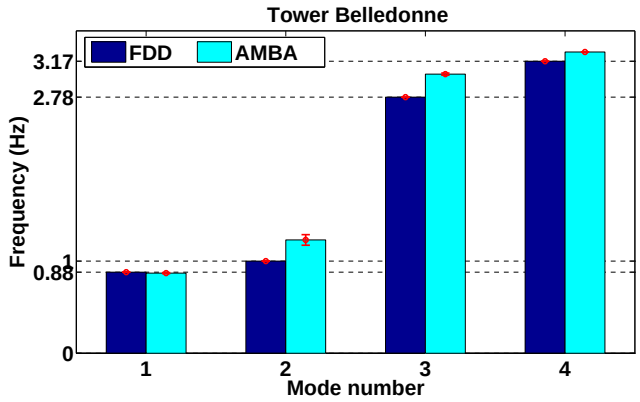

(b)

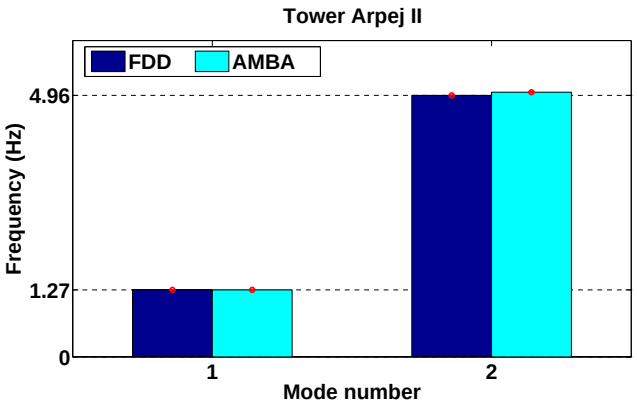

(c)

Figure 6.12: Mean frequency estimates for the different N_{rds} in the region of interest (light blue), and their associated values in [Mik+13, MGC12] using the Frequency Domain Desomposition (FDD) (dark blue), along with their standard deviations using AMBA for (a) Tower Mont-Blanc, (b) Tower Belledonne, and (c) Tower Arpej II.

The rest of this section presents the estimation of frequency and damping ratio by AMBA for the three towers of Grenoble (France). The same procedure that is applied over the towers of Beirut is applied over those of Grenoble.

The same trend as those of Beirut towers is also observed over these of Grenoble towers, *i.e.*, Arpej II tower is half the height of those of Mont-Blanc and Belledonne, and thus as shown in Tab. 6.6, its fundamental frequency is higher and its mean normalized error is the highest. A well matching between the results of AMBA and those of [MGC12, Val+14] is clearly illustrated in Fig. 6.12 for all the three towers.

In figures 6.9 and 6.10 for towers Mont-Blanc and Belledonne respectively, the torsion mode is clearly visible at around 1 Hz. The standard deviation of the torsion mode for both towers is higher than that of the other modes, this can be attributed to the fact that this mode is not in the direction of study of these two signals, *i.e.*, the longitudinal direction. Another mode at around 3 Hz is detected for tower Belledonne, this is the transverse mode that is observed in the longitudinal direction of this building which also explains its unstable damping ratio estimates.

For the frequency estimate, AMBA has shown a very well match with the results of [GVM12, Mik+13, MGC12, Val+14]. Moreover, AMBA was able to do the estimation of all the modes of the signal simultaneously and automatically. More and above, reliable estimates of the damping ratio were also provided by AMBA, the results of the latter were only disturbed when the estimated mode is not in the chosen direction of study.

6.2 Time-tracking of the modal parameters by AMBA: Application to the three towers of Beirut (Lebanon)

This section is devoted to the application of AMBA for a long-term real-time tracking of the modal parameters of actual high-rise buildings. This is held over the three towers of the Cap-sur-ville project of Beirut (Lebanon) (*cf.*, Fig. 6.1). This choice is due to the fact that these buildings share very similar structural design, and they are all founded in the same geological formations, so that the soil-structure won't affect the sensitivity of the buildings response to external conditions.

Seventy-two-hour length of real-time ambient vibration data are continuously collected from the three towers. The starting time of recording is 00:00, 26$^{\text{th}}$ of May, 2011 and the end time is 23:00, 28$^{\text{th}}$ of May, 2011.

In this study, the long-term variation of the frequency and the damping ratio is computed hourly by AMBA, corresponding to 2592, 3348 and 3024 periods of the fundamental mode for the three towers W, V and X respectively (*cf.*, Tab. 6.1). A sampling of one hour is studied, so that only one value of the frequency and the damping for each mode is considered per hour. No overlap was considered between two successive one-hour windows.

For an efficient use of AMBA for the real-time tracking of the modal parameters, the first one-hour window should be treated independently. The first section of this chapter (*cf.*, section 6.1) is used to calibrate the needed *a priori* information about each tower. A reference database of the natural frequencies (f_k), damping ratios (ξ), number of modes (K) $\forall k \in [1, K]$, and the length of the MRDS N_{rds} is thus firstly populated.

These information are tabulated in Tab. 6.5 for the three towers under study. As could be seen in this table, the zone of interest contains more than one value of N_{rds}. For the time-tracking by AMBA, and as per the geologists it is preferable to use the smallest value of N_{rds} from the zone of interest. This could be attributed to the fact that lower N_{rds} yields lower computation time. Accordingly, N_{rds} equals to 8, 6, and 10 periods is considered for towers W, V and X respectively.

Frequency and damping fluctuations are shown in figures 6.13 and 6.14 respectively for the seventy-two-hour length of the three towers in the longitudinal directions. As the tracking of the small variations of both the frequency and the damping ratio is concerned, it is worth noting that the scale of the figures is not unified which allows a reasonable identification of the small variations. Though certain tiny variations might not provide enough insight about the presence of a damage in the building, however, such variations have significant influence on the applicability of AMBA for the long-term real-time tracking of the modal parameters that might be related to the environmental conditions.

Fig. 6.13 shows the variations of the frequency values for the three towers. The first six modes of each tower are considered. We observe small fluctuations in time, the main variations are visible simultaneously on the associated modes of the three towers (black arrows). Nevertheless, we also observe some fast and transient variations here and there only on certain modes and not on the others. These variations could be attributed to the parasitic vibrations (presence of electric motors, machines, lifts, *etc.*).

Near-perfect synchronization is observed in the frequency variations between the three towers for all the associated modes. AMBA being able to detect very small fluctuations (less than 0.2%). Because the buildings are completely independent, the origin of the simultaneous variations over the associated modes of the three towers must be physical. Such physical variations could be directly related to boundary conditions.

Correlation with the daily variations are clear regardless of the buildings and the mode. In our case, only the temperature difference between day and night is affecting the variations of the frequency. The effect of rain and wind is not considered as the studied recorded data is only for three days in May, and there might not have been strong wind or heavy rain during this duration to influence the frequency.

AMBA is also used for the long-term monitoring of the damping ratios in Fig. 6.14. No correlation are clearly put in evidence for damping ratios. Greater scattering are observed for damping than for frequency, but still less than 4%.

We observe an overall positive trend between frequency and damping. That is to say, the

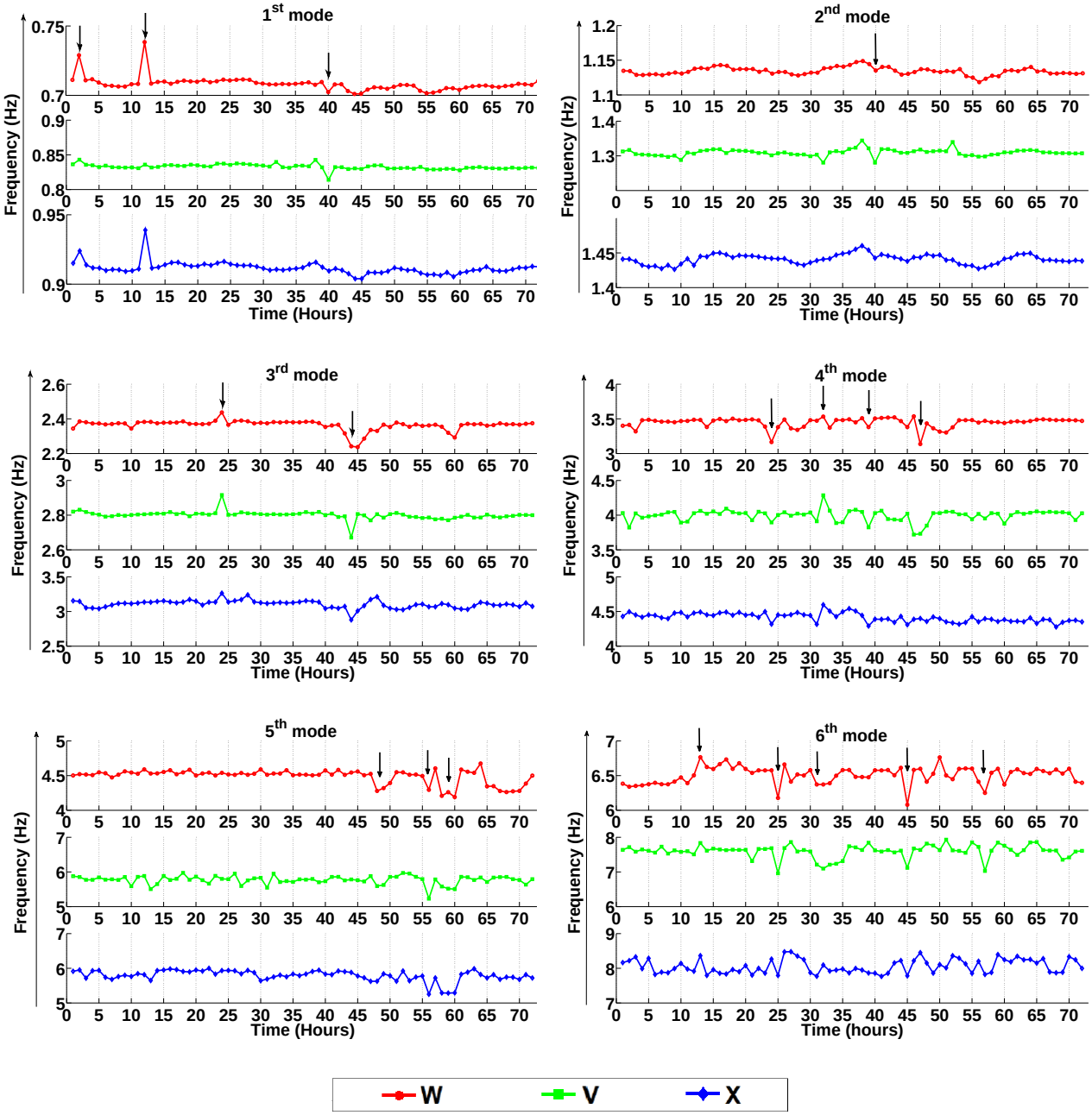

Figure 6.13: Evolution of modal frequency of modes 1 (top left) to 6 (down right) automatically tracked by AMBA during the period from 26/05/2011 to 28/05/2011.

same main variations but with opposite trend (black arrows) is observed for damping, *i.e.*, as the frequency variations are increasing, those of the damping are decreasing.

In conclusion, AMBA has shown its ability to monitor the very small variations in modal frequencies around 0.2%. AMBA provides effective assessment of the building variation tracking over time with an accuracy close to 0.4%. Some variations were attributed to the physical variations of the building, however, additional data is needed to draw definitive conclusion

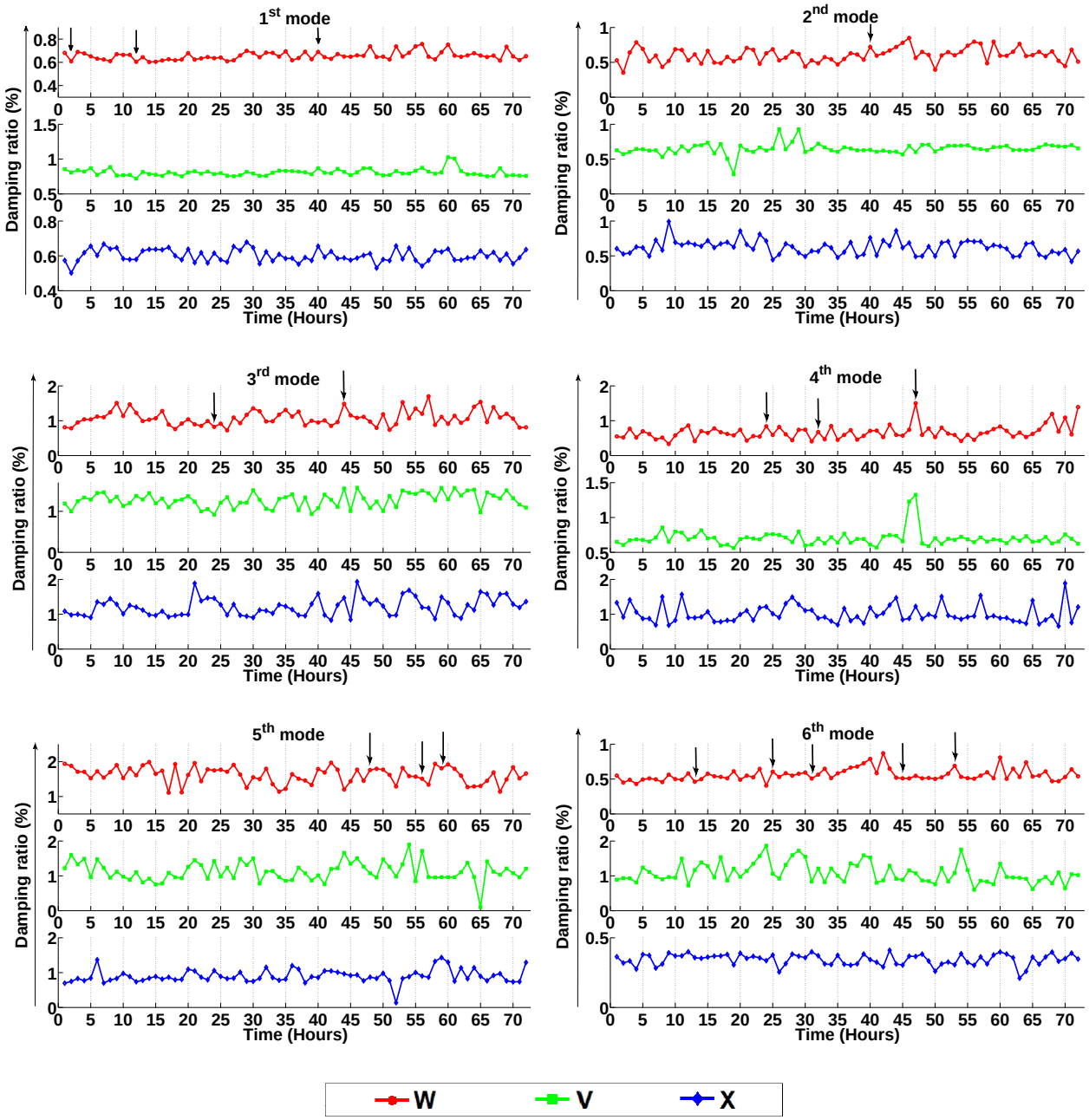

Figure 6.14: Evolution of modal damping of modes 1 (top left) to 6 (down right) automatically tracked by AMBA during the period from 26/05/2011 to 28/05/2011.

on the physical parameters explaining these trends.

6.3 Summary

In this chapter we have analyzed the applicability of the Automatic Model-Based Approach in assessing the two main parameters the frequency and the damping ratio that classically characterize the dynamic response of a building.

This chapter started by applying AMBA over six actual buildings subjected to real-world ambient vibrations. These buildings are of interested characteristics and have been already treated in the literature, which provided a good database to properly validate AMBA.

As the initialization step of AMBA is spectral based, thus the estimated number of modes of the multi-mode Random Decrment Signature is related to the frequency resolution of the used spectrum. To solve this issue, and in order to deal with the multi-component signals that is always the case of the real-world ambient vibrations, we proposed in this chapter a method to choose the best length N_{rds} in the RDT that constitute the basis of AMBA.

All the obtained results of AMBA were cross validated with several references analyzing the same building with a manual modal analysis. AMBA matches well with these results but in a simultaneous and automatic way. Moreover, it is able to provide a reliable estimation of the damping ratio.

The last section of this chapter was devoted to the heart of the matter of the dynamic structural health monitoring, where excessive data of continuously recorded structural response are collected. In this section, the applicability of AMBA in long-term real-time tracking of the modal parameters is tested over three high-rise buildings. The results illustrated a well functionality of AMBA in the time-tracking purposed. However, further validation is needed in this regard.

Chapter 7

Conclusions and perspectives

This thesis proposed an automatic long-term monitoring approach for identifying the frequencies and the damping ratios of all the modes of the signals of ambient vibrations recorded on an actual high-rise building.

The fact of working over actual high-rise buildings subjected to real-world ambient vibrations is faced with several challenges; we cite for example, the time-domain convolution between the system impulse response and the seismic noise, the low, exponential and damped amplitudes of the impulse response, the existence of several components, the presence of closely-spaced frequency modes, and the low signal-to-noise ratio levels.

The proposed approach of this thesis handled the aforementioned challenges simultaneously without the need for the user intervention. This approach is given the name Automatic Model-Based Approach, AMBA for short, and it is introduced in three sequential steps. Each step is responsible to tackle one or more challenge in the aim to provide an automatic and moreover a reliable and robust modal parameter estimation of the studied signals.

At first, we addressed the extraction of a free-decay signature equivalent to the system impulse response. Our approach to this problem has been to use the application of the Random Decrement Technique directly over the multi-component signal in question. This approach skips the filtering process prior to the RDT analysis and leads to the estimation of the Multi-mode Random Decrement Signature. This approach is given the name Filter-Free Random Decrement Technique.

Its main originality is its ability to avoid the difficulties of setting the filtering parameters especially in the critical cases of low signal-to-noise ratio levels, closely-spaced frequency modes and highly damped ones. Furthermore, it avoids the user intervention that disturbs the automatic estimation procedure.

To characterize the estimated Multi-mode Random Decrement Signature, we proposed a signal model. This signal model keeps the same definition of the number of modes, the natural frequencies and the damping ratios as the physical model of the studied building. It is thus able to directly characterize the multi-mode signal.

There are two contributions in the proposed signal model. First, the model is able to deal with the exponentially damped amplitude in the context of the building vibration signals, whose amplitude can be represented by an exponential function. Second, based on this model, the proposed approach is able to estimate an exponential amplitude which is of great

interest to the physicists.

The Filter-Free Random Decrement Technique forms the first step of the proposed AMBA. It mainly contributes to meet the first challenge of overcoming the convolution between the system impulse response and the seismic noise.

The idea was then to deal with the modal estimation of all the modes of the estimated Multi-mode Random Decrement Signature. For this purpose, we proposed a non-parametric spectral-based method. It is based on an averaged Welch spectral estimation from two periodograms calculated over two segments of the Multi-mode Random Decrement Signature. These two segments are of the same length and placed one at the beginning of the Multi-mode Random Decrement Signature and the other at its end. They have an overlapping of 50%. This method is mainly devoted to undertake the challenge of the presence of multi-components in the studied signal beside estimating the associated modal parameters.

Over the averaged Welch spectrum, the modes were identified by finding the corresponding frequencies. Accordingly, we proposed to use the iterative P-pass filtering process proposed by Durnerin [Dur99]. Such a peak detection method associated with the statistical properties of the spectrum estimator allowed for an automatic interpretation of the spectrum contents.

Through the use of the statistical properties of the estimator, the local peaks of the averaged spectrum is detected by a detection method which is insensitive to the settings. It first considers the noise spectrum of such a spectrum, then it detects the peaks emerging from the estimated noise spectrum with a Neyman-Pearson test.

The damping ratios of each of the detected peaks were then calculated from the amplitude variations on the frequency modes of the already estimated two periodograms.

The proposed spectral-based method has the advantage of being applicable over MDOF systems with well-spaced frequency modes. Its main limitations are: (1) being dependent on the resolution of the Fourier spectrum, and (2) the modal estimation is not well adapted for closely-spaced frequency modes, especially with high noise levels. In order to solve these issues, we then proposed a parametric method based on the Maximum-Likelihood Estimator. This method fits well the closely-spaced frequency modes of the non-filtered signal.

The Maximum-Likelihood Estimator is nonlinear and requires a stochastic optimization method for the parameter estimation. For this purpose, we proposed to use the simulated annealing technique which is iterative and requires an initialization step. The already proposed spectral-based method thus serves for this issue. The latter is then called an initialization step and it forms the second step of AMBA.

Once the modal parameters along with the number of modes of the studied signal were estimated by the spectral-based initialization step, the Maximum-Likelihood Estimator procedure was then used. The Maximum-Likelihood Estimator constitutes the last step of AMBA. The modal parameter estimation using the Maximum-Likelihood Estimator was performed by a parametric iterative process. In this way, the bias of the modal estimates from the initialization step was reduced, and thus more reliable and robust estimation was obtained.

The optimization of the MLE via the simulated annealing was strongly inspired by the previous work of Jabloun [Jab+07]. The setting of the parameters of the simulated annealing was modified from those proposed by [Jab+07] to adapt to our problem and to the constraints imposed in our work.

The results on simulated signals generated using a model of high-rise building defined as a continuous beam model indicated the validity of the complete AMBA algorithm. The Filter-Free Random Decrement Technique has automatically estimated a Multi-mode Random Decrement Signature equivalent to the system impulse response. The initialization step has successfully and automatically estimated the number of modes of the Multi-mode Random Decrement Signature and the associated natural frequencies and damping ratios. The last Maximum-Likelihood Estimator step has automatically estimated non-biased and more reliable frequencies and damping ratios of all the detected modes.

Encouraged by these results, AMBA was then validated over real signals recorded over actual buildings subjected to real-world ambient vibrations, the results have proved the efficiency of AMBA and have shown very low estimation error for both the natural frequencies and the damping ratios for closely-spaced frequency modes, highly damped amplitudes ($\xi \leq 5\%$) and very low signal-to-noise ratio level. The error of the natural frequency is less than 5% and that of the damping ratio is around 15%.

In the real-time long-term tracking, one of the ultimate goals of this thesis is to monitor the variations of the natural frequencies and the damping ratios and thus being able to detect the damage in the studied building. This is to avoid any catastrophic failure. AMBA has proved its applicability in such a context. The variations of the natural frequencies and moreover those of the damping ratios were correctly and automatically tracked over seventy-two-hours length of real-time ambient vibration data continuously collected over three actual buildings.

Some prospects are proposed in the following for the continuation and improvement of this work.

Short term prospects:

Reducing the computational load The majority of the computational load for the modal estimation of the signal comes from the Maximum-Likelihood Estimation step of AMBA. Therefore the computation time increases with the number of modes, the size of the signal and the number of iterations in the simulated annealing. To reduce the computation time, we can optimize the programming by using a more efficient programming language other than the Matlab R2012b that we used in this work. Another solution could be to use another stochastic optimization technique other than the simulated annealing to achieve a faster convergence.

Extension to more complex signals It is proposed to extend AMBA for the detection of the intersecting modes in the frequency plane, and for more closely-spaced frequency modes (< 0.01 Hz). The difficulty of the proposed algorithm in the crossing components is related to the spectral representation, which can not provide sufficient resolution to separate the cross components. The first solution could be to use an alternative choice to initialize components. The second solution could be to integrate the estimation of the number of modes

in a parametric model which avoids the dependency between the spectral resolution and the peak detection.

Longer time surveillance Though AMBA has been able to track the variations over the three tested buildings for three consecutive days. However, we believe that AMBA has the potential to be further generalized for testing much longer signals that include several months of different seasons. It could also be of high interest if such signals contain a seismic record as well to provide indicators about the trend of the frequency and the damping ratio evolution.

Long term prospects:

Estimate the number of modes without the initialization step The first solution could be by inserting such an estimation within a modal parameter modelling method or by replacing the stochastic optimization method by a reversible jump MCMC. This could save time and help avoid having the detection of false alarmed peaks.

Other deconvolution methods Further to the above suggestion for the long term future work, the use of another method to extract the impulse response other than the Random Decrement Technique can be considered. The direct estimation of the auto-correlation function of the signal under study could be one of the solutions. This might help avoiding the influential parameters that should be taken into consideration when using the Random Decrement Technique.

Compare the results with Lidar signals recorded over actual buildings The results obtained by our proposed AMBA should be compared with the existing methods in the literature. One of the interested comparisons to be held in the context of *ANR-URBASIS* project is to compare with the signals recorded using the Lidar over the same actual buildings. Such comparison will certainly help in evaluating the damage detection of the buildings under study by different aspects.

Appendix A

Résumé en Français

Sommaire

CE document est un résumé détaillé en français des travaux réalisés dans cette thèse. L'introduction et les conclusions sont traduites directement du manuscrit en anglais pour une meilleure compréhension du contexte. Les chapitres concernant les développements et résultats théoriques sont présentés sous forme synthétique, avec seulement les principaux développements et résultats.

A.1 Introduction

Peu importe la façon dont elles sont construites et conçues, toutes les structures se détériorent au cours de leur durée de vie. L'évaluation de la santé de ces structures, la prévision en temps de leurs dégâts et la détection de toute défaillance possible est essentielle pour des raisons de sécurité.

Le concept de diagnostic de l'état d'une structure est généralement nommé "Structural Health Monitoring". Cette surveillance est largement appliquée à diverses structures, comme

par exemple toutes les formes d'infrastructures civiles, des structures mécaniques et de l'aérospatiale, des instruments acoustiques et des centrales nucléaires.

Dans le domaine du génie civil, l'analyse modale est devenue un outil majeur dans la but de l'identification et de l'amélioration des caractéristiques dynamiques des structures de génie civil. Cet intérêt est principalement attribuable au fait que les paramètres modaux peuvent fournir une base pour la détermination des propriétés physiques telles que la masse, la rigidité et l'amortissement de la structure dû à la relation directe entre le modal et les paramètres physiques.

Dans les deux dernières décennies, l'évaluation de la vulnérabilité sismique a toujours été un sujet d'actualité. Afin de fournir des stratégies propres à réduire les risques sismiques dans les zones urbaines, l'un des besoins essentiels est d'avoir des solutions fiables et abordables pour surveiller le comportement d'un batiment en temps réel et à long terme. La surveillance en temps réel et en continu d'une structure en service permet une utilisation optimale de cette structure, minimise les temps d'arrêt, et permet d'éviter les défaillances catastrophiques. Telle est l'idée de base derrière la surveillance de santé structurale basée sur la vibration continue, et la nécessité des méthodes efficaces et robustes capables d'effectuer un traitement automatique de grandes quantités de données recueillies en continu.

Lorsque la surveillance de la santé structurelle continue à base de vibrations est appliquée sur la structure d'une bâtiment, les excitations ambiantes jouent un rôle important. D'abord, parce que les bâtiments concernés dans cette étude sont caractérisés par leur très grande taille et de conception complexe qui rend difficile une excitation artificielle, et deuxièmement, parce que les vibrations ambiantes sont toujours présentes dans un bâtiment, ce qui en fait un élément utile à enregistrer en continu.

En dépit des efforts remarquables dans ce contexte, le savoir-faire d'utilisateur n'est pas totalement écarté dans la plupart des méthodes proposées d'analyse modale automatiques, en particulier concernant la sélection de certains paramètres. À cet égard, l'idée principale de cette thèse est d'estimer les paramètres modaux de vibrations ambiantes d'une manière fiable, robuste et automatique en relevant les défis suivants:

- Des batiments de grande hauteur;
- Des signaux multi-composantes;
- Des amplitudes faibles et amorties de façon exponentielles;
- Une durée temporelle longue;
- Des modes de fréquences rapprochées;
- Des niveaux faible de rapport signal à bruit.

Les méthodes existantes ont des limitations en plusieurs aspects. De nombreuses méthodes permettant d'estimer automatiquement les paramètres modaux du signal, telles que

une méthode automatique de décomposition dans le domaine frequentiel, ne fournissent pas une estimation fiable du facteur d'amortissement, ce qui est le but principal de cette thèse. D'autres méthodes ne sont pas adaptées au contexte des signaux multi-composants, telle que la technique de décrémentation aléatoire. Pour appliquer ces méthodes sur des signaux multi-composantes, les composantes de signal doivent d'abord être filtrées. Beaucoup des méthodes existantes sont très sensibles au bruit, comme la méthode d'identification automatique de sous-espace où certain modes ne sont pas identifiés. D'autres procédés ne sont pas appropriés pour un suivi temporel de l'analyse modale, comme l'algorithme de classification et le procédé de filtrage dans le domaine temporel. Le premier nécessite une initialisation préliminaire manuelle avant chaque application ce qui reduit son efficacité, et la seconde, devient longue à appliquer dans le cas d'une excitation inconnue, et lors de modes de fréquence rapprochées. La sélection des pôles physiques est une tâche très critique pour presque toutes les méthodes existantes. La plupart consiste à seuiller des pics qui nécessite une phase d'étalonnage avant l'analyse. Ce processus d'étalonnage peut prendre beaucoup de temps selon la structure analysée.

Le type de signaux que nous considérons dans cette thèse est le résultat d'une convolution en temps entre la réponse impulsionnelle du système et la sollicitation du sol. Par conséquent, cette thèse est consacrée à la résolution des problèmes suivants liés à la nature du signal étudié et aux défis susmentionnés :

- Pour estimer les paramètres modaux d'un signal, la réponse impulsionnelle du signal doit être extraite à partir des sollicitations du sol, en mettant l'accent sur l'importance d'obtenir une signature qui est équivalente à la réponse impulsionnelle de système.
- Nous devons concevoir un modèle de signal qui correspond du contexte d'une signature estimée multi-mode.
- Nous devons proposer une méthode pour estimer automatiquement les paramètres modaux de la signature multi-composante. Un tel procédé doit gérer la détection des modes physiques, en tenant compte des modes de fréquences rapprochées et les plus amorties.
- Pour assurer la robustesse de l'approche proposée, nous devons proposer une méthode paramétrique non biaisée, qui ne dépend pas de la résolution de l'estimateur spectrale utilisée.
- Comme la méthode paramétrique est itérative par nature, nous devons proposer une méthode pour résoudre le problème de l'initialisation.

A.2 Technique du décrément aléatoire sans filtre préliminaire

La technique de décrément aléatoire (RDT) est une méthode proposée par Cole [Col68] en 1968 comme une méthode efficace pour extraire une signature notée RDS équivalente à la

réponse impulsionnelle de système. En conséquence, dans le cadre de ce travail, dans le but de relever le défi de la convolution dans le domaine temporel entre la réponse impulsionnelle et le bruit sismique, nous avons proposé d'utiliser d'abord la technique de décrément aléatoire.

Lorsque la technique de décrément aléatoire a d'abord été proposé, elle n'a pas été appliquée directement à une série temporelle au plusieurs composantes, mais uniquement à un système a un seul degré de liberté (SDOF). Les données ont été nécessairement filtrées avant l'application de la RDT (Fig. A.1).

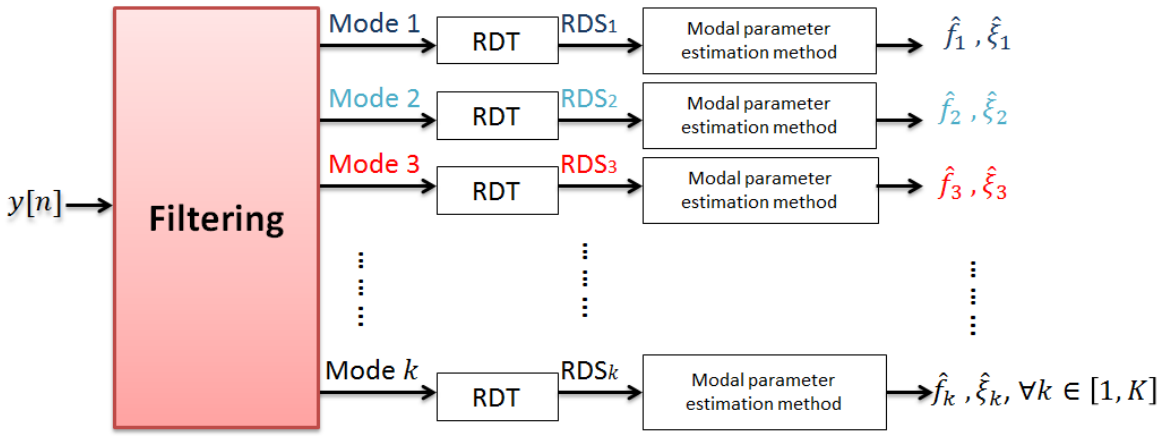

Figure A.1: Le concept général de la technique de décrément aléatoire.

Toutefois, il est bien connu que le processus de filtrage est une étape critique en particulier dans les situations où les données sont difficiles à analyser, à savoir, un faible rapport signal sur bruit, des modes de fréquences proches, et fortement amorties, *etc.*, qui sont les caractéristiques de presque tous les signaux du monde réel qui ont généralement un grand nombre de modes.

En conséquence, le filtrage est une des étapes la plus délicate en traitant avant la RDT. Le réglage manuel du processus de filtrage prends beaucoup de temps, et est totalement dépendant de l'utilisateur. Comme l'objectif principal de ce travail est d'automatiser le processus d'estimation des paramètres modaux en utilisant la RDT, alors le processus de filtrage préliminaire avant l'analyse de RDT est ignoré. Cette procédure est appelée technique de décrément aléatoire sans filtrage qui mène à l'estimation de la signature de décrément aléatoire Multimode (MRDS) (Fig. A.2).

Une MRDS se caractérise par le même nombre de modes K, le même facteur d'amortissement ξ_k et la même fréquence f_k que la réponse impulsionnelle $h[n]$ de la vibration mesurée du bâtiment $y[n]$, mais pas la même phase initiale ni le même amplitude initiale, vu que ces deux paramètres sont modifiés en raison du principe de la moyenne de la RDT.

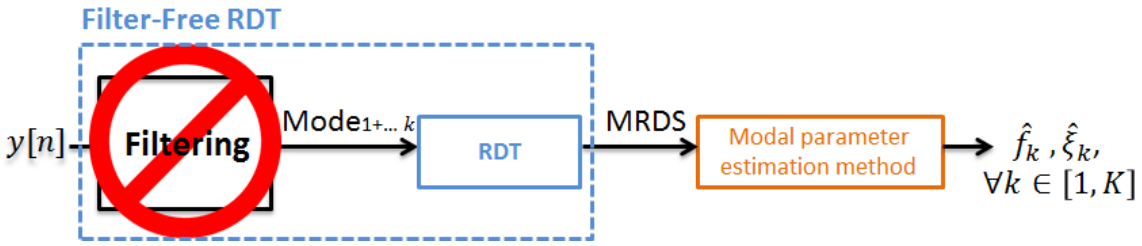

Figure A.2: Illustration de la technique de décrément aléatoire sans filtrage.

La vibration mesurée du bâtiment $y[n]$ est donnée par

$$\begin{aligned} y[n] &= \mathfrak{g}[\mathfrak{n}] + e[n], \\ \text{où} \quad \mathfrak{g}[\mathfrak{n}] &= h[n] * p[n] \end{aligned} \tag{A.1}$$

$$\text{avec} \quad h[n] = \sum_{k=1}^{K} A_{0k} \exp^{-2\pi f_k \xi_k n} \sin(\omega_{Dk} n + \phi_{0k}), \forall k \in [1, K], \tag{A.2}$$

Où n est l'indice temporel discret, $\mathfrak{g}[\mathfrak{n}]$ est la partie exempte de bruit de vibration de la structure, $h[n]$ est la réponse impulsionnelle de cette structure. L'amplitude initiale ($A_{0k} = -1/\omega_{Dk}$), le facteur d'amortissement (ξ_k), la fréquence naturelle (f_k), la phase initiale (ϕ_{0k}), et le nombre de modes (K) sont les paramètres de $h[n]$. $\omega_{Dk} = 2\pi f_k \sqrt{1-\xi_k^2}$ est la pseudo-pulsation amortie, $p[n]$ et applelé le bruit sismique et $e[n]$ est un bruit additif, ces bruits étant supposés blanc gaussien de moyenne nulle et de variance inconnue. L'opérateur de convolution est $*$.

Considérant tout ce qui précède, dans cette étude, nous avons proposé un modèle de signal pour la MRDS estimée $s[n]$

$$s[n] = \mathfrak{h}[\mathfrak{n}] + v[n], \tag{A.3}$$

$$\text{avec} \quad \mathfrak{h}[\mathfrak{n}] = \sum_{k=1}^{K} B_{0k} \exp^{-2\pi f_k \xi_k n} \sin(2\pi f_k n + \varphi_{0k}), \forall k \in [1, K], \tag{A.4}$$

où $v[n]$ est le résidu de la RDT considéré comme un bruit blanc gaussien additif de moyenne nulle et de variance inconnue. $\mathfrak{h}[\mathfrak{n}]$ est un processus multi-mode déterministe qui a les mêmes caractéristiques que $h[n]$ dans (A.2) mais pas pour la phase initiale φ_{0k} et l'amplitude initiale B_{0k}. Il convient de noter que le terme $\sqrt{1-\xi_k^2}$ de l'équation (A.2) est approximativement égale à 1 dans le modèle de signal considéré en raison du fait que le facteur d'amortissement est rarement supérieur à 10 %.

A.3 Estimation préliminaire des paramètres modaux

La question est maintenant de gérer la présence de modes multiples dans les MRDS estimées, dans le but d'estimer pour chaque mode, la fréquence et le facteur d'amortissement. À cette fin, nous avons proposé une méthode spectrale basée sur l'estimation spectrale de Welch

des MRDS. En outre, nous avons proposé d'inclure une méthode de détection, à savoir celle proposée par Durnerin [Dur99], pour détecter automatiquement le nombre de modes dans les MRDS.

A.3.1 Test d'hypothèse pour la détection et la suppression de pics

Le spectre de $s[n]$ de l'équation (A.3) peut être exprimée comme

$$\mathbf{S}_s[f] = \mathbf{S}_\mathfrak{h}[f] + \mathbf{S}_v[f], \tag{A.5}$$

où $\mathbf{S}_\mathfrak{h}[f]$ est le spectre de la partie sans bruit $\mathfrak{h}[\mathfrak{n}]$ et $\mathbf{S}_v[f]$ est le spectre de la partie aléatoire $v[n]$. Le but du détecteur est de décider pour chaque fréquence f du spectre $\mathbf{s}_s[f]$ si $s[n]$ se compose seulement de bruit $v[n]$, ou la somme de $\mathfrak{h}[\mathfrak{n}]$ et de bruit $v[n]$. A cet effet, un test statistique entre les deux hypothèses peut être écrit comme

$$T[f] = \frac{\mathbf{S}_s[f]}{\mathbf{S}_v[f]} \underset{\mathcal{H}_0}{\overset{\mathcal{H}_1}{\gtrless}} \lambda, \tag{A.6}$$

avec $T[f]$ une variable aléatoire, *lambda* le seuil de détection, et les deux hypothèses étant définies comme

$$\begin{aligned} \mathcal{H}_0 &: \mathbf{S}_s[f] = \mathbf{S}_v[f], \\ \mathcal{H}_1 &: \mathbf{S}_s[f] = \mathbf{S}_\mathfrak{h}[f] + \mathbf{S}_v[f], \end{aligned} \tag{A.7}$$

Dans cette étude, la densité de probabilité de $\mathcal{H}_1$ est inconnue. Nous allons considérer le détecteur tel que proposé dans [Dur99]. Une telle détection est basée sur le test de Neyman-Pearson où la probabilité de fausse alarme $\mathcal{PFA}$ est donnée *a priori* pour être en mesure de fixer le seuil λ tel que

$$\mathcal{PFA} = \int_\lambda^{+\infty} p_{T(f)|\mathcal{H}_0}(x)dx, \tag{A.8}$$

$p_{T(f)|\mathcal{H}_0} = \chi_2^r$ est la densité de probabilité de $T(f)$ sous l'hypothèse $\mathcal{H}_0$. En effet, il a été montré dans [Dur99] que tous les estimateurs de Fourier sous l'hypothèse $\mathcal{H}_0$ peuvent être considérés comme proportionnel à une variable aléatoire suivant une loi du χ_2^r à r degré de la liberté, avec r dépendant du nombre de segments et de leur chevauchement.

Le spectre de bruit $\mathbf{S}_v[f]$ de l'équation (A.5) est inconnu et doit donc être estimé afin d'appliquer l'équation (A.6).

A.3.2 Estimation de la ligne de fond de bruit

Deux types d'erreurs peuvent être rencontrées dans l'estimation du spectre de bruit: la sous-estimation et la surestimation. Dans le premier cas, certains des modes peuvent être identifiés

à tort comme du bruit. Dans le second cas, les pics de bruit pourraient être considérés comme des modes et provoquer de fausses alarmes. Ces deux erreurs doivent être évitées afin d'assurer la robustesse de l'approche.

Le spectre de bruit inconnu $\mathbf{S}_v[f]$ est etimée et notée $\hat{\mathbf{S}}_v[f]$ par un processus itératif; à savoir, une technique de filtrage multipasses développée dans [Dur99].

Cette technique est initialisée avec un filtre médian

$$\hat{\mathbf{S}}_{v1}[f] = FILT_{med}\{\mathbf{S}_s[f - \frac{(L_f - 1)}{2}, \cdots, f + \frac{(L_f - 1)}{2}]\}, \tag{A.9}$$

où $\hat{\mathbf{S}}_{v1}[f]$ est l'estimation de bruit de la première itération, $FILT_{med}\{\cdot\}$ est le filtre médian, et L_f est un entier impair spécifiant la longueur de la fenêtre de filtre glissante. Normalement L_f est défini comme

$$3B_{main}(\frac{F_s}{f_{res}}) \leq L_f \leq 4B_{main}(\frac{F_s}{f_{res}}), \tag{A.10}$$

avec B_{main} étant le nombre de bins entre les deux zéros du lobe principal de la fenetre spectrale pour la fenetre de $Hamming$ $B_{main} = 4$. F_s est la fréquence d'échantillonnage du signal, et f_{res} est la résolution en fréquence du spectre.

Le procédé consiste en P itérations de filtrage non linéaire. L'estimation du spectre de bruit est raffiné à chaque itération $\forall p \in [1, P]$ en supprimant les pics appartenant au spectre $\mathbf{S}_p[f]$. Le spectre final correspond à l'estimation de la ligne de fond du bruit $\hat{\mathbf{S}}_p[f]$.

Chaque itération comporte deux étapes. Dans la première étape, les pics correspondants à $\mathcal{H}_1$ sont éliminés par l'application du test d'hypothèse décrite dans la paragraphe A.3.1, avec une probabilité de fausse alarme dénommé $\mathcal{PFA}_v$ et le spectre de bruit estimé $\hat{\mathbf{S}}_{p-1}[f]$. La deuxième étape lisse la partie restante $\mathbf{S}_p[f]$ par un filtre à moyenne glissante de M points. L'estimation du spectre final du bruit $\hat{\mathbf{S}}_v[f]$ est la sortie après p itérations. Le choix du nombre P est fixé à 3 à 5 itérations de sorte que l'estimation du spectre de bruit ne change plus.

A.3.3 Détection des modes et estimation des fréquences

Dès que le spectre de bruit est estimé, les pics du spectre $\mathbf{S}_S[f]$ peuvent être calculés en utilisant l'équation (A.6) où

1- λ dans l'équation (A.6) est déduite d'une probabilité de fausse alarme $\mathcal{PFA}_d$ comme dans l'équation (A.8).

2- $\mathbf{S}_v[f]$ dans l'équation. (A.6) est substitué en utilisant le spectre de bruit $\hat{\mathbf{S}}_v[f]$ du paragraphe A.3.2.

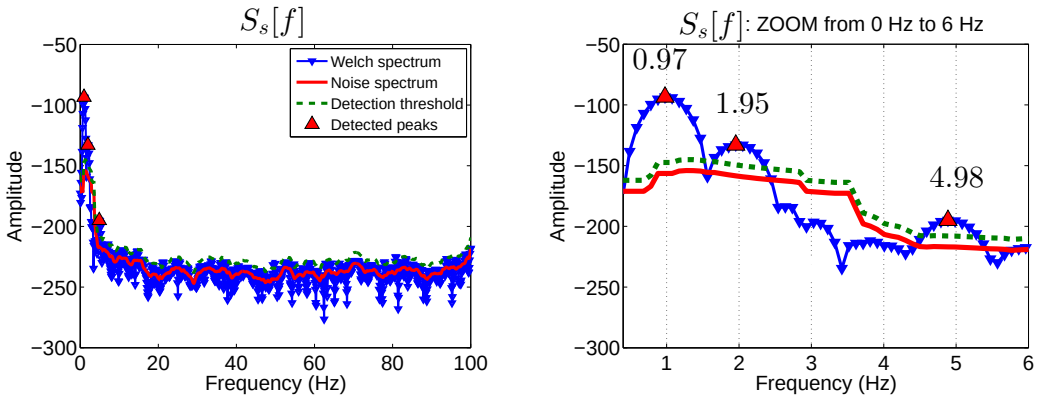

(a) (b)

Figure A.3: (a) Application de la méthode de détection de pic sur le spectre de Welch d'un signal simulé avec $f = 1, 2$ et 5 Hz et $\xi = 1, 2$ et 3%, respectivement, (b) un zoom sur les trois modes détectés.

Les pics sont définis comme étant le sommet des pics au-dessus du seuil de détection λ. Le nombre de modes K de $s[n]$ est estimé comme le nombre de pics détectés. Dans [Dur99] la technique d'adjustement de fenêtre spectrale est utilisée pour estimer la fréquence du pic. Toutefois, dans cette étude, puisque seules des estimations approximatives sont souhaitées dans l'estimation préliminaire des paramètres modaux, le maximum de la forme de cloche est défini comme étant la fréquence f de chaque pic.

La détection de pic est illustrée sur la Fig. A.3 avec un signal simulé de 180000 points, échantillonné à 200 Hz, se composant de trois modes situés à 1 Hz, 2 Hz, et de 5 Hz et amorties à 1%, 2 % et 3% respectivement. Le seuil de détection est calculé avec une probabilité de fausse alarme $\mathcal{PFA}_v = 0,1$, et une autre probabilité de fausse alarme de l'estimation du spectre de bruit $\mathcal{PFA}_d = 0,1$.

La Fig. A.3 illustre la procédure de détection de mode et de l'estimation de la fréquence. Les trois modes d'intérêts sont correctement identifiés sur l'estimation de fréquence, avec une erreur normalisée $e_{\hat{f}'} = |f - \hat{f}'|/f \leq 0.03$ %.

A.3.4 Estimation du facteur d'amortissement

L'estimation du facteur d'amortissement pour tous les modes estimées des MRDS est obtenue en utilisant le rapport des spectres de deux segments voisins sur $s[n]$. Ces deux segments sont de la même longueur $L_t = 2/3L_{rds}$ et décolé de 50 % (Fig. A.4 (a)).

Le périodogramme est calculé sur chaque segment en utilisant une fenêtre dite de *Hamming*. Sur les deux segments ce qui donne deux périodogrammes $\mathbf{S}_1[f]$. (Fig. A.4 (b)) et $\mathbf{S}_2[f]$ (Fig. A.4 (c)).

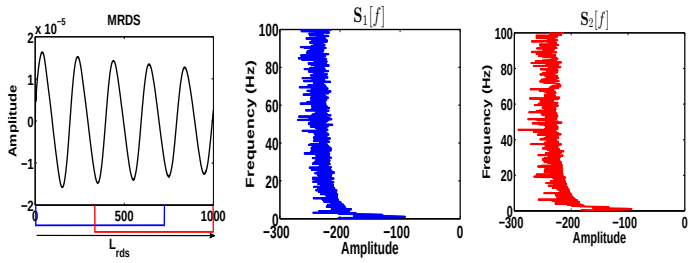

(a) (b) (c)

Figure A.4: (a) La MRDS est divisée en deux segments de longuer égale à 50% de chevauchement, (b) et (c)les périodogrammes de deux segments respectivement.

Ci-après, chaque segment est exprimé dans le domaine du temps sous forme de vecteur

$$\mathbf{s}_1 = [s[1], \cdots, s[\frac{2}{3}L_{rds}]], \tag{A.11}$$

$$\mathbf{s}_2 = [s[1 + \frac{1}{3}L_{rds}], \cdots, L_{rds}]], \tag{A.12}$$

où $\mathbf{s}_1$ et $\mathbf{s}_2$ sont les MRDS sur le premier et le deuxième segment, respectivement. Plus loin, $\mathbf{s}_1$ et $\mathbf{s}_2$ peuvent être décomposées comme la somme des modes

$$\mathbf{s}_j = \sum_{k=1}^{K} \mathbf{s}_{j,k}, \forall k \in [1, K], \tag{A.13}$$

où $j = 1, 2$ et $\mathbf{s}_{1,k} = [s_k[1], \cdots, s_k[2/3L_{rds}]]$, et $s_{2,k} = [s_k[1 + 1/3L_{rds}], \cdots, s_k[L_{rds}]]$ sont les vecteurs RDS du mode k (Eq. (A.3)) sur chaque segment.

Pour chaque segment j

$$\mathcal{FT}\{\mathbf{s}_j\} = \sum_{k=1}^{K} \mathcal{S}_{j,k}[f] = \mathcal{S}_j[f]. \tag{A.14}$$

A

$$\mathcal{FT}\{\mathbf{s}_{j,k}\} = \mathcal{S}_{j,k}[f], \tag{A.15}$$

où $\mathcal{FT}\{.\}$ désigne la transformée de Fourier discrète, et $\mathcal{S}_{j,k}$ est le vecteur du spectre notée $\mathcal{S}_{j,k}[f]$.

Puisque les modes sont répartis de façon indépendante dans le domaine fréquentiel, puis

$$\mathcal{S}_j[f_k] = \mathcal{S}_{j,k}[f_k]. \tag{A.16}$$

Donc

$$\frac{\mathcal{S}_2[f_k]}{\mathcal{S}_1[f_k]} = \frac{\mathcal{S}_{2,k}[f_k]}{\mathcal{S}_{1,k}[f_k]}. \tag{A.17}$$

Si nous supposons que le bruit dans la MRDS est faible, l'équation (A.4)conduit à

$$\frac{\mathcal{S}_2[f_k]}{\mathcal{S}_1[f_k]} = exp^{-\alpha\frac{1}{3}L_{rds}}, \tag{A.18}$$

où $\alpha = 2\pi f_k \xi_k$, avec f_k and ξ_k étant la fréquence et le facteur d'amortissement de la MRDS pour chaque mode k, $\forall k \in [1, K]$. Pour chaque pic détecté sur les fenêtres $1/3L_{rds}$ et $2/3L_{rds}$ le facteur d'amortissement est estimée par

$$\hat{\xi_k'} = \frac{\log\left(\mathcal{S}_1[f_k]\right) - \log\left(\mathcal{S}_2[f_k]\right)}{2\pi f_k \frac{L_{rds}}{3}}. \tag{A.19}$$

A.4 Estimation affinée des paramètres modaux

Une fois que le nombre de modes de la MRDS ainsi que les paramètres modaux associés sont estimés, nous proposons une méthode d'estimation paramétrique afin d'améliorer la résolution en fréquence et être en mesure de mieux séparer les modes de fréquences étroitement espacées par rapport à l'approche non-paramétrique. La méthode est basée sur une approche d'estimation du maximum de vraisemblance. Ainsi, cette méthode convient bien au modes de fréquence rapprochées.

Les paramètres de chaque mode de Eq. (A.3) forment un vecteur $\boldsymbol{\theta}$,

$$\boldsymbol{\theta} = [\boldsymbol{\theta}_1^T, \cdots, \boldsymbol{\theta}_k^T] = [B_{0k}, \xi_k, f_k, \varphi_{0k}]^T, \forall k \in [1, K], \tag{A.20}$$

où ^{T} est le symbole de transposition, et B_{0k}, ξ_k, f_k et φ_{0k} sont l'amplitude initiale, le facteur d'amortissement, la fréquence propre, et la phase initiale de la k^{th} mode respectivement.

L'estimation par le maximum de vraisemblance de $\boldsymbol{\theta}$ est considéré comme équivalent à l'approche des moindres carrés dans l'hypothèse d'un bruit additif gaussien blanc. Ainsi

$$\hat{\boldsymbol{\theta}} = \underset{\boldsymbol{\theta}\in\mathbb{N}^{4k}}{\arg\max}\, l_{MV}(\boldsymbol{\theta}) = \underset{\boldsymbol{\theta}\in\mathbb{N}^{4k}}{\arg\min}\, MC(\boldsymbol{\theta}), \tag{A.21}$$

$$MC(\boldsymbol{\theta}) = \sum_{n=-L/2}^{L/2} |s[n] - \mathfrak{h}[\mathfrak{n}; \boldsymbol{\theta}]|^2. \tag{A.22}$$

$MC(\boldsymbol{\theta})$ est la fonction des moindres carrés. $s[n]$ est la MRDS (Eq. (A.3)), $\mathfrak{h}[\mathfrak{n}; \boldsymbol{\theta}]$ est la partie sans bruit de Eq. (A.3) où tous les paramètres sont définis par $\boldsymbol{\theta}$.

La fonction $MC(\boldsymbol{\theta})$ est multidimensionnelle et non linéaire. Ainsi, une résolution directe de l'équation Eq. (A.22) est difficile en raison de la non-linéarité élevé de la fonction et le nombre de paramètres. Les techniques classiques d'optimisation tels que la descente de gradient, l'algorithme de Gauss-Newton et l'algorithme Espérance Maximisation EM ne garantissent pas la convergence vers le minimum global lorsque les minima locaux sont nombreux. Ce problème peut être résolu avec les approches de méta-heuristique. Dans le cadre de cet article, nous avons proposé d'utiliser la technique de recuit simulé [Kir84] pour son efficacité quand un extremum global désiré est caché dans de nombreux extrema locaux, et aussi à cause de sa mise en œuvre simple.

Cependant, la technique de recuit simulé nécessite l'initialisation de ses paramètres. Dans le cadre de notre travail, la méthode spectrale non-paramétrique proposée est appliquée dns le paragraphe A.3 pour initialiser ces paramètres (*cf.* Fig. A.5).

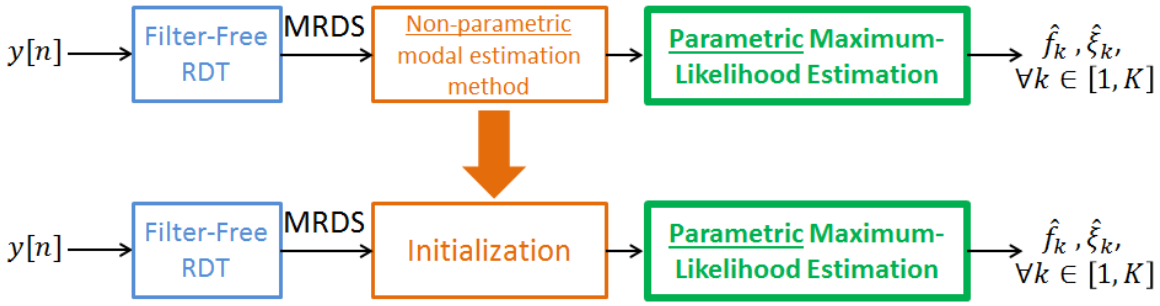

Figure A.5: L'étape non-paramétrique sert d'étape d'initialisation de la méthode paramétrique.

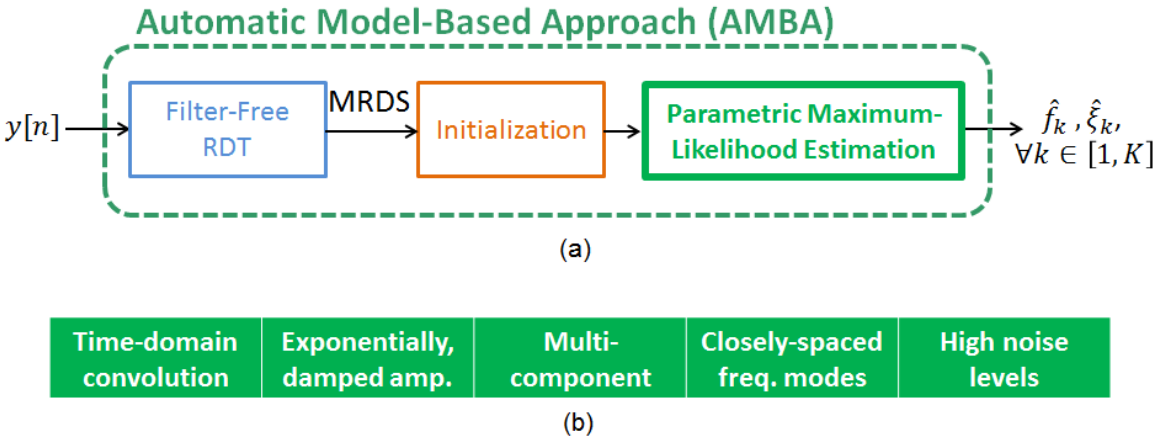

Figure A.6: (a) Les trois étapes proposées constituent la totalité de l'approche proposée AMBA. (b) Les défis de cette thèse que AMBA est capable d'aborder.

Ainsi les trois étapes présentée ci-dessus forment la totalité de l'approche proposée, comme indiqué dans la Fig. A.6, méthode appelée "Automatic Model-Based Approach" ou AMBA. AMBA est alors capable de gérer simultanément tous les défis prédéfinis de cette étude (*cf.*

paragraphe A.1).

A.5 Application de l'approche proposée "AMBA"

Préalablement à l'application de la méthode AMBA sur les signaux à l'étude, les paramètres de configuration de la RDT doivent être fixés.

Dans ce contexte, nous avons accordé une attention particulière aux deux principaux paramètres qui intéressent principalement les physiciens, à savoir le N_{sig} la longueur du signal en périodes et N_{rds} la longueur de la MRDS en périodes. Cette paragraphe est réalisée en simulant la réponse d'un système SDOF avec un seul degré de liberté $K = 1$ dans l'équation (A.2).

La présente étude a conclu à la meilleure combinaison de N_{sig} et N_{rds} comme indiqué dans la Fig. A.7.

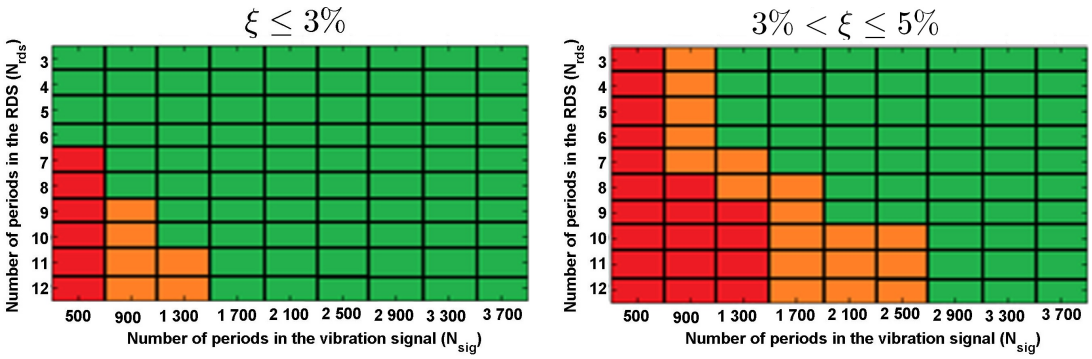

Figure A.7: L'erreur d'estimation E de: (a) $\xi \leq 3\%$ et (b) $3\% < \ xi \leq 5\%$. Bonnes régions en vert avec $E \leq 10\%$, régions intermédiaires en orange avec $10\% < E \leq 20\%$ et les mauvaises régions en rouge avec $E > 20\%$.

où l'erreur d'estimation E est calculée comme suit

$$E = \frac{1}{D} \sum_{i=1}^{D} \frac{|\xi - \hat{\xi}_i|}{\xi}, \tag{A.23}$$

où ξ est le facteur d'amortissement simulé, D est le nombre de réalisations de bruit, $\hat{\xi}_i$ est le facteur d'amortissement estimée $\forall i \in [1, D]$.

La région verte indique une erreur d'estimation $E \leq 10\%$, la région orange 10% $E \leq 20\%$, et la région rouge $E > 20\%$. En conséquence, il est toujours recommandé d'être dans la région verte pour une estimation du facteur d'amortissement acceptables.

A.5.1 Sur des signaux simulés

L'application de l'AMBA en termes de précision et de fiabilité des estimations est d'abord étudié sur des données simulées. Ces données sont générées en utilisant un modèle de bâtiment de grande hauteur défini comme un modèle de poutre continue [Per+13].

Six modèles des bâtiments de 50 étages sont simulés comme indiqué dans le tableau Tab. A.1.

Table A.1: Les six signaux simulés désignés par Top_1, Top_2, Top_3, Top_4, Top_5, et Top_6, où f indique la fréquence simulée en (Hz) et ξ le facteur d'amortissement simulé en (%).

	Bien-espacées				Quasi-espacés				Étroitement-espacés			
	Top_1		Top_2		Top_3		Top_4		Top_5		Top_6	
mode k	f	ξ	f	ξ	f	ξ	f	ξ	f	ξ	f	ξ
1^{ere}	1	1	1	0.5	0.4	1	0.4	0.5	1	1	1	0.5
2^{eme}	2	2	2	0.7	1.2	2	1.2	0.7	1.2	2	1.2	0.7
3^{eme}	5	3	5	1	2	3	2	1	NA	NA	NA	NA
4^{eme}	7	4	7	1.5	NA	NA	NA	NA	NA	NA	NA	NA

Les six signaux simulés sont générés avec une longueur de 360000 de points, et une fréquence d'échantillonnage de 200 Hz. L'application de la méthode AMBA est testée avec différents niveaux de rapport signal sur bruit (RSB) 0 dB, 9 dB, et 15 dB.

La RDT sans filtre est appliquée sur les signaux simulés multi-composantes. Les MRDS estimées sont ensuite décimés à une fréquence de Nyquist de 20 Hz.

Lorsque l'estimation non-paramétrique préliminaire du paragraphe A.3 est appliquée sur les signaux simulés, il est clairement visible dans Fig. A.8, Fig. A.9, et Fig. A.10, que tous les modes d'intérêt pour chacun des signaux à l'étude sont correctement identifiés, même pour les cas de modes de fréquences rapprochées avec un très haut niveau de rapport signal-sur-bruit.

Ensuite, pour chacun des modes identifiés, une estimation de leur fréquence et de leur facteur d'amortissement est représentée sur la Fig. A.11 et la Fig. A.12. Il pourrait être considéré que ces estimations sont moins fiables pour le cas des modes de fréquences rapprochées en particulier lorsque le niveau de RSB est très élevé, ces estimation présentant une valeur moyenne des biais d'estimation inférieure à 10% pour la fréquence et à 15% pour le facteur d'amortissement.

Une telle estimation est améliorée par l'application de la méthode paramétrique présentée dans le paragraphe A.4. Comme on le voit dans la Fig. A.13 et la Fig. A.14 l'estimation de la fréquence et du facteur d'amortissement pour chacun des modes identifiés est plus fiable. La valeur moyenne des biais d'estimation de la fréquence et du facteur d'amortissement est inférieur à 5% et 10% respectivement.

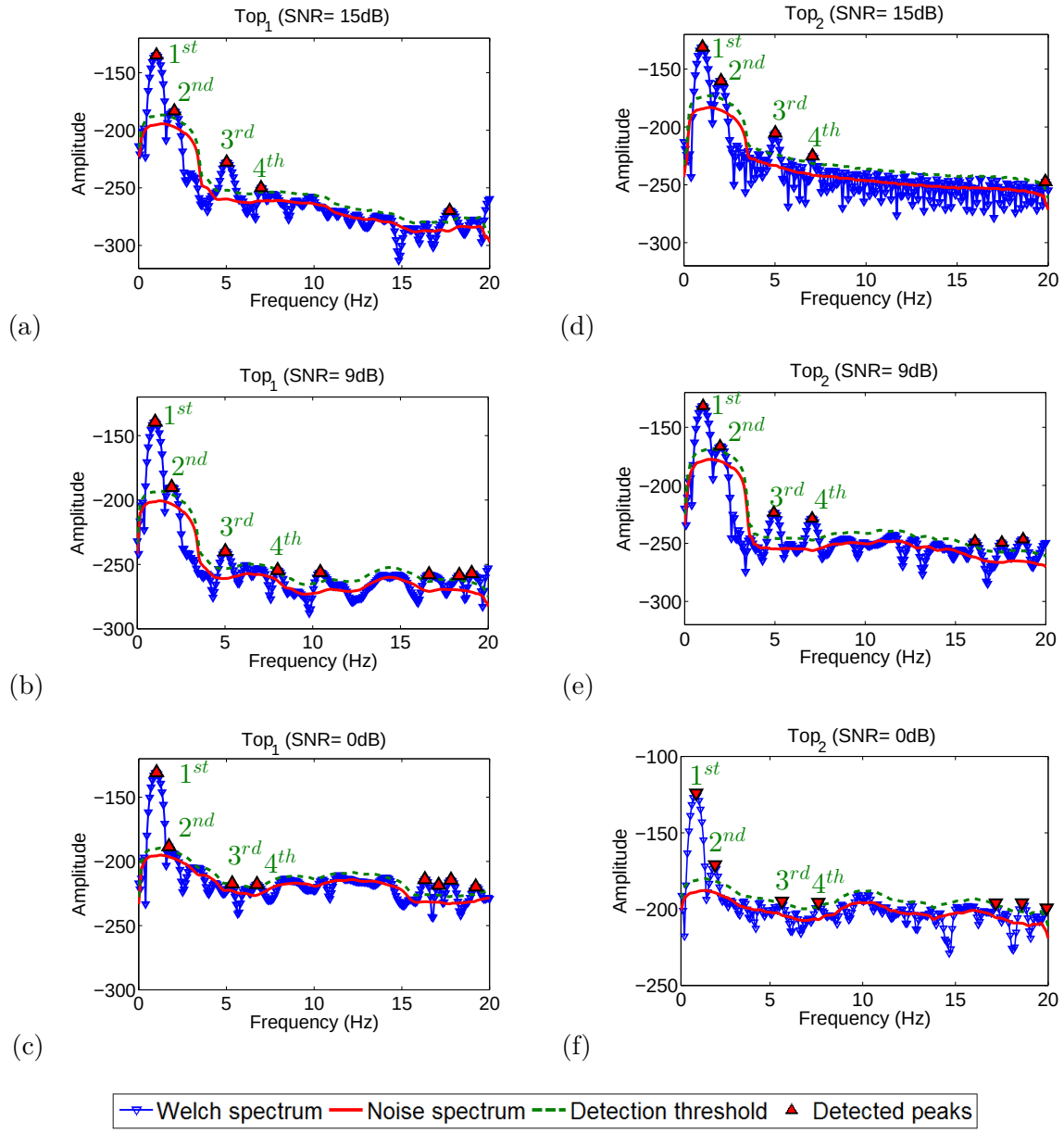

Figure A.8: Application de la méthode automatique de détection de pic sur le spectre de Welch de la MRDS de Top_1 avec un niveau de RSB (a) 15 dB, (b) 9 dB, et (c) 0 dB, et sur celui de Top_2 avec le niveau de (d) 15 dB, (e) 9 dB, et (f) 0 dB RSB. Les modes d'intérêt sont marqués en vert.

A des fins de comparaison, la RDT classique avec in processus de filtrage manuel préliminaire est appliquée sur les six signaux simulés. Un filtre de *Butterworth* est utilisé pour filtrer les signaux. Afin d'obtenir l'ordre et de la bande passante nécessaire pour filtrer chaque mode k, le filtre a été conçu avec une bande passante fréquence W_p, une fréquence bande d'arrêt W_s, une ondulation de la bande passante R_p, et une bande d'arrêt d'atténuation R_S.

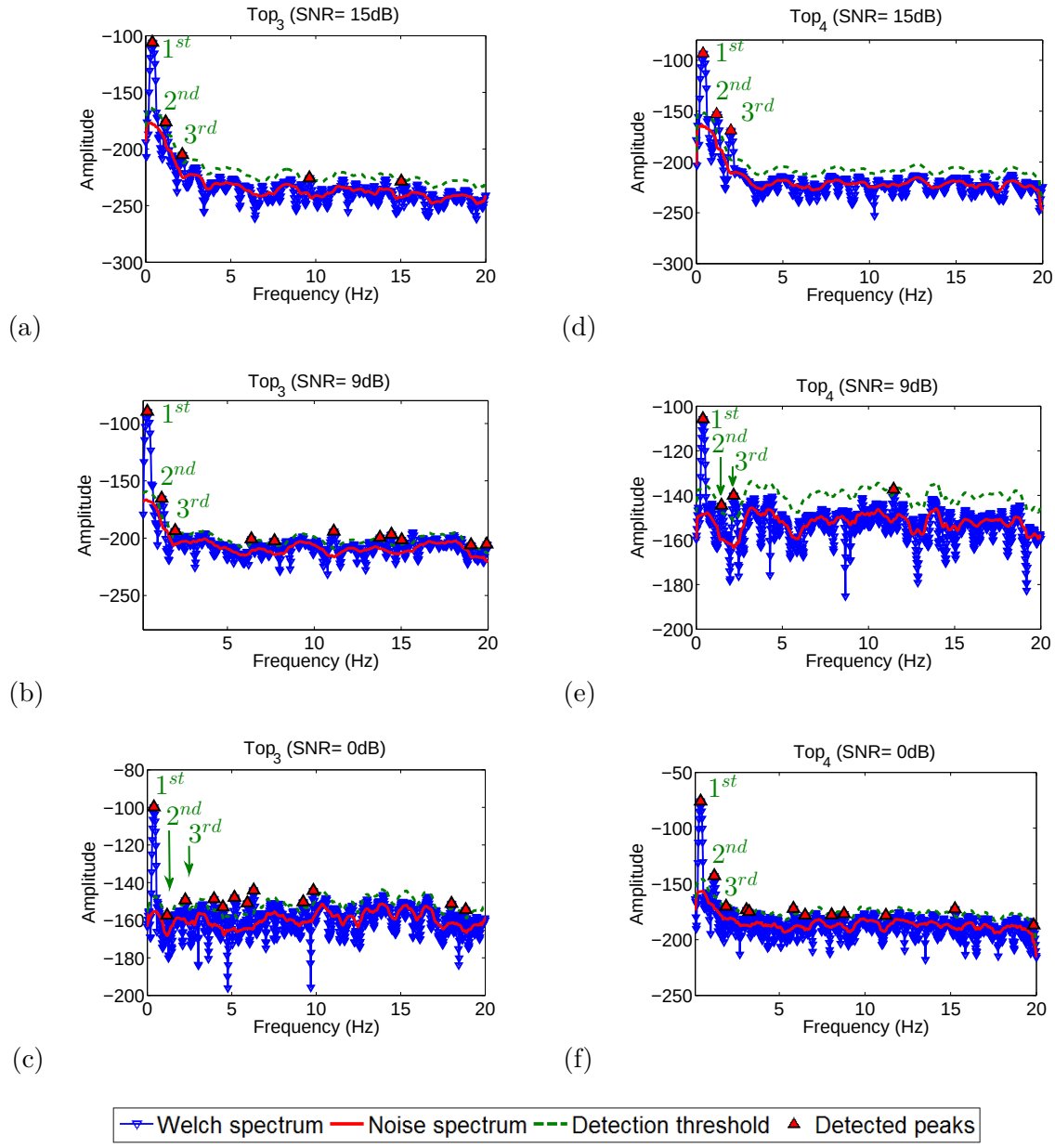

Figure A.9: Application de la méthode automatique de détection de pic sur le spectre de Welch de la MRDS de Top_3 avec un niveau de RSB (a) 15 dB, (b) 9 dB, et (c) 0 dB, et sur celui de Top_4 avec le niveau de (d) 15 dB, (e) 9 dB, et (f) 0 dB RSB. Les modes d'intérêt sont marqués en vert.

Les résultats comparatifs comme représentés sur les Fig. A.15 et Fig. A.16 indiquent la fiabilité de l'approche automatique proposée (AMBA) dans cette thèse. AMBA est capable de donner des résultats très précis automatiquement pour l'ensemble des modes. En outre, il montre son importance pour les cas où le filtrage devient très difficile comme dans le cas des modes rapprochées, d'où l'importance du la suppression du processus de filtrage avant l'application de la RDT.

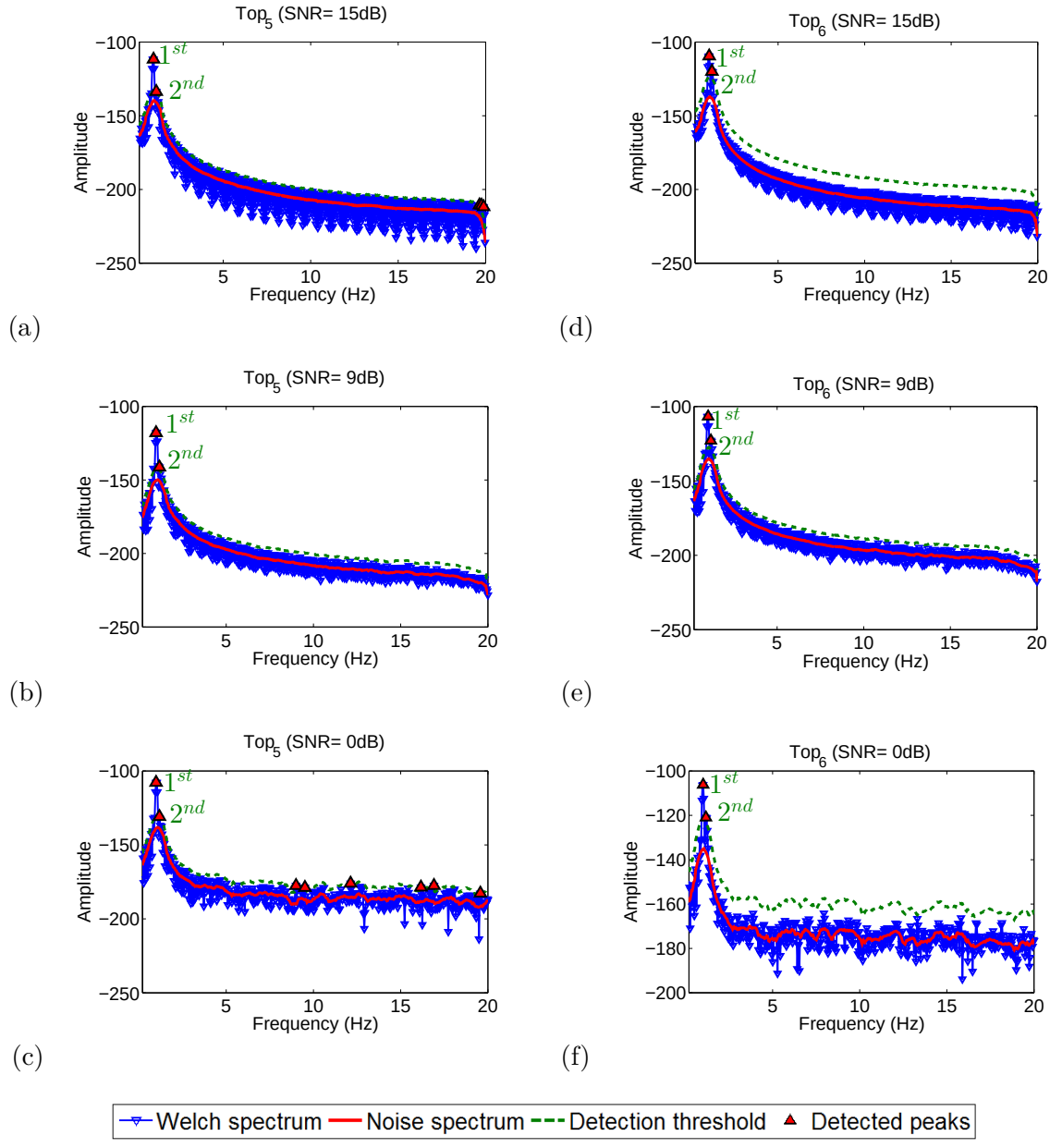

Figure A.10: Application de la méthode automatique de détection de pic sur le spectre de Welch de la MRDS de Top_5 avec un niveau de RSB (a) 15 dB, (b) 9 dB, et (c) 0 dB, et sur celui de Top_6 avec le niveau de (d) 15 dB, (e) 9 dB, et (f) 0 dB RSB. Les modes d'intérêt sont marqués en vert.

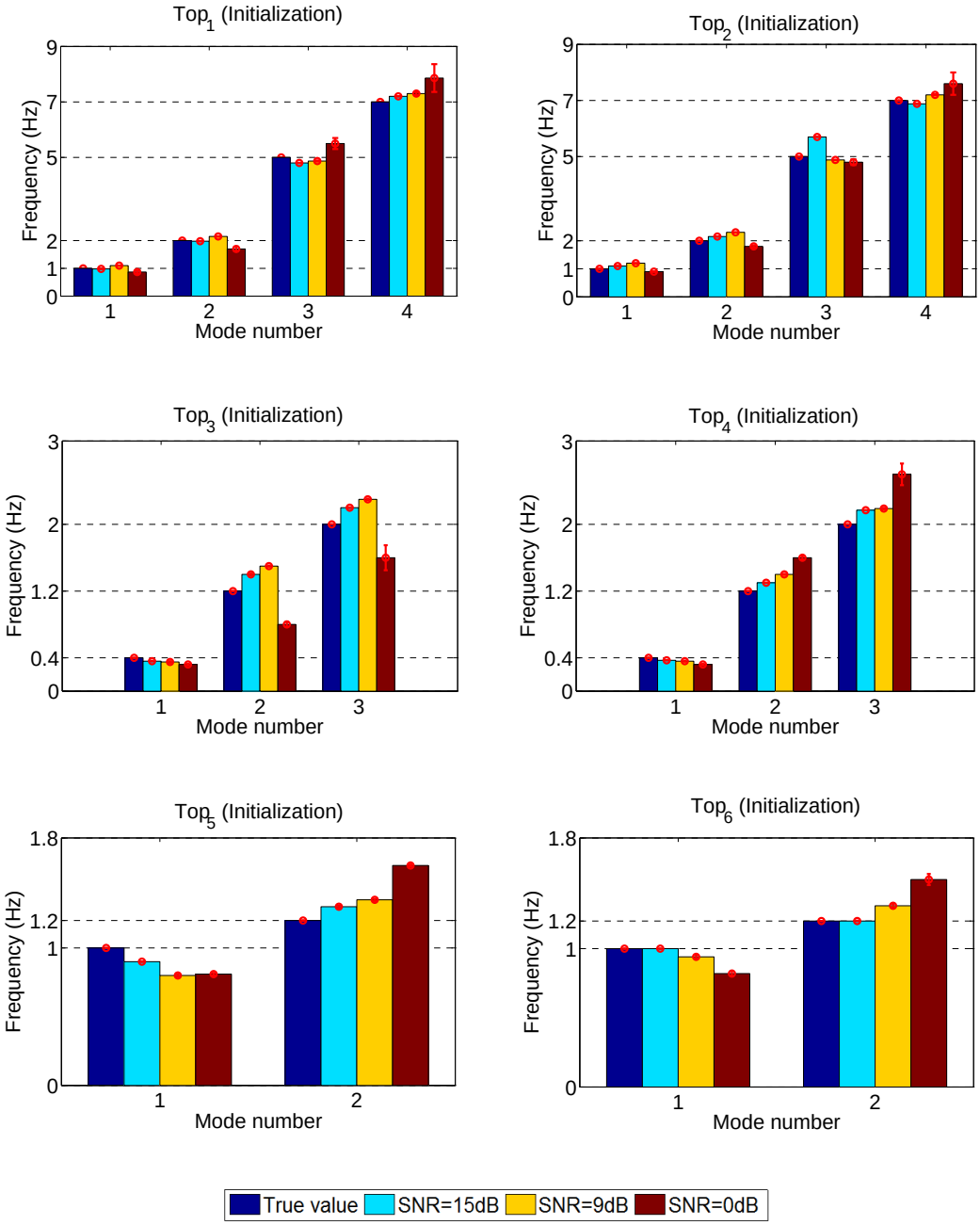

Figure A.11: Moyenne des estimations de fréquence par l'étape d'initialisation pour les trois niveaux de SNR différents ($15dB$ bleu, $9dB$ jaune, $0dB$ de rouge foncé), et leurs vraies valeurs associées (bleu foncé), avec leurs écarts-types de Top_1 (en haut à gauche) pour Top_6 (en bas à droite).

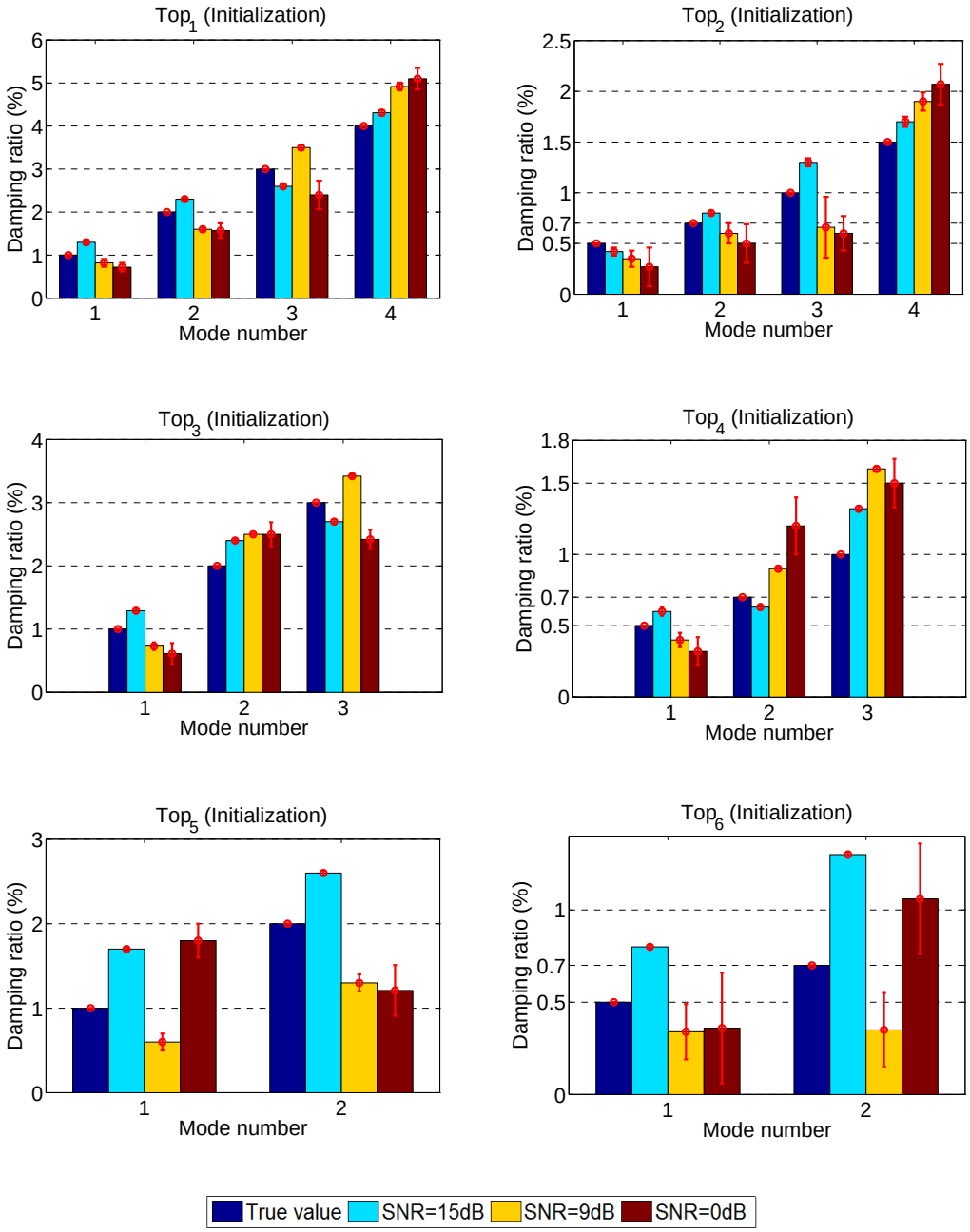

Figure A.12: Moyenne des estimations du facteur d'amortissement estimé par l'étape d'initialisation pour les trois niveaux de RSB différents ($15dB$ bleu, $9dB$ jaune, $0dB$ de rouge foncé), et leurs vraies valeurs associées (bleu foncé), avec leurs écarts-types de Top_1 (en haut à gauche) pour Top_6 (en bas à droite).

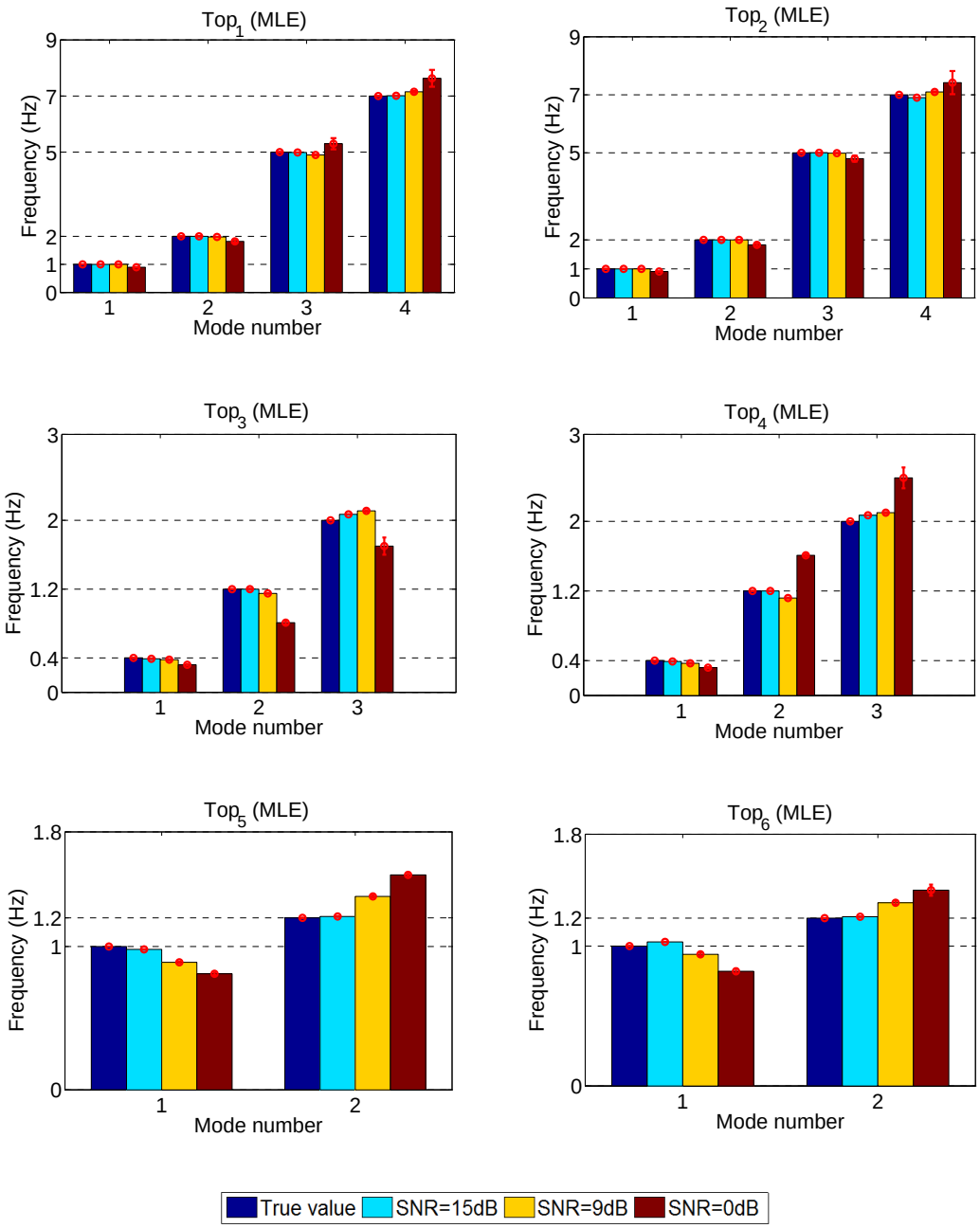

Figure A.13: Moyenne des estimations de fréquence estimé par l'étape de MV pour les trois niveaux de RSB différents ($15dB$ bleu, $9dB$ jaune, $0dB$ de rouge foncé), et leurs vraies valeurs associées (bleu foncé), avec leurs écarts-types de Top_1 (en haut à gauche) pour Top_6 (en bas à droite).

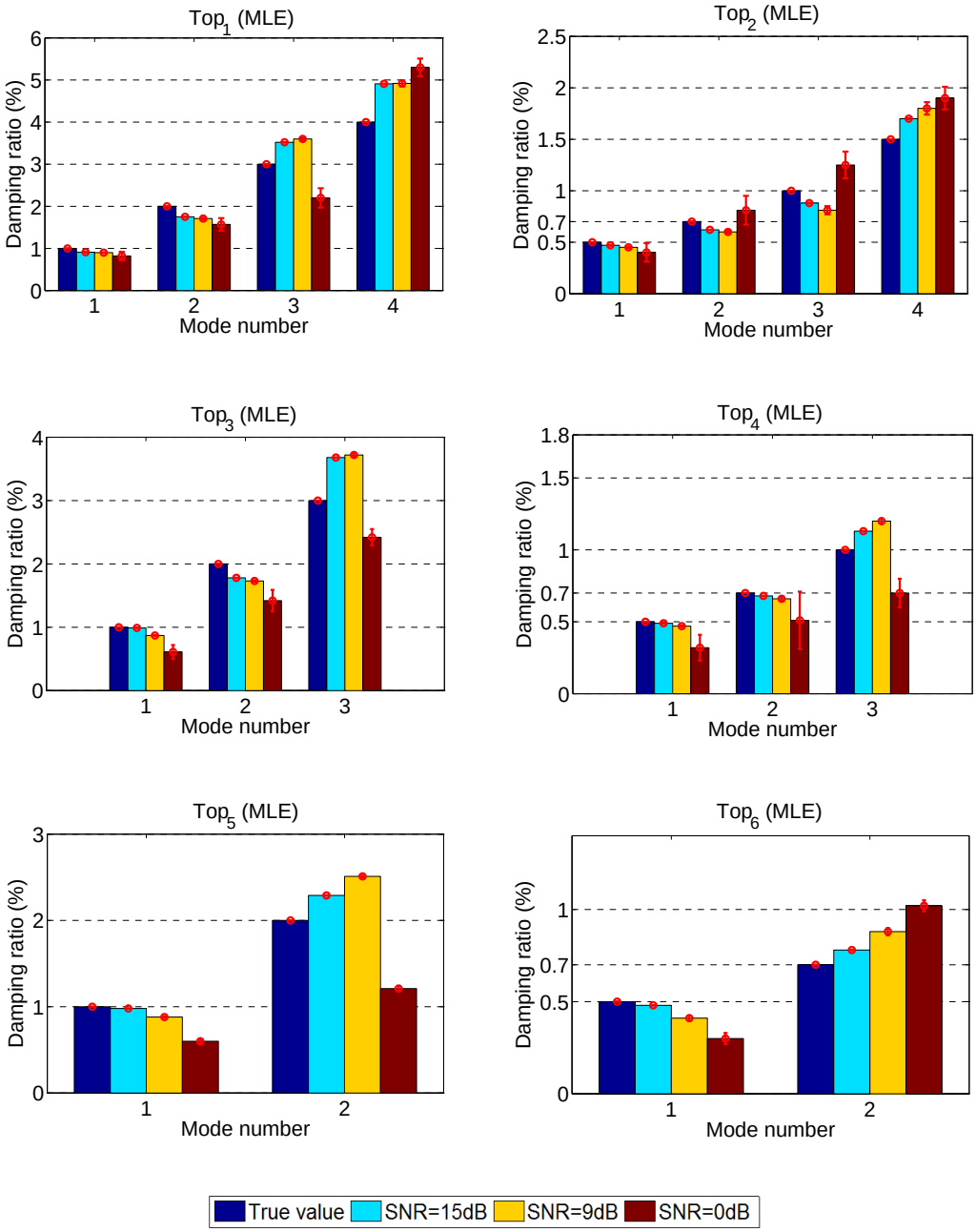

Figure A.14: Moyenne des estimations du facteur d'amortissement estimé par l'étape de MV pour les trois niveaux de RSB différents ($15dB$ bleu, $9dB$ jaune, $0dB$ de rouge foncé), et leurs vraies valeurs associées (bleu foncé), avec leurs écarts-types de Top_1 (en haut à gauche) pour Top_6 (en bas à droite).

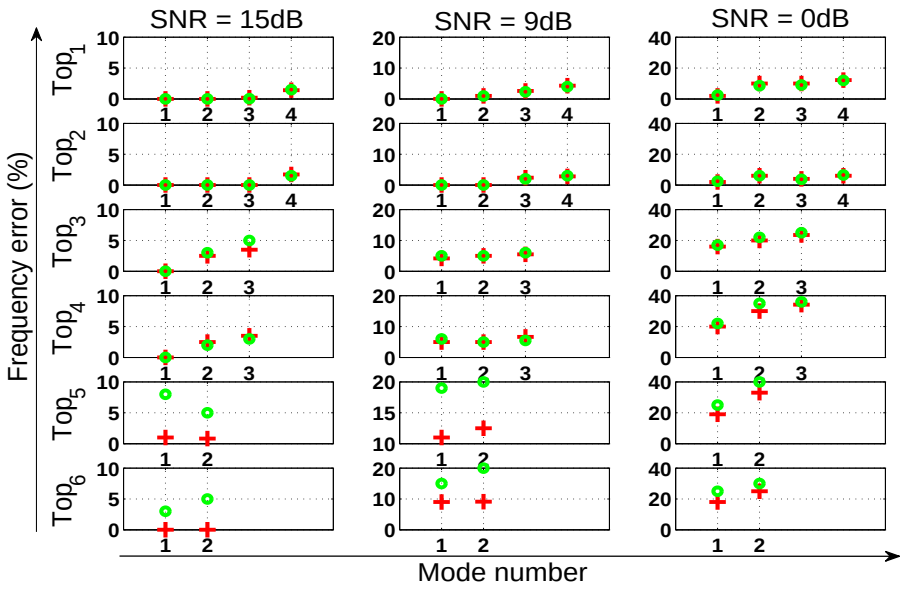

Figure A.15: Fréquence estimé par la méthode AMBA d'estimation automatique (+) (RDT sans filtre), et par une approche d'estimation manuelle (RDT pré-traitées par filtrage) (o).

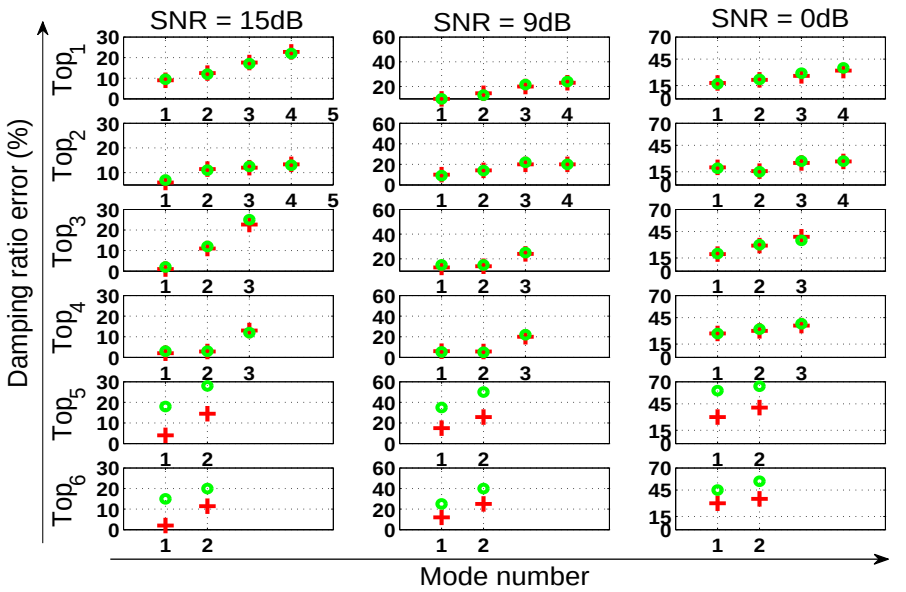

Figure A.16: Facteur d'mortissement estimé par la méthode AMBA d'estimation automatique (+) (RDT sans filtre), et par une approche d'estimation manuelle (RDT pré-traitées par filtrage) (o).

A.5.2 Sur des signaux réel

Ce paragraphe vise à étudier de la précision et l'efficacité de l'approche AMBA pour l'estimation de la fréquence et du facteur d'amortissement lorsqu'il est appliqué sur les bâtiments réels soumis à des vibrations ambiantes.

A cet effet, six signaux réels ont été choisis. Trois d'entre eux sont issus de batiments à Beyrouth (Liban) et les trois autres à Grenoble (France). Par souci de synthèse, seulement l'application de la méthode AMBA sur les tours de Beyrouth sera présentée dans ce paragraphe.

Les trois tours de Beyrouth sont ceux du projet Cap-sur-Ville. Ils sont nommés W (21 étages), V (18 étages) et X (16 étages), ils corresponde à 1 heure d'enregistrement(720 000 points) et échantillonné a $F_s = 200$ Hz.

La fréquence estimée et le facteur d'amortissement évalués par la méthode AMBA appliquée sur les tours W, X et V à Beyrouth sont respectivement présenté dans les figures A.17, A.18, et A.19. Les figures sont divisées en différentes zones par des lignes verticales noires, sur la base des valeurs de l'N_{rds} et les estimations connexes de la fréquence et du facteur d'amortissement. Le processus de fractionnement est lié à des critères pour classer le meilleur N_{rds} qui est capable de:

- détecter le nombre maximum de modes dans la mesure où une interprétation physique peut être établie,
- fournir l'erreur normalisée E la plus stable E (Eq. A.24.), par rapport à N_{rds}, ce qui indique unse stabilité des fréquences et les facteur d'amortissement. où l'erreur normalisée est définie comme

$$E = \frac{\sum_n |s[n] - \hat{s}[n]|^2}{\sum_n (s[n])^2}. \tag{A.24}$$

Les trois bâtiments ont été étudiés dans la direction longitudinale. Les figures A.17, A.18 et A.19 présentent respectivement l'estimation de fréquence, du facteur d'amortissement et l'erreur normalisée des tours W, X et V. Comme on le voit sur ces figures, tous les modes d'intérêt ont été correctement identifiés par la méthode de AMBA avec leur fréquence associée et facteur d'amortissement, ainsi que la région d'intérêt qui indique une plus grande stabilité de l'estimation des facteurs d'amortissement et des fréquences.

Les lignes en pointillés dans les trois figures sont considérées comme présentant des modes de torsion qui ont été observée dans la direction longitudinale seulement. Généralement, l'estimation des paramètres modaux est moins fiable lorsque des directions différentes sont considérées.

Le Tab. A.2 présente l'estimation moyenne du fréquence et du facteur d'amortissementpour les bâtiments de Beyrouth.

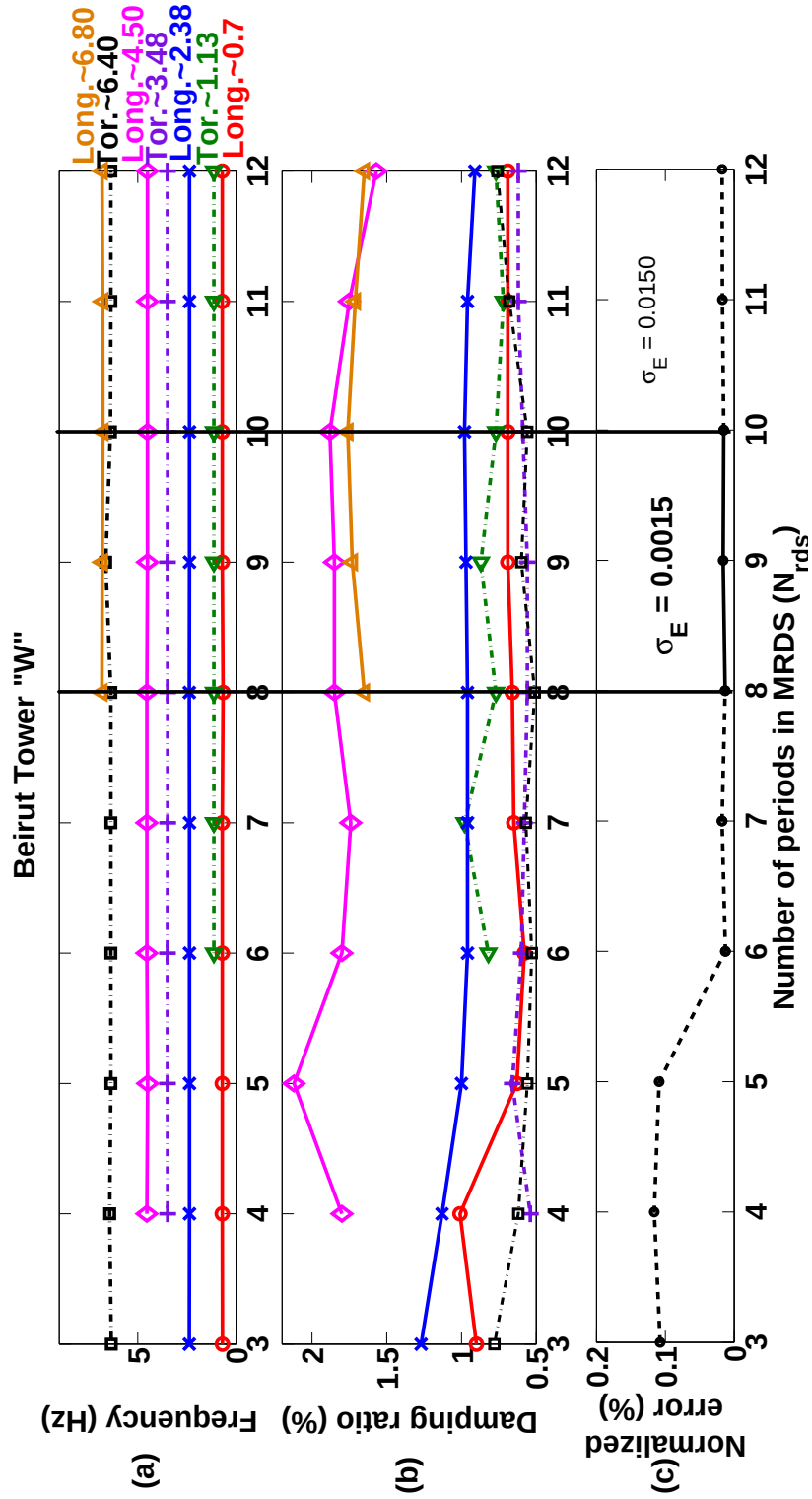

Figure A.17: (a) La fréquence, (b) le facteur d'amortissement et (c) l'erreur normalisée estimée par la méthode AMBA pour la tour W à Beyrouth (Liban) dans la direction longitudinal (long.). Tor. indique les modes de torsion observés dans la direction longitudinale. $sigma_E$ est l'écart type de l'erreur normalisée. La région d'intérêt est indiquée par σ_E en gras.

Table A.2: La moyenne et l'écart type de l'estimation de la fréquence et du facteur d'amortissement par la méthode AMBA des modes d'intérêt des signaux de tours de W, V et X.

	Tower W				Tower V				Tower X			
Region of interest	$8 \leq N_{rds} \leq 10$				$6 \leq N_{rds} \leq 8$				$10 \leq N_{rds} \leq 12$			
mode	$\bar{f}$	σ_f	$\bar{\xi}$	σ_ξ	$\bar{f}$	σ_f	$\bar{\xi}$	σ_ξ	$\bar{f}$	σ_f	$\bar{\xi}$	σ_ξ
1	0.69	0.0010	0.68	0.0173	0.83	0.0057	0.80	0.0306	0.90	0.0035	0.59	0.0057
2	*1.13*	0.0065	0.80	0.0577	*1.30*	0.0058	0.60	0.1442	*1.43*	0.0061	0.59	0.0119
3	2.37	0.0057	0.97	0.0100	2.81	0.00058	1.27	0.0306	3.12	0.0058	1.15	0.0503
4	*3.48*	0.0058	0.57	0.0173	*4.06*	0.0058	0.69	0.0635	*4.50*	0.0058	0.91	0.0228
5	4.52	0.0017	1.86	0.0173	5.57	0.0417	1.16	0.0200	5.92	0.0172	0.84	0.0300
6	*6.46*	0.011	0.55	0.0451	*7.49*	0.0936	1.07	0.1002	*8.07*	0.0172	0.33	0.0308
7	6.88	0.011	1.68	0.0153	NA	NA	NA	NA	NA	NA	NA	NA
Normalized Error E:												
$\bar{E}$	0.0014				0.0077				0.0205			
σ_E	0.0015				0.0011				0.0004			

Par rapport aux tours W et V, la fréquence fondamentale légèrement supérieure de la tour X comme indiqué dans le Tab. A.2 et la Fig. A.18 est expliquée par l'hauteur le moins grand de cette tour. Le rapport signal sur bruit de cette tour est le plus bas, sachant que ce rapport est connu pour augmenter avec le nombre d'étages. Cette tour est donc la plus sensible au bruit.

A.5.3 Suivi à long terme de variation modale

Ce paragraphe présente l'application de la méthode AMBA pour le suivi à long terme des variations modales. L'étude se déroule sur les trois tours de Beyrouth (Liban). Soixante-douze heures de données de vibration ambiante sont collectées en continu sur les trois tours. L'enregistrement démarre à 00:00, le 26 ^{eme} de mai 2011 et se termine à 23h00, le 28 ^{eme} mai 2011.

A partir de notre expérience de la méthode de AMBA et le suivi de variation modale, il est constaté que la première heure des enregistrements doit être traité séparément afin d'estimer certains paramètres *a priori*, comme K, f_k, ξ_k and N_{rds}. Dans ce cas, les résultats du paragraphe A.5.2 fournissent de tels paramètres nécessaires tels que présentés dans le Tab. A.2.

Comme le montrent les figures A.20 et A.21, le méthode de AMBA est capable de suivre les variations modales sur tous les modes des bâtiments étudées. La flèche noire dans les chiffres indiquent les variations simultanées sur les trois tours. Dans cette étude, une telle variation simultanée a été attribuée à des conditions environnementales plutôt du'à une détérioration physique dans le bâtiment. Ceci est, en fait, parce que les trois bâtiments sont très proches les uns des autres (environ 50 m de distance), et il a été supposé que les trois bâtiments ont subi les mêmes conditions environnementales.

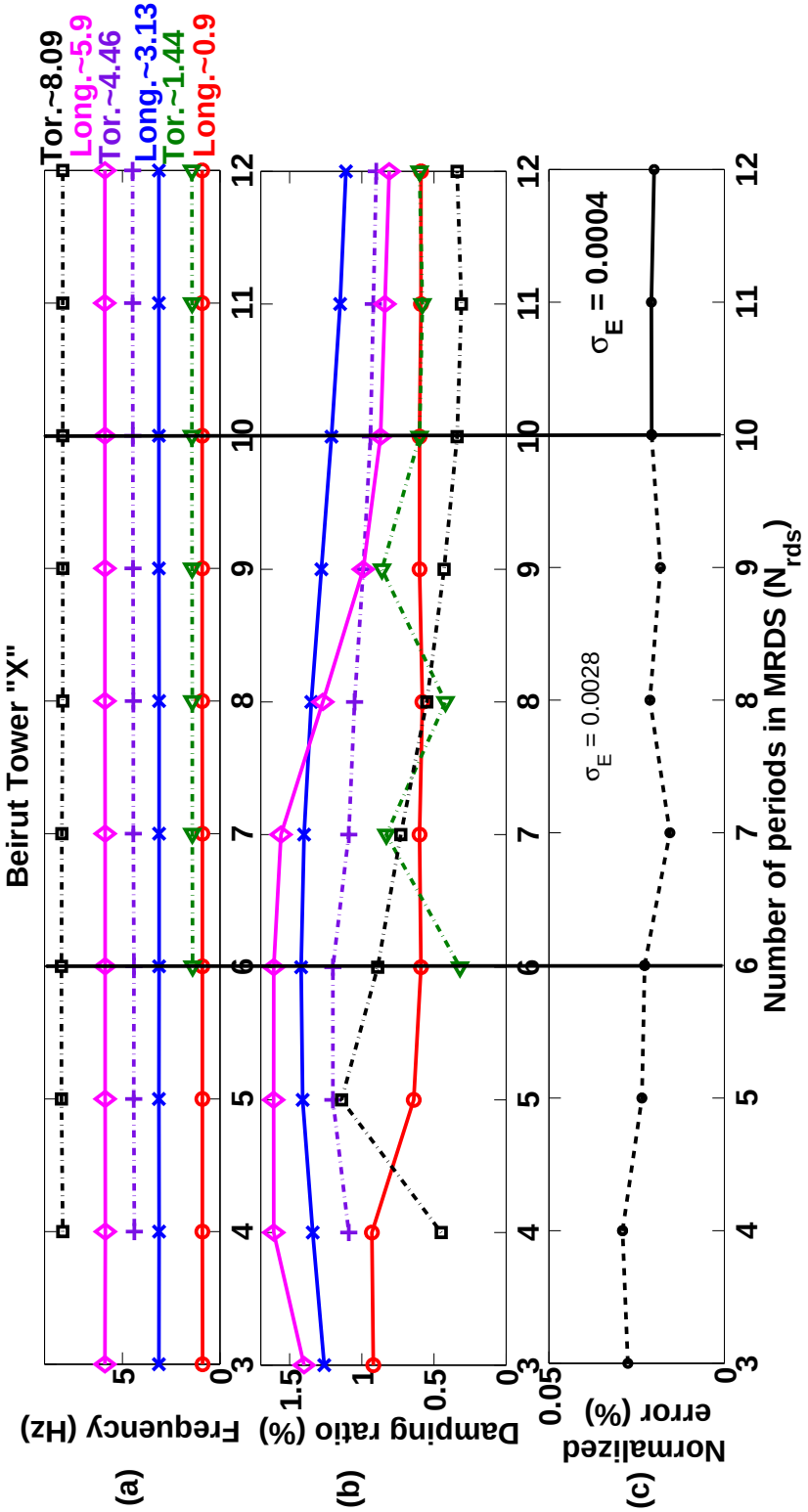

Figure A.18: (a) La fréquence, (b) le facteur d'amortissement et (c) l'erreur normalisée estimée par la méthode AMBA pour la tour X à Beyrouth (Liban) dans la direction longitudinal (long.). Tor. indique les modes de torsion observés dans la direction longitudinale. $sigma_E$ est l'écart type de l'erreur normalisée. La région d'intérêt est indiquée par σ_E en gras.

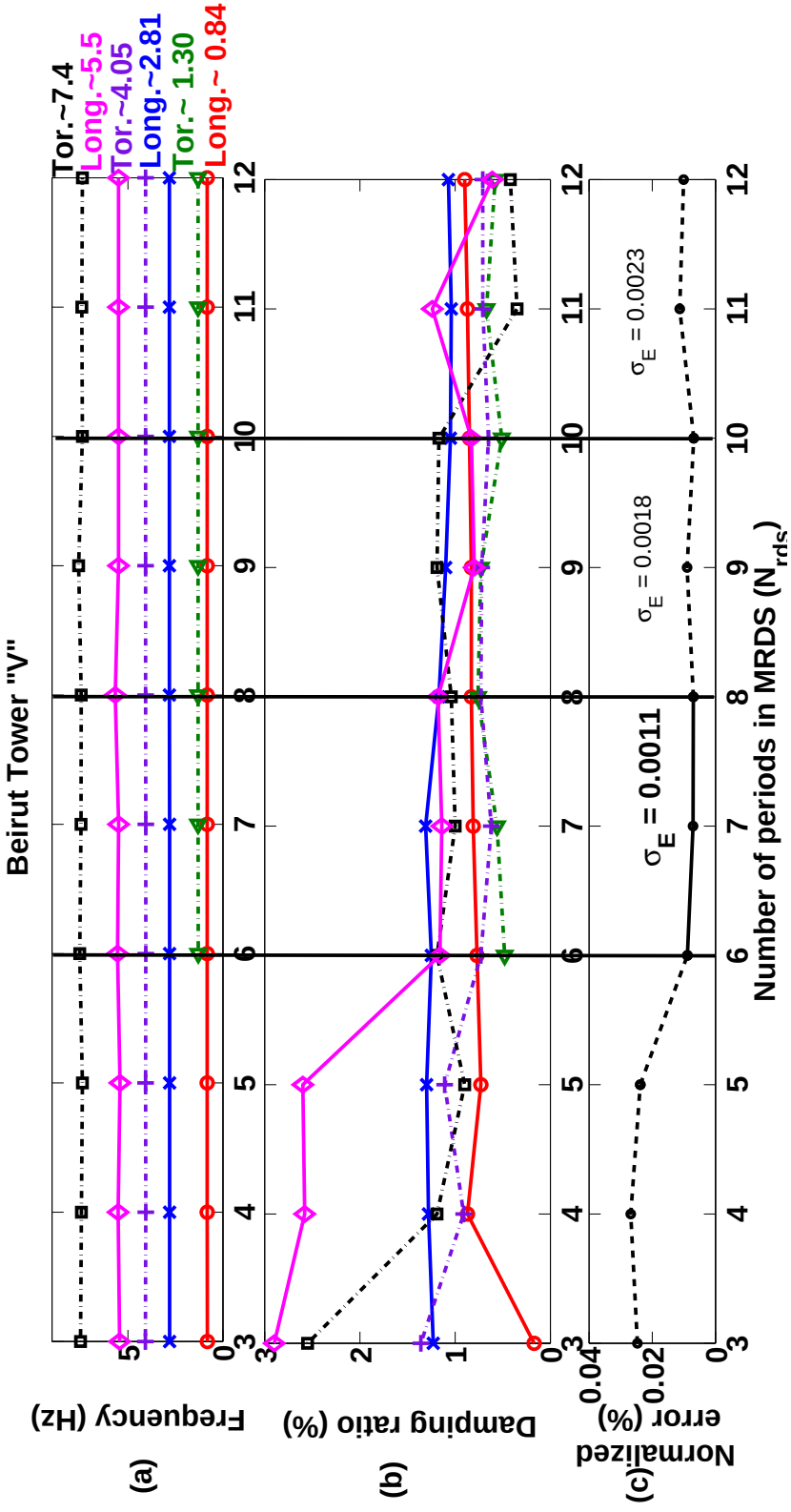

Figure A.19: (a) La fréquence, (b) le facteur d'amortissement et (c) l'erreur normalisée estimée par la méthode AMBA pour la tour V à Beyrouth (Liban) dans la direction longitudinal (long.). Tor. indique les modes de torsion observés dans la direction longitudinale. $sigma_E$ est l'écart type de l'erreur normalisée. La région d'intérêt est indiquée par σ_E en gras.

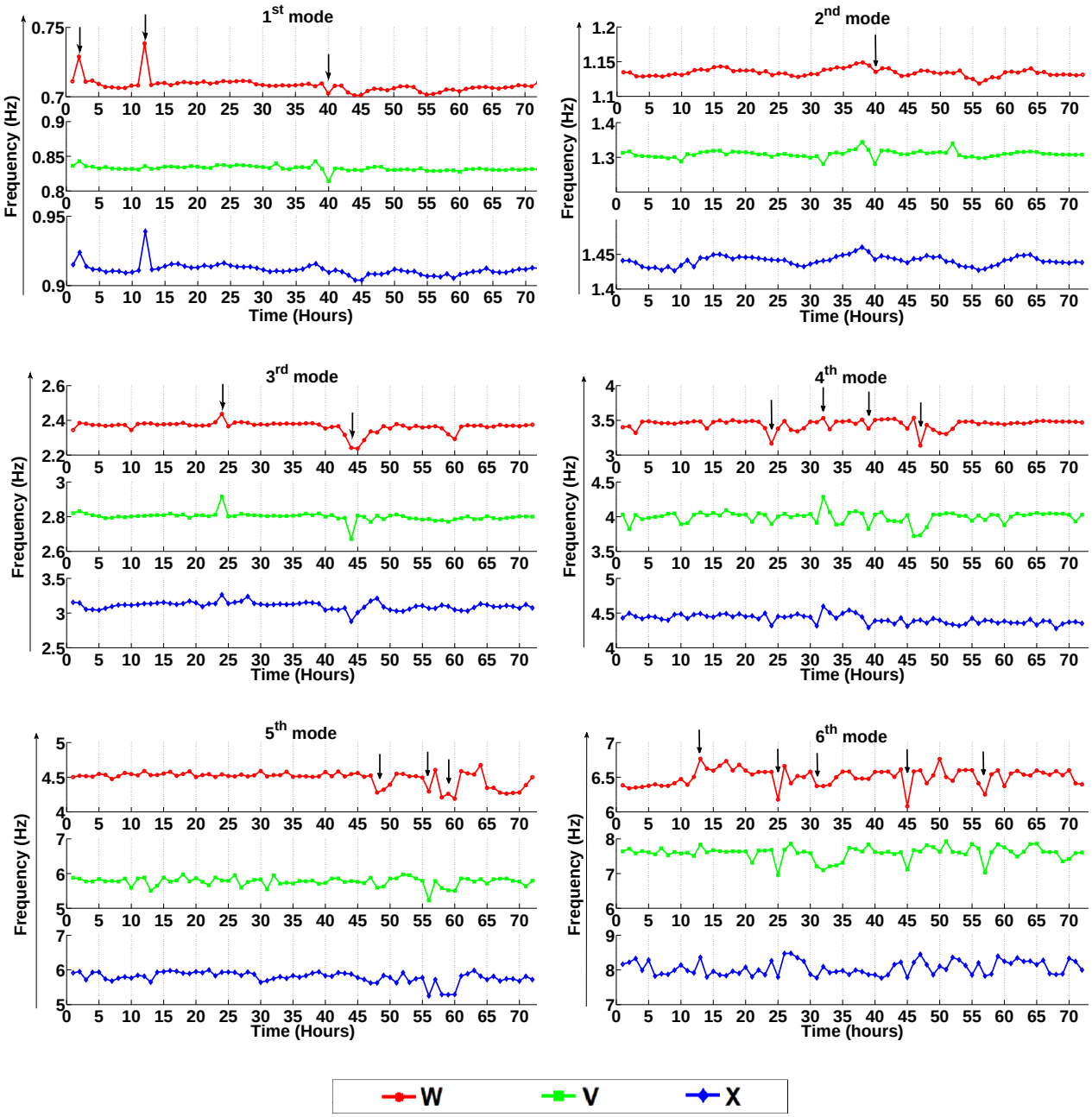

Figure A.20: Evolution de la fréquence modale des modes 1 (en haut à gauche) à 6 (en bas à droite) automatiquement suivis par le méthode de AMBA pendant la période du 26/05/2011 au 28/05/2011.

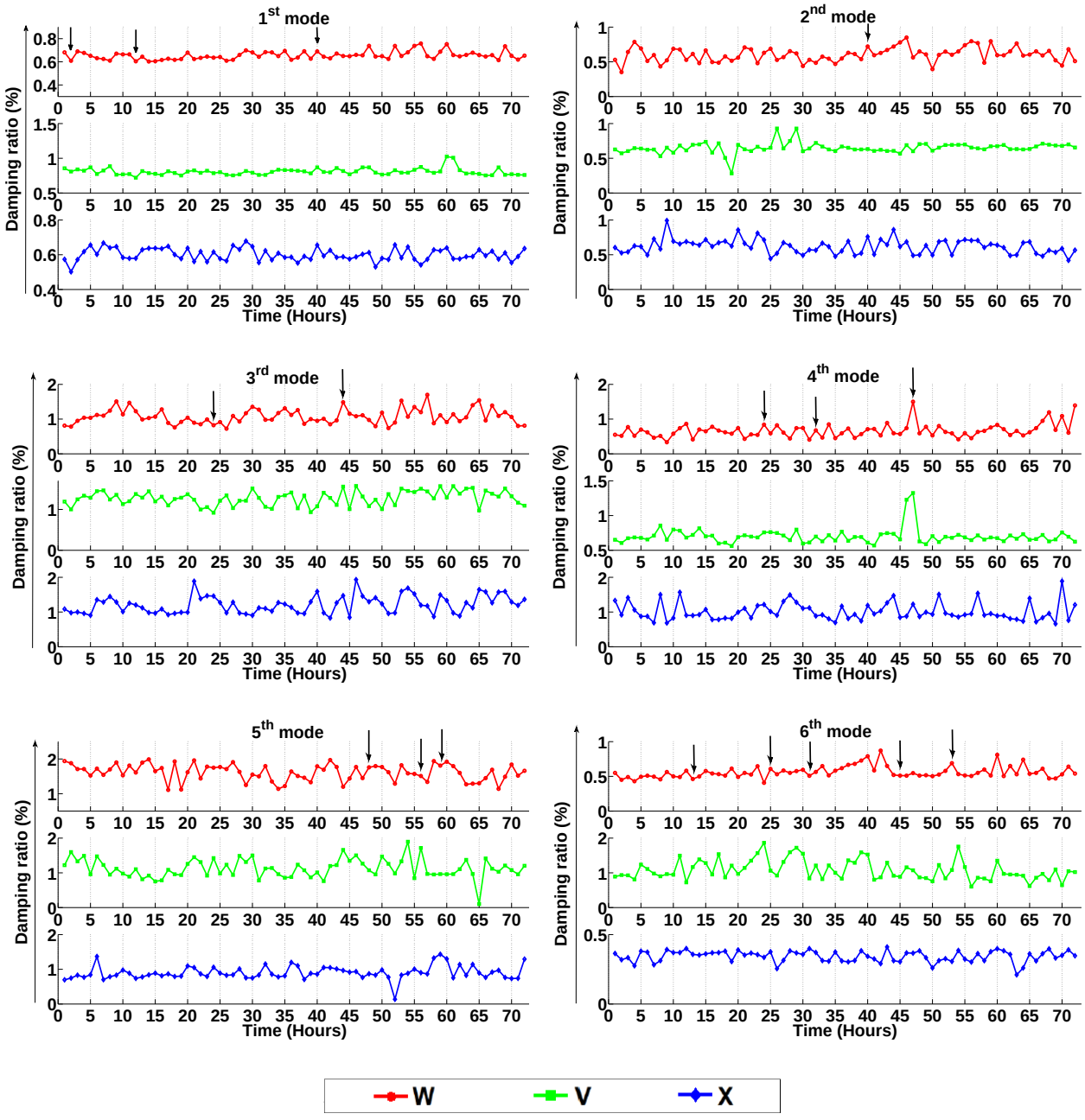

Figure A.21: Evolution du facteur d'amortissement des modes 1 (en haut à gauche) à 6 (en bas à droite) automatiquement suivis par le méthode de AMBA pendant la période du 26/05/2011 au 28/05/2011.

A.6 Conclusions et perspectives

Cette thèse propose une approche automatique de surveillance à long terme pour identifier les fréquences et les facteurs d'amortissement des modes propres des bâtiments exités par des vibrations ambiantes.

Le fait de travailler sur les bâtiments réels de grande hauteur soumis à des vibrations ambiantes est confronté à plusieurs défis; nous citerons par exemple, la convolution dans le domaine temporel entre la réponse impulsionnelle de système et le bruit sismique, les amplitudes faibles, et amorties de façon exponentielles de la réponse impulsionnelle, l'existence de plusieurs composants, la présence de modes de fréquences étroitement espacées, et les faibles niveaux de rapport signal sur bruit.

L'approche proposée dans cette thèse a relevé les défis susmentionnés simultanément sans la nécessité de l'intervention de l'utilisateur. Cette approche intitulé Automatic Model-Based Approach, AMBA, se déroule en trois étapes successives. Chaque étape relève un ou plusieurs des défis dans le but de fournir une méthode automatique et une estimation de paramètres modaux fiable et robuste.

Dans un premier temps, nous avons abordé l'extraction d'une signature équivalente à la réponse impulsionnelle de système. Nous avons utilisé la technique de décrément aléatoire directement sur le signal multi-composants. Cette approche supprime le processus de filtrage avant l'analyse RDT et conduit à l'estimation d'une signature multi-Mode.

L'originalité de cette technique est sa capacité: (1) à éviter les difficultés rencontrées dans le processus de filtrage en particulier dans les situations où les données sont difficiles à analyser, *ie*, avec un faible rapport signal sur bruit, ou avec des modes étroitement espacés en fréquence, et fortement amortis, et (2) à supprimer l'intervention.

Pour caractériser la signature multi-Mode obtenue par la technique de décrément aléatoire, nous avons proposé un modèle de signal. Ce modèle conserve la même définition du nombre de modes, les même fréquences et les même facteurs d'amortissement que le modèle physique du bâtiment.

Il y a deux contributions dans le modèle de signal proposé. Tout d'abord, ce modèle considére une amplitude amortie exponentielle. Deuxièmement, sur la base de ce modèle, l'approche proposée est capable d'estimer une amplitude exponentielle.

Le technique de décrément aléatoire sans-filtrage constitue la première étape de la méthode AMBA. Elle contribue principalement à relever le premier défi concernant la convolution entre la réponse impulsionnelle de système et le bruit sismique.

Dans l'étape suivante concernant l'estimation modale de tous les modes de la signature obtenue par le décrément aléatoire. Nous avons proposé une méthode spectrale non-paramétrique basé sur une estimation spectrale de Welch. Cette méthode est principalement consacrée à relever le défi de la présence de plusieur composantes dans le signal étudié.

La recherche des fréquences utilisée un filtrage multi-passe itératif proposé par DURNERIN [Dur99]. Un tel procédé de détection de pic associée à des propriétés statistiques de l'estimateur de spectre a permis une interprétation automatique du contenu du spectre.

Grâce à l'utilisation des propriétés statistiques de l'estimateur, les pics du spectre sont détectés par un procédé qui est insensible aux réglages. Les pics émergents du spectre de bruit estimé sont dètectès par un test de Neyman-Pearson.

Les facteurs d'amortissement de chacun des pics détectés ont ensuite été calculées à partir des variations d'amplitude des modes estimés sur deux périodogrammes consecutifs.

La méthode proposée a l'avantage d'être applicable sur les systèmes MDOF avec des modes de fréquence bien espacées, mais ses principales limites sont les suivantes: (1) les résultats dépendent de la résolution du spectre de Fourier, et (2) l'estimation est pas bien adaptée pour les modes de fréquences rapprochées, notamment avec des niveaux de bruit élevés. Afin de résoudre ces problèmes, nous avons ensuite proposé une méthode paramétrique basée sur l'estimateur du maximum de vraisemblance. Cette méthode a la capacitè à sèparer des fréquences rapprochées.

L'estimateur du maximum de vraisemblance est non linéaire et nécessite une méthode d'optimisation stochastique pour l'estimation des paramètres. À cette fin, nous avons utilisé la technique de recuit simulé qui est itérative et nécessite une étape d'initialisation. La méthode spectrale déjà proposée est utilisée dans ce but et sert donc d'une étape d'initialisation. La méthode du Maximum de Vraisemblance produit des estimations moins biaisées.

Les résultats sont prèsentès sur des signaux simulés générés en utilisant un modèle de bâtiment défini comme une poutre continue. AMBA a ensuite été validée sur des signaux réels mesurès sur les bâtiments soumis à des vibrations ambiantes, les résultats ont prouvé l'efficacité de méthode AMBA et ont montré une très faible erreur d'estimation pour les paramètres modaux avec des amplitudes très amorties ($\xi \leq 5\%$) et un très faible niveau de rapport signal-sur-bruit. Les erreurs sur l'estimation de les fréquences est inférieures à 5 % et celles sur les facteurs d'amortissement sont d'environ 15%.

Dans le suivi long terme en temps réel, l'un des buts ultimes de cette thèse est de surveiller les variations des fréquences et les facteurs d'amortissement et donc d'être en mesure de détecter les domages dans le bâtiment étudié. AMBA a prouvé son applicabilité dans un tel contexte. Les variations des fréquences et surtout des facteurs d'amortissement ont été correctement et automatiquement suivis pendant soixante-douze heures, les données de vibration ambiante en temps réel étant recueillies en continu sur trois bâtiments réels.

Certaines perspectives sont proposées dans la suite pour la poursuite et l'amélioration de ce travail.

Perspectives à court terme:

Réduction de la charge de calcul La majorité de la charge de calcul pour l'estimation des paramètres modaux du signal provient de l'étape d'estimation du maximum de vraisemblance de méthode AMBA. Par conséquent, le temps de calcul augmente avec le nombre de modes,

la longueur du signal et le nombre d'itérations dans le recuit simulé. Pour réduire le temps de calcul, nous pouvons optimiser la programmation en utilisant un langage de programmation plus efficace autre que le R2012b Matlab que nous avons utilisé dans ce travail. Une autre solution pourrait être d'utiliser une technique d'optimisation stochastique autre que le recuit simulé pour parvenir à une convergence plus rapide.

Extension à des signaux plus complexes Il est proposé d'étendre AMBA pour la détection des modes qui se croisent dans le plan de fréquence, et pour les modes de fréquences plus rapprochées ($< 0{,}01$ Hz). La difficulté de l'algorithme proposé dans ce contexte est liée à la représentation de Fourier, qui ne peut pas fournir une résolution suffisante pour séparer les composants qui se croisent. La première solution serait d'utiliser une autre méthode pour l'étape d'initialisation. La seconde solution consistait à intégrer l'estimation du nombre de modes dans un modèle paramétrique a qui évitait la dépendance avec la résolution spectrale.

Surveillance à plus long terme AMBA a été en mesure de suivre les variations modales des trois bâtiments testés pendant trois jours consécutifs. Cependant, le méthode AMBA a le potentie pour être testé sur plusieurs mois. d'amortissement.

Perspectives à long terme:
Estimer le nombre de modes sans l'étape d'initialisation. Une piste serait d'insérer ce paramétre dans le modéle paramétrique et d'utiliser une méthode d'optimisation stochastique tel que un saut réversible MCMC.

Autres méthodes de déconvolution L'utilisation d'une autre méthode pour extraire la réponse impulsionnelle autre que la technique de décrément aléatoire peuvent être envisagée. L'estimation directe de la fonction d'auto-corrélation du signal pourrait être une des solutions.

Comparez les résultats avec des signaux lidar enregistrées sur les bâtiments réels Les résultats obtenus par AMBA devrait être comparé avec les méthodes existant dans la littérature. Une des comparaisons intéressante dans le cadre du projet URBASIS serait de comparer les résultats avec ceux obtenus avec les signaux Lidar mesurés sur les mêmes bâtiments réels.

Bibliography

[AB98] J. C. Asmussen and R. Brincker. "A new approach for predicting the variance of random decrement functions". In: *Proceedings of The 16th International Modal Analysis Conference, Santa Barbara*. 1998a (Cited on page 22).

[AEB11] J. Antoni and M. El Badaoui. "The Discrete-Time Random Decrement Technique: Closed-form Solutions for the Blind Identification of SIMO Systems". In: *Proceedings of The International Conference on Structural Sytem Identification*. 2011 (Cited on pages 21, 22).

[AF87] S. Anily and A. Federgruen. "Simulated annealing methods with general acceptance probabilities". *Journal of Applied Probability* (1987), pp. 657–667 (Cited on page 57).

[AIB97] J. C. Asmussen, S. R. Ibrahim, and R. Brincker. "Application of vector triggering random decrement". In: *Proceedings of The 15th International Modal Analysis Conference, Orlando, Florida*. Vol. II. 1997, pp. 1165–1171 (Cited on page 21).

[And+07] P. Andersen, R. Brincker, M. Goursat, and L. Mevel. "Automated modal parameter estimation for operational modal analysis of large systems". In: *Proceedings of The 2nd International Operational Modal Analysis Conference (IOMAC)*. 2007, pp. 299–308 (Cited on page 14).

[Asm97] J. C. Asmussen. "Modal analysis based on the random decrement technique: application to civil engineering structures". PhD thesis. Department of Building Technology and Structural Engineering University of Aalborg, Denmark, 1997 (Cited on pages 20, 22, 24, 26).

[BAJ07] R. Brincker, P. Andersen, and N. J. Jacobsen. "Automated frequency domain decomposition for operational modal analysis". In: *Proceedings of The 25th International Modal Analysis Conference (IMAC), Orlando, Florida*. 2007 (Cited on pages 13–15).

[BC04] S. Bonnefoy-Claudet. "Nature du bruit de fond sismique: implications pour les études des effets de site". PhD thesis. Université Joseph-Fourier-Grenoble I, France (In french), 2004 (Cited on page 7).

[BC07] J. M. W. Brownjohn and E. P. Carden. "Tracking the effects of changing environmental conditions on the modal parameters of Tamar Bridge". In: *Proceedings of The 3rd international conference on structural health monitoring and intelligent infrastructure*. 2007 (Cited on page 14).

[BCCB06] S. Bonnefoy-Claudet, F. Cotton, and P. Y. Bard. "The nature of noise wavefield and its applications for site effects studies: a literature review". *Earth-Science Reviews* 79, 3 (2006), pp. 205–227 (Cited on pages 6, 7).

[BKJ91] R. Brincker, S. Krenk, and J. L. Jensen. "Estimation of Correlation Functions by the Random DEC Technique". In: *Proceedings of The 9th International Modal Analysis Conference and Exhibit, Florence, Italy*. 1991 (Cited on page 20).

[BKR91] R. Brincker, P. H. Kirkegaard, and A. Rytter. "Identification of System Parameters by the Random Decrement Technique". In: *Proceedubgs of the Florence Modal Analysis conference. Florence. Italy*. 1991a (Cited on page 21).

[Bou+05] C. Boutin, S. Hans, E. Ibraim, and P. Roussillon. "In situ experiments and seismic analysis of existing buildings. Part II: Seismic integrity threshold". *Earthquake engineering & structural dynamics* 34, 12 (2005), pp. 1531–1546 (Cited on page 41).

[Bou+99] C. Boutin, S. Hans, I. Erdin, and M. Loriot. "Approche de la vulnérabilité sismique par l'étude du comportement de bâtiments réels". *Rapport de recherche ENTPE, Lyon* (1999) (Cited on page 11).

[BR05] R. Brincker and J. Rodrigues. "Application of the random decrement technique in operational modal analysis". In: *Proceedings of The 1st International Operational Modal Analysis Conference (IOMAC)*. 2005 (Cited on page 22).

[Bro70] C. G. Broyden. "The convergence of a class of double-rank minimization algorithms 1. general considerations". *IMA Journal of Applied Mathematics* 6, 1 (1970), pp. 76–90 (Cited on page 56).

[BVA01] R. Brincker, C. Ventura, and P. Andersen. "Damping estimation by frequency domain decomposition". In: *Proceedings of The 19th International Modal Analysis Conference*. 2001, pp. 698–703 (Cited on page 12).

[BZA00] R. Brincker, L. Zhang, and P. Andersen. "Modal identification from ambient responses using frequency domain decomposition". In: *Proceedings of The 18th 'International Modal Analysis Conference (IMAC), San Antonio, Texas*. 2000 (Cited on pages 12, 15).

[CA02] F. N. Catbas and A. E. Aktan. "Condition and damage assessment: issues and some promising indices". *Journal of Structural Engineering* 128, 8 (2002), pp. 1026–1036 (Cited on page 9).

[Car36] D. S. Carder. "Observed vibrations of buildings". *Bulletin of the Seismological Society of America* 26, 3 (1936), pp. 245–277 (Cited on page 11).

[CB02] I. Cohen and B. Berdugo. "Noise estimation by minima controlled recursive averaging for robust speech enhancement". *Signal Processing Letters, IEEE* 9, 1 (2002), pp. 12–15 (Cited on page 35).

[CBH08] C. Chesnais, C. Boutin, and S. Hans. "TO WHAT TYPE OF BEAM CAN BE ASSOCIATED A BUILDING?" In: *Proceeding in The 14th World Conference on Earthquake Engineering, Beijing, China*. 2008 (Cited on page 40).

[CCW03] K. P. Chong, N. J. Carino, and G. Washer. "Health monitoring of civil infrastructures". *Smart Materials and structures* 12, 3 (2003), p. 483 (Cited on page 9).

[CF04] E. P. Carden and P. Fanning. "Vibration based condition monitoring: a review". *Structural Health Monitoring* 3, 4 (2004), pp. 355–377 (Cited on page 10).

[Cli+06] J. F. Clinton, S. C. Bradford, T. H. Heaton, and J. Favela. "The observed wander of the natural frequencies in a structure". *Bulletin of the Seismological Society of America* 96, 1 (2006), pp. 237–257 (Cited on pages 11, 12).

[Col68] H. A. Cole. "On-The-Line Analysis of Random Vibrations". *AIAA Paper* (1968), pp. 68–288 (Cited on pages 20–22, 24, 26, 43, 96).

[Col71a] H. A. Cole. "Failure detection of a space shuttle wing by random decrement". *NASA TMX-62,041* (1971) (Cited on pages 22, 26).

[Col71b] H. A. Cole. "Method and apparatus for measuring the damping characteristics of a structure". *United States Patent No. 3,620,069* (1971) (Cited on pages 22, 26).

[Col73] H. A. Cole. "On-line failure detection and damping measurement of aerospace structures by random decrement signatures". *National Aeronautics and Space Administration* 2205, (1973) (Cited on pages 22, 23, 26, 47).

[Cre87] S. Creed. "Assessment of large engineering structures using data collected during in-service loading". In: *Procedings of structural assessment based on full and large scale testing*. 1987 (Cited on page 12).

[CT08] S. Chauhan and D. Tcherniak. "Clustering approaches to automatic modal parameter estimation". In: *Proceedings of the International Modal Analysis Conference (IMAC)*. 2008 (Cited on page 14).

[CZJ99] K. S. Chhipwadia, D. C. Zimmerman, and G. H. James. "Evolving autonomous modal parameter estimation". In: *Proceedings of the 17th IMAC, Kissimmee, FL*. 1999 (Cited on page 13).

[Der+08] A. Deraemaeker, E. Reynders, G. De Roeck, and J. Kullaa. "Vibration-based structural health monitoring using output-only measurements under changing environment". *Journal of Mechanical systems and signal processing* 22, 1 (2008), pp. 34–56 (Cited on page 14).

[Doe+96] S. W. Doebling, C. R. Farrar, M. B. Prime, and D. W. Shevitz. *Damage identification and health monitoring of structural and mechanical systems from changes in their vibration characteristics: a literature review*. Tech. rep. No. LA-13070-MS Los Alamos National Laboratory, Los Alamos, NM (United States), 1996 (Cited on pages 5, 10, 13).

[Dré+03] J. Dréo, A. Pétrowski, É. D. Taillard, and P. Siarry. "Métaheuristiques pour l'optimisation difficile". *Eyrolles, 61, Bld Saint-Germain, Paris, ISBN : 2-212-11368-4* (2003) (Cited on page 56).

[Dun05] F. Dunand. "Pertinence du bruit de fond sismique pour la caractérisation dynamique et l'aide au diagnostic sismique des structures de génie civil". PhD thesis. Université Joseph-Fourier-Grenoble I, France (In French), 2005 (Cited on page 12).

[Dur99] M. Durnerin. "Une stratégie pour l'interprétation en analyse spectrale. Détection et caractérisation des composantes d'un spectre." PhD thesis. Institut National Polytechnique de Grenoble-INPG, France (In French), 1999 (Cited on pages 33–35, 46, 91, 99–101, 124).

[Ewi00] David John Ewins. *Modal testing: theory, practice and application*. Vol. 2. Research studies press Baldock, 2000 (Cited on pages 11, 16).

[Far+97] C. R. Farrar, S. W. Doebling, P. J. Cornwell, and E. G. Straser. "Variability of modal parameters measured on the Alamosa Canyon Bridge". In: *In Proceedings of IMAC 15, Orlando, FL, USA*. 1997, pp. 257–263 (Cited on page 12).

[FDN01] C. R. Farrar, S. W. Doebling, and D. A. Nix. "Vibration–based structural damage identification". *Philosophical Transactions of the Royal Society of London. Series A: Mathematical, Physical and Engineering Sciences* 359, 1778 (2001), pp. 131–149 (Cited on pages 5, 11).

[FF99] L. Frenkel and M. Feder. "Recursive expectation-maximization (EM) algorithms for time-varying parameters with applications to multiple target tracking". *IEEE Transactions on Signal Processing* 47, 2 (1999), pp. 306–320 (Cited on page 35).

[GKS05] H. Guan, V. M. Karbhari, and C. S. Sikorski. "Time-domain output only modal parameter extraction and its application". In: *Proceedings of the 1st International Operational Modal Analysis Conference, Copenhagen, Denmark*. 2005, pp. 577–584 (Cited on page 14).

[Gue+14] Philippe Gueguen, Mickael Langlais, Philippe Roux, Jakub Schinkmann, and Isabelle Douste-Bacqué. "Frequency and Damping Wandering in Existing Buildings Using the Random Decrement Technique". In: *Proceeding of the 7th European Workshop on Structural Health Monitoring - EWSHM*. 2014 (Cited on page 22).

[GVM12] P. Gueguen, C. Voisin, and A. Mariscal. "Wandering of the modal parameters in existing building: application to structural health monitoring and seismic vulnerability analysis." In: *Proceedings of The 15th WCEE, LISBOA*. 2012 (Cited on pages 68–73, 77, 85).

[HS89] B. Hajek and G. Sasaki. "Simulated annealing—to cool or not". *Systems & control letters* 12, 5 (1989), pp. 443–447 (Cited on page 57).

[IAB97] S. R. Ibrahim, J. C. Asmussen, and R. Brincker. "Vector triggering random decrement technique for higher identification accuracy". In: *Proceeding of the IMAC XV. Orlando. Florida*. 1997 (Cited on page 21).

[Ibr77] S. R. Ibrahim. "Random decrement technique for modal identification of structures". *Journal of Spacecraft and Rockets* 14, 11 (1977), pp. 696–700 (Cited on page 21).

[ITT00] S. S. Ivanovic, M. D. Trifunac, and M. I. Todorovska. "Ambient vibration tests of structures-a review". *ISET Journal of Earthquake Technology* 37, 4 (2000), pp. 165–197 (Cited on page 11).

[Jab+07] M. Jabloun, F. Leonard, M. Vieira, and N. Martin. "A new flexible approach to estimate the IA and IF of nonstationary signals of long-time duration". *IEEE Transactions on Signal Processing* 55, 7 (2007), pp. 3633–3644 (Cited on pages 55, 56, 92).

[JAB06] N. J. Jacobsen, P. Andersen, and R. Brincker. "Using enhanced frequency domain decomposition as a robust technique to harmonic excitation in operational modal analysis". In: *International Conference on Noise and Vibration Engineering (ISMA), Leuven, Belgium*. 2006 (Cited on page 12).

[Jab07] M. Jabloun. "Modélisation de signaux fortement non stationnaires à phase et à amplitude locales polynomiales." PhD thesis. Institut National Polytechnique de Grenoble-INPG, France (In French), 2007 (Cited on page 59).

[Jea86] A. P. Jeary. "Damping in tall buildings—a mechanism and a predictor". *Earthquake engineering & structural dynamics* 14, 5 (1986), pp. 733–750 (Cited on page 12).

[Jea96] A. P. Jeary. "The description and measurement of nonlinear damping in structures". *Journal of wind engineering and industrial aerodynamics* 59, 2 (1996), pp. 103–114 (Cited on page 12).

[Jea97] A. P. Jeary. "Damping in structures". *Journal of wind engineering and industrial aerodynamics* 72, (1997), pp. 345–355 (Cited on page 12).

[JIZC99] G. H. James III, D. C. Zimmerman, and K. S. Chhipwadia. "Application of autonomous modal identification to traditional and ambient data sets". In: *Proceedings in the International Modal Analysis Conference (IMAC)*. Society of Photo-Optical Instrumentation Engineers. 1999, pp. 840–845 (Cited on page 13).

[KGV83] S. Kirkpatrick, C. D. Gelatt, and Jr. M. P. Vecchi. "Optimization by simmulated annealing". *science* 220, 4598 (1983), pp. 671–680 (Cited on page 56).

[Kir84] Scott Kirkpatrick. "Optimization by simulated annealing: Quantitative studies". *Journal of statistical physics* 34, 5-6 (1984), pp. 975–986 (Cited on page 104).

[KK02] T. Kijewski and A. Kareem. "On the reliability of a class of system identification techniques: insights from bootstrap theory". *Structural Safety* 24, 2 (2002), pp. 261–280 (Cited on page 26).

[Li+00] Q. S. Li, D. K. Liu, J. Q. Fang, A. P. Jeary, and C. K. Wong. "Damping in buildings: its neural network model and AR model". *Engineering Structures* 22, 9 (2000), pp. 1216–1223 (Cited on page 12).

[LRP04] J. Lanslots, B. Rodiers, and B. Peeters. "Automated pole-selection: proof-of-concept & validation". In: *Proceedings of the ISMA International Conference on Noise and Vibration Engineering, Leuven, Belgium*. 2004 (Cited on page 14).

[Mar11] N. Martin. "Spectral Analysis, Parametric, Non-parametric and Advanced Methods". *WILEY-VCH* (2011) (Cited on page 34).

[MCC12] F. Magalhães, A. Cunha, and E. Caetano. "Vibration based structural health monitoring of an arch bridge: from automated OMA to damage detection". *Mechanical Systems and Signal Processing* 28, (2012), pp. 212–228 (Cited on page 13).

[Met+53] N. Metropolis, A. W. Rosenbluth, M. N. Rosenbluth, A. H. Teller, and E. Teller. "Equation of state calculations by fast computing machines". *The journal of chemical physics* 21, 6 (1953), pp. 1087–1092 (Cited on page 56).

[MG10] C. Michel and P. Guéguen. "Time-frequency analysis of small frequency variations in civil engineering structures under weak and strong motions using a reassignment method". *Structural health monitoring* 9, 2 (2010), pp. 159–171 (Cited on page 11).

[MGB08] C. Michel, P. Guéguen, and P. Y. Bard. "Dynamic parameters of structures extracted from ambient vibration measurements: An aid for the seismic vulnerability assessment of existing buildings in moderate seismic hazard regions". *Soil Dynamics and Earthquake Engineering* 28, 8 (2008), pp. 593–604 (Cited on page 11).

[MGC12] C. Michel, P. Gueguen, and M. Causse. "Seismic vulnerability assessment to slight damage based on experimental modal parameters". *Earthquake Engineering & Structural Dynamics* 41, 1 (2012), pp. 81–98 (Cited on pages 69–72, 84, 85).

[Mic+10] C. Michel, P. Guéguen, S. El Arem, J. Mazars, and P. Kotronis. "Full-scale dynamic response of an RC building under weak seismic motions using earthquake recordings, ambient vibrations and modelling". *Earthquake Engineering & Structural Dynamics* 39, 4 (2010), pp. 419–441 (Cited on page 11).

[Mic07] C. Michel. "Vulnérabilité Sismique de l'échelle du bâtiment à celle de la ville-Apport des techniques expérimentales in situ-Application à Grenoble". PhD thesis. Université Joseph-Fourier-Grenoble I, France (In french), 2007 (Cited on pages 8, 41, 42).

[Mik+13] A. Mikael, P. Guéguen, P. Y. Bard, P. Roux, and M. Langlais. "The Analysis of Long-Term Frequency and Damping Wandering in Buildings Using the Random Decrement Technique". *Bulletin of the Seismological Society of America* 103, 1 (2013), pp. 236–246 (Cited on pages 22, 69–72, 84, 85).

[MS97] N. M. M. Maia and J. M. M Silva. "Theoretical and experimental modal analysis". *Taunton: Research Studies Press* (1997) (Cited on page 11).

[MSZ99] C. Modena, D. Sonda, and D. Zonta. "Damage localization in reinforced concrete structures by using damping measurements". *Key engineering materials* 167, (1999), pp. 132–141 (Cited on page 12).

[Nas+13] F. Nasser, Z. Y. Li, N. Martin, and P. Guéguen. "Automatic Parameter Setting of Random Decrement Technique for the Estimation of Building Modal Parameters". In: *Proceeding in the International Conference Surveillance 7*. 2013, 13–p (Cited on page 27).

[PDR01] B. Peeters and G. De Roeck. "One-year monitoring of the Z 24-Bridge: environmental effects versus damage events". *Earthquake engineering & structural dynamics* 30, 2 (2001), pp. 149–171 (Cited on pages 13, 14).

[Per+13] M. Perrault, P. Guéguen, A. Aldea, and D. Sorin. "Reducing the uncertainties of the fragility curves using experimental testing in existing buildings: the case of the BRD Tower of Buccarest (Romania)". *Earthquake Engineering and Engineering Vibration* 12, 4 (2013) (Cited on pages 41, 106).

[PJZ98] R. S. Pappa, G. H. James, and D. C. Zimmerman. "Autonomous modal identification of the space shuttle tail rudder". *Journal of Spacecraft and Rockets* 35, 2 (1998), pp. 163–169 (Cited on page 13).

[PKG08] F. Poncelet, G. Kerschen, and J. C. Golinval. "In-orbit vibration testing of spacecraft structures". In: *Proceeding in the International Conference on noise and vibration Engineering*. 2008 (Cited on page 15).

[PWJ97] R. S. Pappa, S. E. Woodard, and J. N. Juang. "A benchmark problem for development of autonomous structural modal identification". In: *Proceedings in the International Modal Analysis Conference (IMAC)*. 1997, pp. 1071–1077 (Cited on page 13).

[Rai+12] C. Rainieri, G. Fabbrocino, G. Manfredi, and M. Dolce. "Robust output-only modal identification and monitoring of buildings in the presence of dynamic interactions for rapid post-earthquake emergency management". *Engineering Structures* 34, (2012), pp. 436–446 (Cited on page 13).

[RB05] J. Rodrigues and R. Brincker. "Application of the random decrement technique in operational modal analysis". In: *Proceeding in the 1st International Operational Modal Analysis Conference*. 2005, pp. 191–200 (Cited on page 20).

[RBA04] J. Rodrigues, R. Brincker, and P. Andersen. "Improvement of frequency domain output-only modal identification from the application of the random decrement technique". In: *Proceeding of the 23rd International Modal Analysis Conference, Deaborn, MI*. 2004 (Cited on page 22).

[RF10] C. Rainieri and G. Fabbrocino. "Automated output-only dynamic identification of civil engineering structures". *Journal of Mechanical Systems and Signal Processing* 24, 3 (2010), pp. 678–695 (Cited on page 13).

[RFC07] C. Rainieri, G. Fabbrocino, and E. Cosenza. "Automated Operational Modal Analysis as structural health monitoring tool: theoretical and applicative aspects". *Key Engineering Materials* 347, (2007), pp. 479–484 (Cited on page 14).

[RFC08] C. Rainieri, G. Fabbrocino, and E. Cosenza. "Integrated systems for Structural Health Monitoring: worldwide applications and perspectives". In: *Proceedings of the 4th European Workshop on Structural Health Monitoring*. 2008, pp. 978–1 (Cited on page 13).

[RFC10] C. Rainieri, G. Fabbrocino, and E. Cosenza. "Some remarks on experimental estimation of damping for seismic design of civil constructions". *Shock and Vibration* 17, 4 (2010), pp. 383–395 (Cited on pages 6, 13).

[RMB07] L. Rankine, M. Mesbah, and B. Boashash. "IF estimation for multicomponent signals using image processing techniques in the time–frequency domain". *Signal Processing* 87, 6 (2007), pp. 1234–1250 (Cited on page 33).

[Ryt93] A. Rytter. "Vibrational based inspection of civil engineering structures". PhD thesis. Aalborg, Denmark, University of Aalborg, 1993 (Cited on page 10).

[Sal97] O. S. Salawu. "Detection of structural damage through changes in frequency: a review". *Engineering structures* 19, 9 (1997), pp. 718–723 (Cited on pages 11, 13).

[Sat+03] N. Satake, K. Suda, T. Arakawa, A. Sasaki, and Y. Tamura. "Damping evaluation using full-scale data of buildings in Japan". *Journal of structural engineering* 129, 4 (2003), pp. 470–477 (Cited on page 12).

[Sik99] C. Sikorsky. "Development of a health monitoring system for civil structures using a level IV non-destructive damage evaluation method". In: *Proceeding of the 2nd International Workshop on Structural Health Monitoring*. 1999, pp. 68–81 (Cited on pages 9, 10).

[Sod77] T. Soderstrom. "On model structure testing in system identification". *International Journal of Control* 26, 1 (1977), pp. 1–18 (Cited on page 14).

[Soh+04] H. Sohn, C. R. Farrar, F. M. Hemez, D. D. Shunk, D. W. Stinemates, B. R. Nadler, and J. J. Czarnecki. "A review of structural health monitoring literature: 1996-2001". *Report Number LA-13976-MS, Los Alamos National Laboratory, Los Alamos, NM* (2004) (Cited on pages 5, 10).

[Soh+99] H. Sohn, M. Dzwonczyk, E. G. Straser, A. S. Kiremidjian, K. H. Law, and T. Meng. "An experimental study of temperature effect on modal parameters of the Alamosa Canyon Bridge". *Earthquake engineering & structural dynamics* 28, 8 (1999), pp. 879–897 (Cited on page 12).

[SS10] O. V. Shiryayev and J. C. Slater. "Detection of Fatigue Cracks Using Random Decrement Signatures". *Structural Health Monitoring* 9, 4 (2010), pp. 347–360 (Cited on page 22).

[Ste88] M. K. Steven. "Modern Spectral Estimation: Theory and Application". *Editor A.V. Oppenhein, Prentice Hall, Englewood Cliffs, New Jersey* (1988) (Cited on page 56).

[Tam+92] Y. Tamura, A. Sasaki, T. Sato, and R. Kousaka. "Evaluation of Damping Ratios of Buildings During Gusty Wind Using the Random Decrement Technique". In: *Proceeding in the 12th Wind Engineering Symposium*. 1992 (Cited on page 26).

[TYY94] Yukio Tamura, Masaaki Yamada, and Haruhiko Yokota. "Estimation of structural damping of buildings". In: *Proceeding in ASCE Structures Congress and IASS International Symposium, Atlanta*. ASCE. 1994, pp. 1012–1017 (Cited on page 12).

[Val+14] M. Valla, P. Gueguen, B. Augere, D. Goular, and M. Perrault. "Remote Modal Study of Reinforced Concrete Buildings Using a Multipath Lidar Vibrometer". *ASCE Journal of Structural Engineering (2014)* 141, 1 (2014) (Cited on pages 69–72, 85).

[Van+82] J. K. Vandiver, A. B. Dunwoody, R. B. Campbell, and M. F. Cook. "A mathematical basis for the random decrement vibration signature analysis technique". *Journal of Mechanical Design* 104, 2 (1982), pp. 307–313 (Cited on pages 20, 21, 23, 26, 27).

[Ver+02] P. Verboven, E. Parloo, P. Guillaume, and M. Van Overmeire. "Autonomous structural health monitoring—part I: modal parameter estimation and tracking". *Journal of Mechanical Systems and Signal Processing* 16, 4 (2002), pp. 637–657 (Cited on page 13).

[Wan03] H. Wan. "Two-pass quantile based noise spectrum estimation". *Center of Spoken Language Understanding, OGI School of Science and Engineering at OHSU* (2003) (Cited on page 35).

[WDR97] M. A. Wahab and G. De Roeck. "Effect of temperature on dynamic system parameters of a highway bridge". *Structural Engineering International* 7, 4 (1997), pp. 266–270 (Cited on page 12).

[YAB04] K. V. Yuen, S. K. Au, and J. L. Beck. "Two-stage structural health monitoring approach for phase I benchmark studies". *Journal of Engineering Mechanics* 130, 1 (2004), pp. 16–33 (Cited on page 9).

[YD80] J. C. S. Yang and N. G. Dagalakis. "Detection of incipient failure in structure using random decrement technique". In: *Proceeding of the Fall Meeting of Society of Experimental Stress Analysis, Ft. Lauderdale, Fla.* 1980, p. 43 (Cited on page 20).

[YDH80] J. C. S. Yang, N. G. Dagalakis, and M. A. Hirt. "Application of the random decrement technique in the detection of an induced crack on an offshore platform model". In: *Computational Methods for Offshore Structures. The winter annual meeting of the American Society of Mechanical Engineers.* Vol. 37. ICOM-CONF-1980-002. American Society of Mechanical Engineers, New York. 1980, pp. 55–67 (Cited on pages 20, 26).

Author's Publications

International Journals

- **F. NASSER**, Z-Y. LI, P. GUEGUEN, N. MARTIN, "On the Estimation of Natural Frequencies and Damping Ratios of Real-World High-rise Builidngs Subjected to Ambient Vibrations using an Automatic Model-Based Approach". *Submitted to the journal of Mechanical Systems and Signal Processing journal, March 2015.*
- **F. NASSER**, Z-Y. LI, N. MARTIN, P. GUEGUEN, "An Automatic Approach towards Modal Parameter Estimation for High-Rise Buildings of Multicomponent Signals under Ambient Excitations via Filter-free Random Decrement Technique". *Submitted to the journal of Mechanical Systems and Signal Processing journal, Oct. 2014 (Under major revision).*

International Conferences

- **F. NASSER**, Z-Y. LI, N. MARTIN, P. GUEGUEN, "Non-biased estimation of modal parameters of multi-component ambient vibrations in high-rise buildings using a self-governed random decrement technique". *Eleventh International Conference on Condition Monitoring and Machinery Failure Prevention Technologies. CM 2014 and MFPT 2014. Manchester, UK, 10-12 June 2014.*
- **F. NASSER**, Z-Y. LI, N. MARTIN, P. GUEGUEN, "Automatic parameter setting of Random Decrement Technique for the estimation of building modal parameters". *International Conference Surveillance 7. Chartres, France, October 29-30, 2013.*
- **F. NASSER**, Z-Y. LI, N. MARTIN, M. VIEIRA, P. GUEGUEN, Invited Keynote Address, "Seismic Response Analysis of Different Buildings using Time- Invariant and Time- Variant Damping Coefficients". *Ninth International Conference on Condition Monitoring and Machinery Failure Prevention Technologies. CM 2012 and MFPT 2012. London, UK, 12-14 June 2012.*

Title: Automatic Modal Variation Tracking via a Filter-Free Random Decrement Technique Application to ambient vibration recordings on high-rise buildings

Abstract: This thesis proposes a novel approach to automatically monitor the variations of the frequencies and the damping ratios of actual high-rise buildings subjected to real-world ambient vibrations. The approach aims at dealing simultaneously with the following challenges: multi-component signals recorded over the aforementioned buildings and having closely-spaced frequency modes with low, exponential and damped amplitudes of their impulse responses and contaminated with high additive noises. The approach relies on the application of the Random Decrement Technique directly over the multi-component signal under study which leads to the extraction of a Multi-mode Random Decrement Signature equivalent to the system impulse response. To characterize such a signature, we propose a signal model based on the physical structure of the building from where the modal parameters can be estimated. For the purpose of non-biased modal estimate, we propose to use an iterative method based on a Maximum-Likelihood Estimation optimized by a simulated annealing technique. In order to initialize the parameters of the latter, a first step is designed which can be considered as an independent estimator of the modal parameters. The originality of this step lies in its ability to automatically define the number of modes of the estimated signature through the use of the statistical properties of a Welch spectrum. The modal parameters estimated by the spectral-based initialization step are finally refined by the Maximum-Likelihood Estimation step. The latter reduces the bias in the estimation and yields more reliable and robust results. All these steps are defined in order to be able to automatically monitor the health of a building via a long-term real-time tracking of the modal variations over time without the need to any user intervention . In addition, the proposed approach has paid very special attention to the automatic estimation of the most problematic modal parameter, *i.e.*, the damping ratio. Such features making two of the original features as compared to existing techniques. The adaptability and functionality of AMBA is validated over six actual buildings excited by real-world ambient vibrations. From the obtained results, AMBA proved high efficiency in automatically estimating the frequencies and moreover the damping ratios in case of closely-spaced frequency modes and very low signal-to-noise ratio level. AMBA as well demonstrated a good performance for tracking the modal variations over time.

Keywords: automatic modal analysis, random decrement technique, modal variation, building monitoring, time-tracking.

Titre : Suivi automatique de variations modales à l'aide du technique de décrément aléatoire sans filtrage
Application à des enregistrements de vibrations ambiantes des batiments

Résumé : Cette thèse propose une nouvelle approche pour surveiller automatiquement les variations des fréquences et des taux d'amortissement des batiments de grande hauteur soumis à des vibrations ambiantes. L'approche vise à relever simultanément avec les défis suivants: signaux multi-composants enregistrées sur les bâtiments mentionnés ci-dessus avec des réponses impulsionnelles ayant des modes de fréquences rapprochées, des amplitudes faibles, exponentielles et amorties noyées dans des bruits additifs élevés. La méthode repose sur l'application de la technique de décrément aléatoire directement sur le signal multi-composante ce qui conduit à l'estimation d'une signature de décrément aléatoire multi-mode équivalente à la réponse impulsionnelle de système. Pour caractériser une telle signature, nous proposons un modèle de signal basé sur la structure physique du bâtiment à partir de laquelle les paramètres modaux peuvent être estimés. Dans le but d'avoir une estimation non biaisée, nous proposons d'utiliser une méthode itérative sur la base d'une estimation du maximum de vraisemblance optimisé par une technique de recuit simulé. Afin d'initialiser les paramètres de ce dernier, une première étape est conçu qui peut être considéré comme un estimateur indépendant des paramètres modaux. L'originalité de cette étape réside dans sa capacité à définir automatiquement le nombre de modes de la signature estimé grâce à l'utilisation des propriétés statistiques d'un spectre estimé par une transformée de Fourier. Les paramètres modaux estimés par l'étape d'initialisation sont finalement affinés par l'étape d'estimation du maximum de vraisemblance. Celui-ci réduit le biais de l'estimation et donne des résultats plus fiables et plus robustes. Toutes ces étapes sont définies de manière à être en mesure de surveiller automatiquement l'état de santé d'un bâtiment par l'intermédiaire d'un suivi long terme en temps réel des variations modales dans le temps sans que l'intervention de l'utilisateur soit nécessaire. En outre, l'approche proposée a accordé une attention toute particulière à l'estimation automatique du paramètre modal les plus problématique, c'est-à-dire, le taux d'amortissement. Ces deux caractéristiques sont des atouts originaux par rapport aux techniques existantes. L'adaptabilité et la fonctionnalité de l'AMBA a été validé sur six bâtiments réels excités par des vibrations ambiantes. D'après les résultats obtenus, AMBA a prouvé une grande efficacité dans l'estimation automatique des fréquences et des taux d'amortissement dans le cas de modes de fréquences rapprochées et avec un très faible rapport signal-sur-bruit. AMBA a ainsi démontré une bonne performance pour suivre les variations modales au fil du temps.

Mots clés : analyse modale automatique, technique du décrément aléatoire, variation modale, surveillance des batiments, suivi temporel.

GIPSA-lab, 11 rue des Mathématiques, Grenoble Campus BP 46,
F-38402 Saint Martin d'Hères CEDEX